United States
Environmental Protection
Agency

Industrial Environmental Research
Laboratory
Research Triangle Park NC 27711

EPA-600/7-79-232a
October 1979

EPA

Assessment of Diesel Particulate Control: Filters, Scrubbers, and Precipitators

Interagency Energy/Environment R&D Program Report

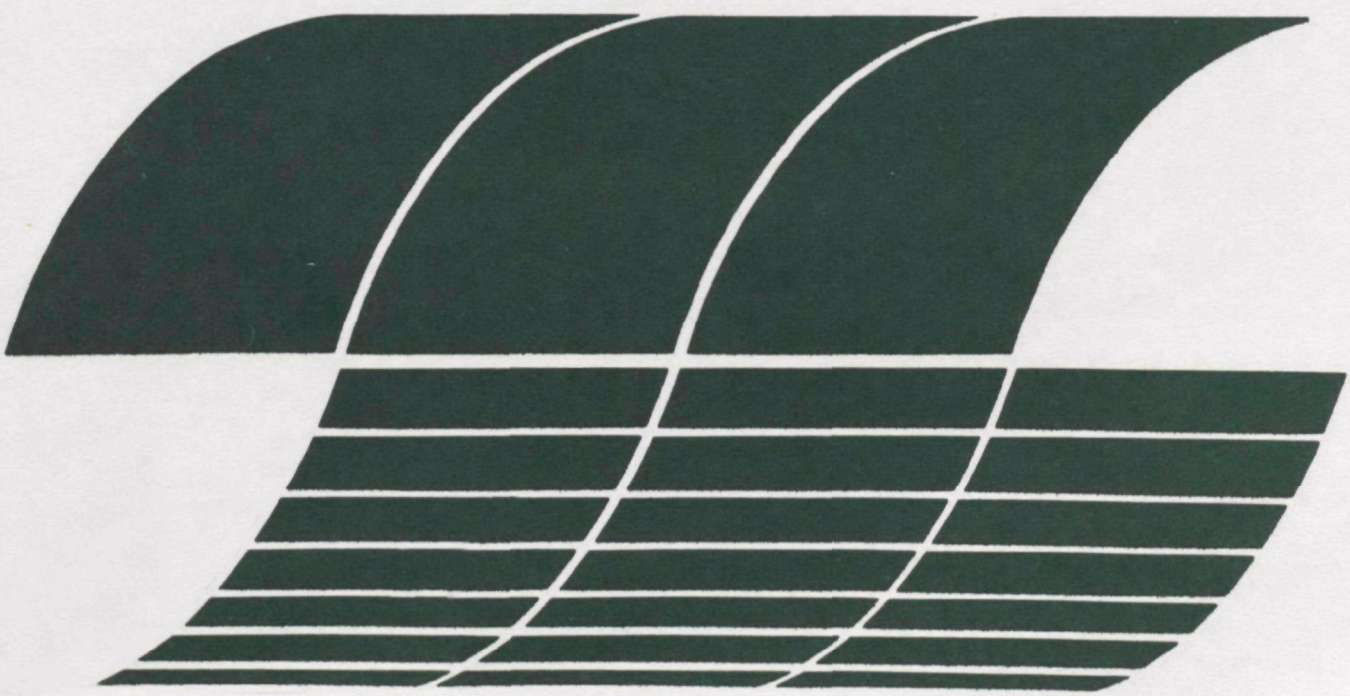

RESEARCH REPORTING SERIES

Research reports of the Office of Research and Development, U.S. Environmental Protection Agency, have been grouped into nine series. These nine broad categories were established to facilitate further development and application of environmental technology. Elimination of traditional grouping was consciously planned to foster technology transfer and a maximum interface in related fields. The nine series are:

1. Environmental Health Effects Research
2. Environmental Protection Technology
3. Ecological Research
4. Environmental Monitoring
5. Socioeconomic Environmental Studies
6. Scientific and Technical Assessment Reports (STAR)
7. Interagency Energy-Environment Research and Development
8. "Special" Reports
9. Miscellaneous Reports

This report has been assigned to the INTERAGENCY ENERGY-ENVIRONMENT RESEARCH AND DEVELOPMENT series. Reports in this series result from the effort funded under the 17-agency Federal Energy/Environment Research and Development Program. These studies relate to EPA's mission to protect the public health and welfare from adverse effects of pollutants associated with energy systems. The goal of the Program is to assure the rapid development of domestic energy supplies in an environmentally-compatible manner by providing the necessary environmental data and control technology. Investigations include analyses of the transport of energy-related pollutants and their health and ecological effects; assessments of, and development of, control technologies for energy systems; and integrated assessments of a wide range of energy-related environmental issues.

EPA REVIEW NOTICE

This report has been reviewed by the participating Federal Agencies, and approved for publication. Approval does not signify that the contents necessarily reflect the views and policies of the Government, nor does mention of trade names or commercial products constitute endorsement or recommendation for use.

This document is available to the public through the National Technical Information Service, Springfield, Virginia 22161.

EPA-600/7-79-232a

October 1979

Assessment of Diesel Particulate Control: Filters, Scrubbers, and Precipitators

by

M.G. Faulkner, E.B. Dismukes, J.R. McDonald,

D.H. Pontius, and A.H. Dean

Southern Research Institute
2000 Ninth Avenue South
Birmingham, Alabama 35205

Contract No. 68-02-2610
Task No. 14
Program Element No. EHE624A

EPA Project Officer: Dennis C. Drehmel

Industrial Environmental Research Laboratory
Office of Environmental Engineering and Technology
Research Triangle Park, NC 27711

Prepared for

U.S. ENVIRONMENTAL PROTECTION AGENCY
Office of Research and Development
Washington, DC 20460

DISCLAMIER

This report has been reviewed by the Industrial Environmental Research Laboratory, U.S. Environmental Protection Agency, Research Triangle Park, North Carolina 27711, and approved for publication. Approval does not signify that the contents necessarily reflect the views and policies of the U.S. Environmental Protection Agency, nor does mention of trade names or commercial products contribute endorsement or recommendation for use.

EXECUTIVE SUMMARY

Introduction

As a result of the Federal Government's requirement that the average fuel mileage of U.S. automobile manufacturers be at least 27.5 mi/gal. by 1985, there is increased interest in the widespread use of diesel engines for light-duty vehicles because of the diesel's superior fuel economy. Unfortunately, the diesel engine produces a high level of combustion by-products that are potentially hazardous, and therefore the Environmental Protection Agency has proposed emission standards which would require up to 70% particulate removal efficiencies for some current models.

Several approaches for controlling particulate emissions are under investigation by automobile researchers, including fuel modification, combustion modification, and aftertreatment of the exhaust in a control device. The purpose of this report is to examine the potential applicability to diesel particulate control of stationary source particulate control technology employing electrostatic precipitation, filtration, and wet scrubbing as collection processes. The removal of particulate by catalyzed or uncatalyzed oxidation is another aftertreatment concept that is being investigated elsewhere, but which may ultimately need to be considered as a disposal strategy in connection with particulate removal by a filtration or electrostatic precipitation device.

A consideration of diesel particulate characteristics yields some insight into the difficulty of designing a practical control device. The size distribution of the material has a mass median diameter (mmd) of about 2×10^{-7} m (0.2 μm), which is the particle size at which conventional control concepts are least effective. If suitable collection is achieved, the bulk density of the soot is only about 120 kg/m^3, which creates a storage and disposal problem. For example, if 90% particulate control is achieved on an Oldsmobile 350 CID diesel, about 0.019 m^3 (5 gal.) of material would be accumulated in 4,800 km (3,000 mi) if no compaction were achieved. The approach used in this study has been to identify and select for screening studies control concepts which, on the basis of existing knowledge of the fundamental collection processes, offer potential for effective particulate

capture without adversely influencing the engine performance. Those concepts that continue to appear promising after the screening data have been evaluated can then be further investigated with more emphasis on particulate storage and disposal.

Filtration

Filtration is a complex process involving several particle collection mechanisms for which theoretical models are not entirely adequate. Filtration theory attempts to predict overall particle removal in a filter based on an understanding of the interaction of particles with a single filter element, which may consist of a fiber, a granule, or a previously collected particle. The currently available filtration theory was employed to estimate the performance of various filter designs. The approach used was to select a reasonable filter volume and path length and then to examine the performance of filters varying in both volume and path length. Both fiber bed and granular bed filters were considered, and the porosity of each was fixed at a reasonable value. The fiber and granule diameter were fixed, and the properties of the gas and aerosol were fixed at a base-case condition of 200°C, with 0.14 m^3/s (300 ft^3/min) of exhaust gas transporting 7 x 10^{-5} kg/m^3 (0.03 gr/ft^3) of particulate with an mmd of 0.2 μm.

The analysis resulted in the selection for further study of a fibrous filter with uniform 10-μm diameter fibers used as packing at a porosity of 99%. Fibrous filter packing of this type is currently available and is considered typical with respect to filtration and pressure drop characteristics. Stainless steel is a possible material for the fibers. A sketch of this proposed prototype is shown in Figure E-1. The estimated pressure drop through this device is 732 Pa (2.9 in. of water) and the estimated maximum lifetime is 20,900 km (13,000 miles) at an emission rate of 5 x 10^{-4} kg/mi and a bulk density of 120 kg/m^3. This is the maximum possible lifetime based on the simplistic approach of estimating how long it would take to fill the void volume with collected particles, and it ignores the increase in pressure drop as porosity decreases. The lifetime expected in actual practice would therefore always be less than the lifetime calculated from the void-filling approach. Efficiency of collection is estimated as 82% using size distribution data obtained by Southern Research Institute from an Oldsmobile 350 CID diesel.

Uncertainties in the calculations which were used in the development of the above design, beyond the accuracy of the predictive equations themselves, include the effects of 1) condensation of hydrocarbons or water, especially during cold starts, 2) reentrainment and bounce of collected particles, and 3) dust load. Uncertainties regarding the effects of dust load are such that empirical verification of the practicality of the above configuration is required.

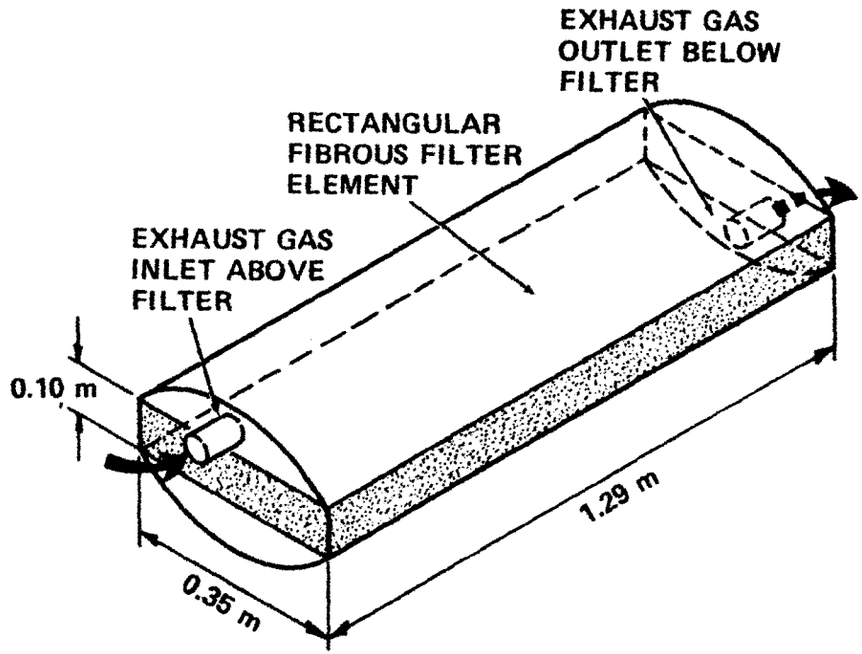

Figure E-1. Prototype fibrous filter.

Several authors have reported on the use of filtration as a means of collecting diesel particulate. Springer and Stahman tested a total of 48 combinations of devices and identified a best system for particulate removal. The system consisted of two alumina-coated, steel wool-packed filters and initially reduced the exhaust particulate by 64%. However, the collection efficiency decreased rapidly with distance, accompanied by a sharp increase in system backpressure. The high backpressure of the system had no great effect on the fuel economy of the test vehicle, but the acceleration rate, already a weak point on diesels, was reduced by 20%.

Sullivan et al. examined six different filter materials in a study concerned with emission of underground diesel engines. Although good collection efficiencies were reported, relatively high backpressures were experienced, and the rate of increase of backpressure was too high for automotive use. General Motors has also tested a number of filter materials including both paper and metal mesh filters. The paper filters exhibited high collection efficiencies, but high backpressures were experienced. The metal mesh filters showed efficiency degradation and, in some cases, evidence of filter destruction from incineration was observed.

The Eikosha Company in Japan has been conducting developmental work on a particulate collection device called an Aut-Ainer intended for use on both gasoline and diesel vehicles. Figure E-2 shows one of these. The initial concept for this device was to provide for the collection of emissions by condensation growth with collection on a mesh material. The original system consisted of a number of expansion chambers followed by regions filled with metal mesh to serve as a collection medium. A ram air cooling tube was also provided down the center on the device. This device has been carried through a number of stages of development using an empirical approach. At the current stage of development, the device has a collection efficiency of about 70% when clean. However, it is necessary to clean it every 2,000 km (1,200 mi). Without cleaning, the device will act as an agglomerator. For this reason, the developers are investigating the use of a post-collection device. One scheme is shown in Figure E-2. After the gases pass through the mesh material, they swirl through the cyclone dumping the spilled particles into a collection bag. This portion of the system still needs a lot of work, but the approach seems promising.

The review of published work on filtration devices has not revealed data on collection efficiency as a function of particle size or on the applicability of existing filtration theory to the various devices which have been tested. It is therefore not possible to directly relate the proposed fibrous filter prototype discussed previously with the prior studies without additional experimentation.

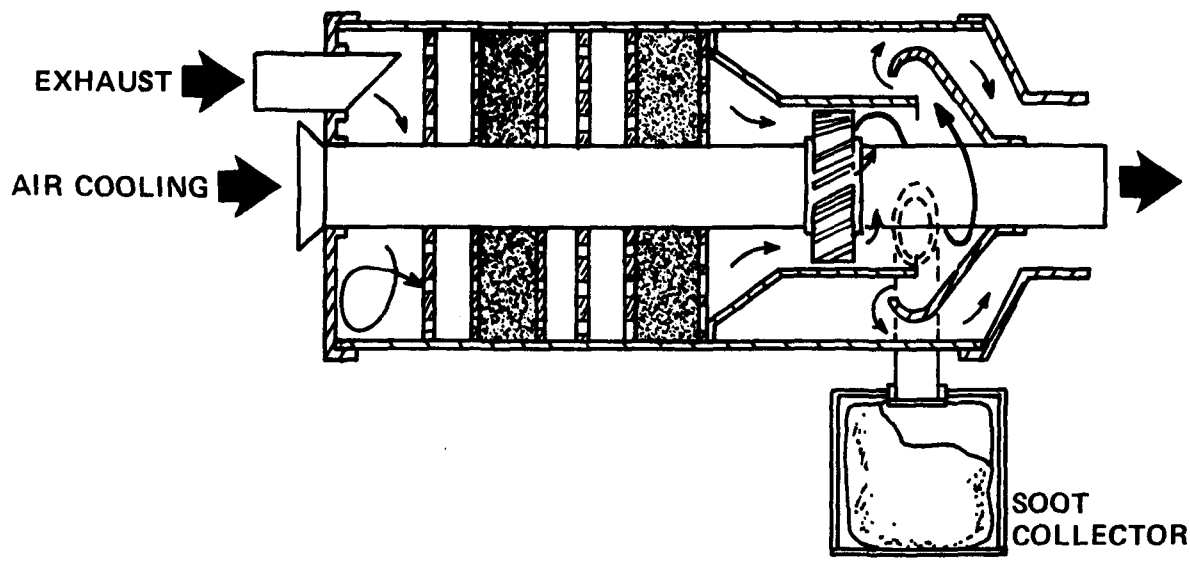

Figure E-2. Aut-Ainer filter with cyclone soot collector.

Electrostatic Precipitation

The electrostatic precipitation process consists of the fundamental steps of particle charging, particle collection, and the removal of the collected material from the collection and discharge electrodes. The particle charging process is accomplished through the creation of an electric field and a corona current by applying a large potential difference between a small-radius electrode and a much larger electrode, where the two electrodes are separated by a region of space containing an insulating gas. Particle charging is essential to the precipitator process because the electrical force that causes a particle to migrate toward the collection electrode is directly proportional to the charge on the particle. The most significant factors influencing particle charging are particle diameter, applied electric field, current density, and exposure time. Particle collection rates for a given value of particle charge are a function of particle size, the electric field in the region of the collection electrode, gas flow rate, gas viscosity, and electrode geometry. Removal of the collected material is usually accomplished by mechanical vibrations of the collection and discharge electrodes, but irrigated electrode systems are also in use which employ sprays of liquid to clean the electrodes. The electrical resistivity of the particulate matter for dry applications strongly influences the collection efficiency which can be achieved with a given electrode geometry.

An electrostatic control device for diesel particulate has the potential advantage of providing high efficiency collection of small particles with low backpressure and low energy consumption. However, there are two serious problems, namely particle reentrainment and current leakage through conductive films on high voltage insulators, which must be overcome in order to allow a practical electrostatic device to be employed. Removal and disposal of the collected particulate matter must also be accomplished in a practical manner.

As a result of the effectiveness of electrostatic precipitation in small particle collection, two prototype devices have been proposed for construction and evaluation. Both devices separate the particle charging and particle collection step as a result of the special requirements needed for diesel particulate collection. Figure E-3 is a conceptual sketch indicating the basic features of a device conceived by Southern Research Institute, which employs a periodic wet flushing scheme to clean the collected particulate thoroughly from all internal surfaces of the system. A vertically oriented, cylindrical geometry appears best suited to such a cleaning method, and optimum from the standpoint of structural strength. A two-stage device was selected to provide a maximum collecting surface with the space

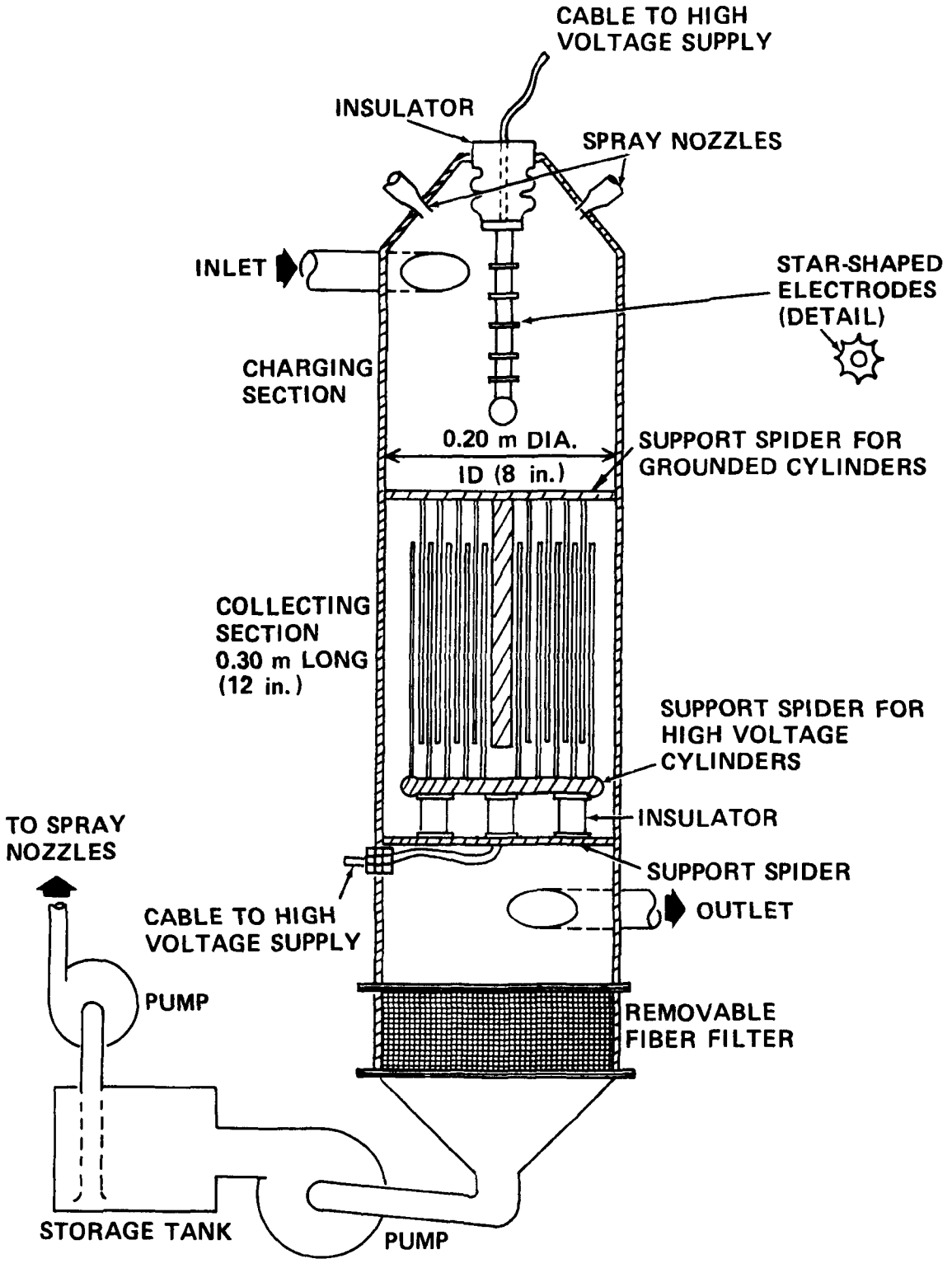

Figure E-3. First prototype electrostatic precipitator for collecting diesel particulate.

limitations of a vehicular installation. The exhaust gas from the engine enters the precipitator tangentially so as to avoid immediate impaction on the high voltage insulators. The cyclonic motion of the gas in the first stage (upper half) of the precipitator has little effect on particulate collection by impaction, since most of the particles are very fine; however, the circular path allows for adequate charging time for the particles before they enter the collecting stage.

Particle charging is achieved by means of an electrical corona discharge from flat, star-shaped electrodes mounted on the axial rod extending downward from the insulator at the top of the device. A corona ball on the end of the rod suppresses discharges to the grounded plates in the collecting stage. This structure is preferred over a more conventional fine-wire corona discharge electrode because of its ruggedness.

The collecting stage consists of a set of concentric cylinders. In sequence of decreasing diameter, the odd-numbered cylinders are connected to electrical ground, and the even-numbered cylinders are connected to the output of a high voltage power supply. The high voltage cylinders are connected together by a metal bus bar and nested between the grounded insulators. Insulating spacers between cylinders are avoided in order to minimize leakage resistance due to fouling by low resistivity material. Three stand-off insulators are used to support the entire array of high voltage cylinders.

The precipitator is to be cleaned periodically by spraying a nonvolatile liquid through the nozzles at the top of the device. The liquid is pulled through a filter at the bottom of the precipitator and then pumped into a storage tank for the next cleaning cycle. The period between flushing operations would probably be governed by the length of time required for the particulate buildup on the insulators to develop a significant current leakage path between high voltage components and ground. Provisions would be required to bypass the precipitator during the cleaning operation, which might take 30 to 60 s.

The 0.20-m diameter and 0.15-m long charging region and the collection area of this device allow an estimation of collection efficiency to be made using mathematical relationships that describe the particle charging and collection processes. If favorable electrical conditions can be maintained, the collection efficiency of 0.2-μm diameter particles from an exhaust gas stream of 0.14 m^3/s is estimated to be 80%.

A second electrostatic device that has been proposed by Castle for diesel exhaust is a radial flow device, which uses dielectric filter material in the collection region. This device, shown in Figure E-4, has the following features:

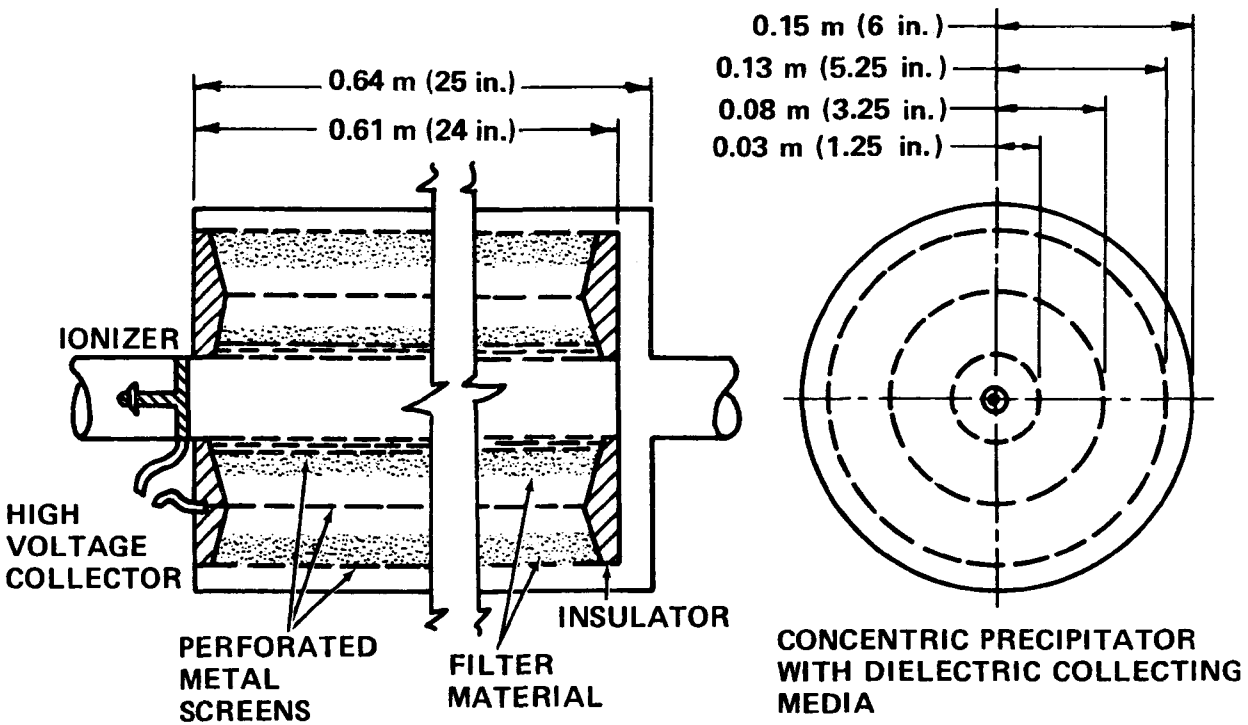

Figure E-4. Second prototype electrostatic precipitator for collecting diesel particulate.

a) two stage operation, thus minimizing ozone generation and power consumption,

b) adaption of high velocity gas throughput in small diameter ducts to low radial velocities for collection, thereby reducing reentrainment,

c) high efficiency for the submicron particle size range,

d) utilization of a combination of mechanical collection forces as well as coulombic, dielectrophoretic, and image electrical forces,

e) convenient geometry for using electrified media in the collection stage and ready adaptation to removable cartridge form.

It is believed that the most effective form of collector would involve a gradation using three collection zones. The first would be a mechanical impaction collector utilizing the high velocity jets of gas produced by the inner perforated screen that changes the gas flow from the axial to the radial direction. The second zone could be a relatively coarse fibrous bed of collection media with superimposed electrostatic field. The final zone would be finer graded bed of fibrous media with a superimposed electrostatic field.

The efficiency of this device is harder to predict. If the effects of the dielectric material are neglected and the particles are assumed to have acquired the same charge as in the wire-cylinder example earlier in this section (admittedly a bad assumption), then using the metal collection plate area of 1.2 m^2 an efficiency of 70% can be calculated. The effect of the dielectric material will be to increase the collection efficiency. Figure E-5 shows the results of using various geometries of dielectric material in a similar device. Note that the collection efficiency for the device was improved with any dielectric inserted and that the most efficient case was for a fibrous bed similar to that proposed here.

This device does have two possible design drawbacks. The first of these is the susceptibility to conductive contamination on the insulators. This will probably be worse on the ionizer and may necessitate the use of a different type of ionizer. The second is the increase in backpressure that will result when the dielectric fiber bed becomes loaded with particles. The magnitude of this problem can only be determined experimentally.

Wet Scrubber

The collection of particulate in a wet scrubber is accomplished through various mechanisms, including inertial impaction,

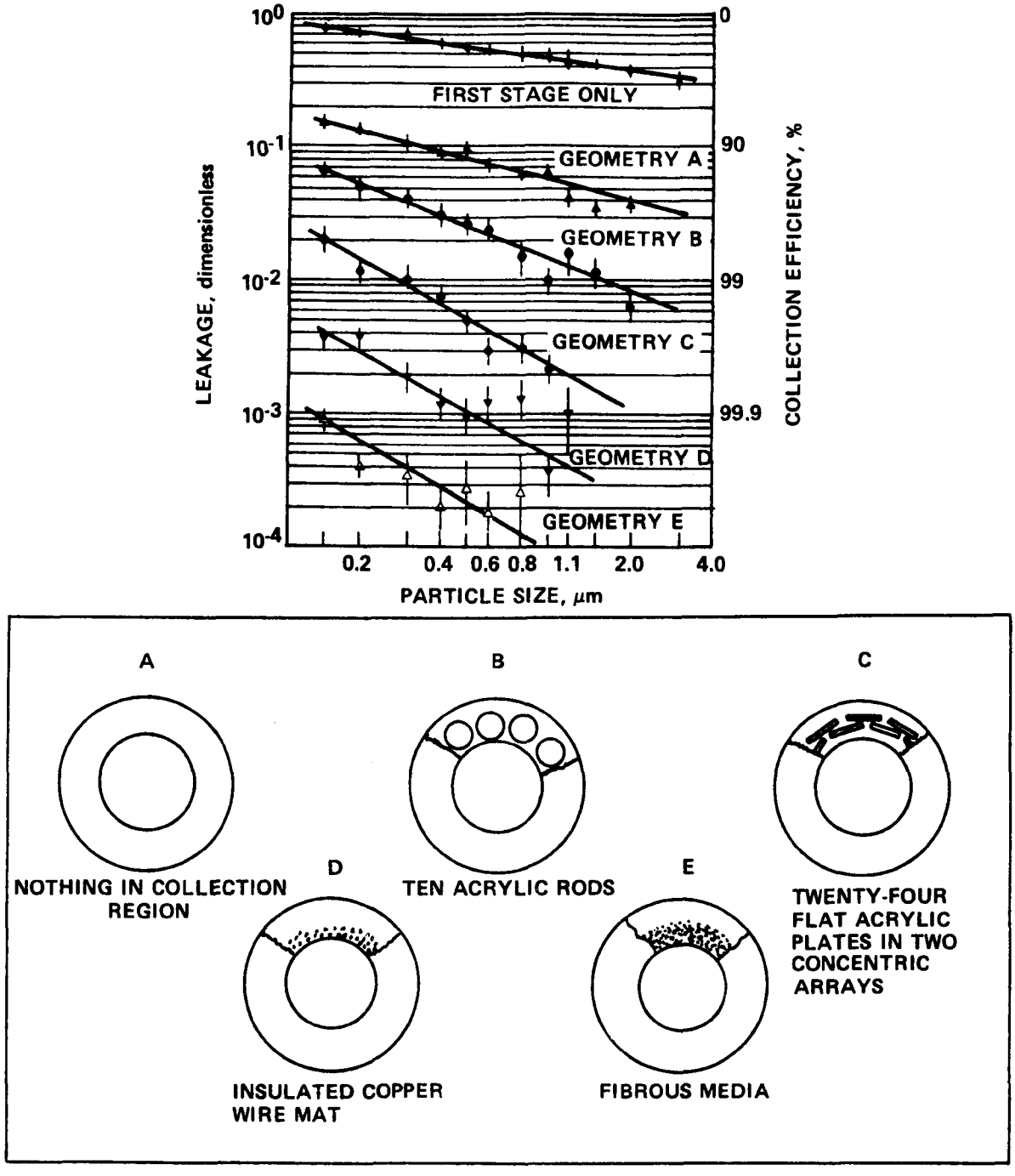

Figure E-5. Collection efficiency of a concentric precipitator with dielectric collection media.[49]

gravitational collection, diffusion, electrostatic collection, and thermophoresis and diffusiophoresis. Mathematical descriptions of these mechanisms were employed to calculate particle collection efficiencies in various scrubber designs that might be employed for collection of diesel particluate. The general conclusion derived from these calculations was that wet scrubbers are not suitable for removing particulate from diesel exhaust.

Under the constraint of a 2,500-Pa pressure drop (10 in. of water), scrubbers are not efficient enough in removing the fine particles present in diesel smoke. A possible exception is the charged droplet scrubber, but it is not clear that this device would be preferable to some other type of electrostatic device.

The above conclusions are reinforced by consideration of the rate of water loss by evaporation in a wet scrubber. Diesel exhaust entering a scrubber at 200°C at a rate of 0.14 m^3/s (300 ft^3/min) will contain about 3% by volume water vapor as the result of fuel combustion in the engine. This rate corresponds to the flow of 1.97 g/s of water vapor. On leaving the scrubber at 50°C with water vapor at the saturation level (concentration, 12.17% by volume), the gas stream will carry water away at the rate of 8.83 g/s. Thus, water will be lost at the rate of 6.86 g/s. This is equivalent to about 6.86×10^{-6} m^3/s. For comparison, the rate of fuel consumption may be calculated by assuming that the exhaust flow rate corresponds to a highway speed of 1.61 km/s (60 mi/h) and that the fuel consumption rate is 2.52×10^{-6} m^3/s (25 mi/gal. or 0.04 gal./min). The conclusion, therefore, is that water would be consumed at 2.7 times the rate of consumption of diesel fuel.

Conclusion

From the preceeding discussion, it is possible to draw some conclusions regarding the applicability of scrubbers, electrostatic devices, and filters to the problem of controlling diesel particulate emissions. The first of these, scrubbers, can be eliminated from further consideration due to the large size required to obtain adequate efficiencies at reasonable backpressures, and to the high rate of water consumption.

Second, electrostatic devices merit further consideration for the important reasons that they present very little backpressure to the system and that they maintain a relatively high collection efficiency over the 0.1- to 0.8-μm particle size range over which, according to theory, a dip in filter efficiecy occurs. To offset this, they have the severe disadvantage of dysfunction due to conductive particle contamination. Further research will have to be performed to design a system which can eliminate this difficulty. A lesser problem is that of disposal of the collected

particulate. A method must be developed whereby the device may be cleaned and the collected particulate properly and safely disposed of as a matter of routine maintenance.

The third mechanism, filtration, demonstrates the same problem of disposal of the collected particulate. Another problem area is the possibility of high backpressure. Although it is possible to design a device of appropriately low backpressure when new, only experimentation will determine the amount of particulate the filter can collect without elevating the backpressure beyond allowable limits and adversely effecting engine performance. The problem of surface seal over can be avoided by utilizing a filter with a large face area such as the proposed prototype. The advantage of filtration is that it is a mechanically simpler concept. Filters, while not necessarily simple to design, are simpler to build and maintain in the field than electrostatic devices and as a consequence should be cheaper and more convenient in use.

Both electrostatic devices and filtration devices show promise of becoming workable solutions to the diesel exhaust problem. However, more research is needed on both types of devices. Prototypes need to be fabricated and tested on actual diesel exhaust streams. Determinations of collection efficiency as a function of particle size would be useful in the study of the collection mechanisms involved, which should in turn lead to the development of improved collection devices. Testing of prototype devices will also yield additional insights into the particulate problems that affect each device.

Additional study is also needed on the effect of gas stream temperature on the hydrocarbon portion of the particulate. A study by Black and High indicates that most of the condensation and subsequent adsorption of vaporous hydrocarbons occurs in the last few feet of the vehicle's tail pipe. This implies that a temperature reduction in the exhaust system would increase the amount of hydrocarbons which condense and can therefore be collected as particulate. Supportive evidence has been given by Masuda, who reports that Eikosha has seen a 20% by volume increase in collected particulate occur when the cooling air flow on the Aut-Ainer filter was increased.

CONTENTS

FIGURES

FIGURES (concluded)

TABLES

TABLES (concluded)

ACKNOWLEDGEMENTS

In addition to the authors of this report, certain other members of the staff of Southern Research Institute made significant contributions to the report. These staff members are:

- Grady B. Nichols, Associate Director of Engineering and Applied Sciences. (Mr. Nichols made a trip to Japan to investigate the use of filters in that country for the control of diesel particulate.)

- William E. Farthing, Research Physicist.

- Ralph B. Spafford, Research Chemist.

In addition to staff members of the Institute, other contributors who served as consultants in various areas were as follows:

- David H. Leith, Tom Kalinowski, and Mike Ellenbacker of Leith Environmental Research Corporation, Newton, Massachusetts 02164 — particulate control by filtration.

- G.S.P. Castle, University of Western Ontario, London, Ontario (Canada) N6A5B9 — electrostatic precipitation.

- M.J. Pilat, B.D. Wright, and J.M. Wilder, University of Washington, Seattle, Washington 98195 — wet scrubbing.

SECTION 1

INTRODUCTION

The Federal Government has issued a regulation that requires the average fuel mileage for each auto manufacturer to be at least 27.5 mi/gal. by the year 1985. The diesel engine, according to various estimates, yields 25 to 75% better fuel mileage than does a gasoline engine of the same displacement. For this reason, the automobile manufacturers are showing an interest in widespread use of diesel engines in light-duty vehicles. General Motors, in particular, has indicated that it may have to depend on the diesel to meet the 1985 requirement.

Unfortunately, one characteristic of the diesel engine is a high level of combustion by-products. Light-duty diesels produce particulate at rates ranging from 0.25 g/mi (Volkswagen Rabbit) to 0.80 g/mi (General Motors 350).* These amounts are 50 to 100 times as much particulate as is produced by engines using unleaded gasoline.[1] The source of this particulate lies in the combustion process. In a diesel engine, fuel is sprayed into hot compressed air in the cylinder where it vaporizes and ignites spontaneously. Most of the fuel is burned in this process, but a small amount is cracked, polymerized, or partially oxidized into a large array of compounds including elemental carbon. The variables which affect this process are summarized in Figure 1. In the exhaust cycle, the products of combustion enter the relatively cooler exhaust system where they are subject to agglomeration and condensation. Beyond the exhaust system, the exhaust enters the outside environment where it is diluted and further cooled.

The particulate that results from diesel combustion consists largely of agglomerates of very small particles of carbon (on the order of 0.01 μm in diameter),[3] which have condensed hydrocarbons adsorbed onto them. These particles have a mass median diameter (mmd) of 0.3 μm, and 70% have diameters smaller than 1 μm[4] (Reference 4 is included in this report as Appendix I).

---

* EPA has defined particulate as everything collected on a 52°C (125°F) filter after dilution with ambient air in a dilution tunnel.

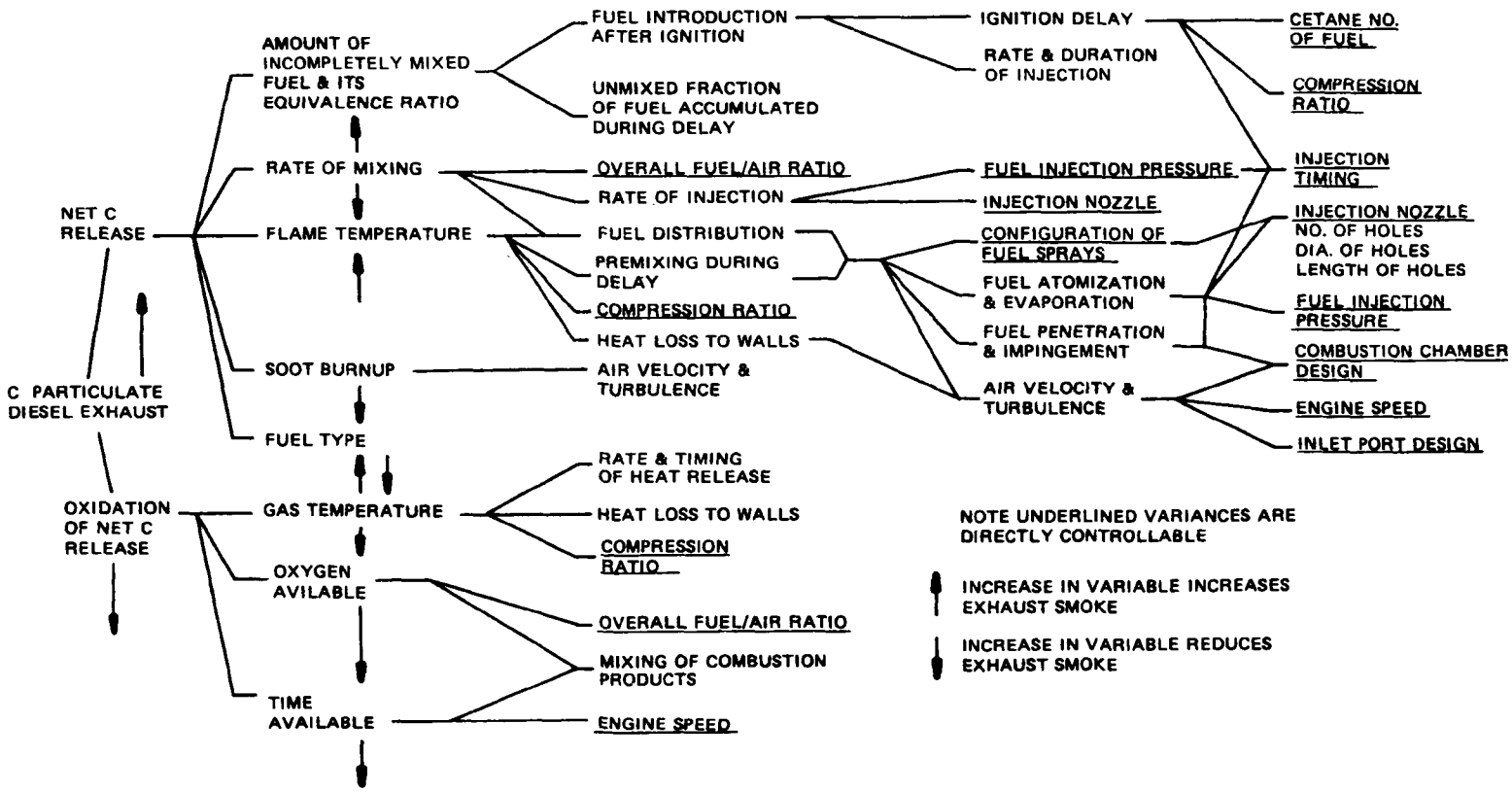

Figure 1. Summary of diesel engine variables effecting soot particulate formation.[2]

Particles of this size remain airborne for extended periods of time as shown in Table 1. According to this table, a 0.1-μm particle will take 5 days to fall 40 cm from the exhaust pipe to the ground in still air. Of course, the air will be quite turbulent, which means that the particles may be transported to greater heights, so that they remain airborne longer. Alternatively, the particles may impact onto the ground or onto other particles, thus reducing the time in suspension. In general, however, the suspension time may be measured in days.[3] Since these particles fall into the respirable size range, the suspension time is directly related to the exposure time for human beings.

TABLE 1. RATE OF FALL OF SPHERICAL PARTICLES IN STILL AIR[5]

Particle diameter (μm)	Rate of fall (cm/sec)
100	30
10	0.3
1	0.003
0.1	0.00009

Laboratory tests on the hydrocarbons derived from diesel particulate show a high level of toxicity. Some of the compounds, notably the polynuclear aromatics such as benzo(a)pyrene, are known to be carcinogenic. Others have been found to be mutagenic in the Ames Salmonella test but have not yet been proven carcinogenic. However, mutagenicity in the Ames test has been shown to have 85 to 90% correlation to carcinogenicity in animal tests.[6] Still other compounds that are known to be noncarcinogenic and nonmutagenic, such as perylene, have been transformed to mutagenic substances by exposure to low concentration of NO (about 1 ppm) in the presence of traces of HNO as is found in common photochemical smog.[7] The transformation of a normally nonmutagenic pollutant into a mutagen by another pollutant indicates the complexity of the air pollution problem and the danger of attempting to isolate the effects of any one pollution element.

The Environmental Protection Agency has proposed standards for regulating diesel emission.[8] These standards are given in Table 2. The particulate emission characteristics for several diesel automobiles are shown in Table 3. From this table, it can be seen that several manufacturers are not affected by the 1981 particulate standard, although all of the General Motors vehicles are affected. However, all manufacturers are affected by the 1983 standard.

TABLE 2. PROPOSED EMISSION STANDARDS FOR LIGHT-DUTY VEHICLES[8]

Type of emission	1981*	1983*
Hydrocarbons (total)	0.41	0.41
Carbon monoxide	3.4	3.4
Nitrogen oxides	1.0	1.0
Particulates	0.6	0.2

* Emission rates are in g/mi.

TABLE 3. PARTICULATE EMISSION RATES FROM LIGHT-DUTY DIESELS TESTED OVER THE EPA RECOMMENDED TEST PROCEDURE[8]

Type of vehicle	Grams per mile
Typical gasoline-powered vehicle (catalyst equipped)	0.008
VW Rabbit	0.23
Peugeot 504	0.29
VW Dasher	0.32
Mercedes 300SD	0.45
IHC Scout (with Nissan diesel)	0.47
Mercedes 240D	0.53
Chevrolet pick-up (with Oldsmobile 350 diesel)	0.59-0.61
Dodge pick-up (with Mitsubishi diesel)	0.81
Oldsmobile 260	0.73-1.02
Mercedes 300D	0.83
Oldsmobile 350	0.84

In order to meet these standards, automobile researchers are considering a wide variety of particulate control methods. Many of these are outside the scope of this report but will be briefly mentioned here for completeness. The first of these is fuel modification. General Motors has shown a 27% reduction in particulate emission on the 1975 Federal Test Procedure by using special blends of fuel in their 350 CID Oldsmobile. General Motors has also demonstrated a 17% particulate reduction by using additives in standard fuels. A third modification is the use of a water-in-fuel emulsion. The theory is that, on injection, the water explodes into super-heated steam which shatters the fuel droplet into a finer mist, thereby providing a better fuel-air mixture. General Motors has shown a 7% particulate reduction using water-in-fuel emulsions.[9]

Another direction of investigation involves improving the combustion mechanism in the engine. Several investigators are examining the possibility of redesigning the combustion chamber for greater efficiency. With current designs, however, lower particulate emissions have been achieved by turbocharging, which increases the available oxygen in the combustion chamber and promotes better fuel-air mixing by increasing turbulence. An example of this approach is the Mercedes 300SD, which emits 0.45 g/mi of particulate, compared to 0.83 g/mi for the Mercedes 300D.[8]

A third direction for reduction of particulate emissions is aftertreatment of the exhaust gases. Aftertreatment offers the possibility of much greater effectiveness than fuel or engine modifications. However, it has the disadvantages of requiring separate maintenance and allowing relative ease of circumvention. One form of aftertreatment that will not be discussed in depth in this report is catalysis. Although devices for reducing the gaseous output of diesel engines are commercially available, removal of particulate by catalysis is a largely unexplored area being investigated elsewhere.

Some other devices for exhaust aftertreatment are scrubbers, electrostatic devices, and filters. These are devices which have found widespread application for controlling emissions of stationary sources. Their extension to control of mobile diesel particulate is the subject of this report. The following chapters discuss the theory of operation of each of these devices and the applicability of each of these devices to the diesel control problem. In addition, a survey of previous attempts to use these devices on mobile diesel sources is presented along with designs of prototype devices which may be fabricated and tested.

SECTION 2

CHARACTERISTICS OF DIESEL EMISSIONS

The particulate emissions from diesel combustion have the form of branched chains of particles about 0.01 μm in diameter.[3] These agglomerates have an mmd of 0.3 μm with 70% smaller than 1 μm.[4] Figure 2 illustrates the size distribution data measured at temperatures from 270 to 430°C on an Oldsmobile diesel by Southern Research Institute. These data show good agreement with size distribution data measured on other vehicles.[3,6,10] Although the density of the soot particles, which are primarily elemental carbon, is about 2,000 kg/m^3, the open structure of the diesel particulate gives rise to a very low bulk density of 120 kg/m^3.[11] If this bulk density is used with the emission data from Table 3, it can be seen that the output volume per 1,000 mi ranges from 2.1 x 10^{-3} m^3 (0.55 gal.) for the Volkswagen Rabbit to 6.9 x 10^{-3} m^3 (1.8 gal.) for the Oldsmobile 350. At highway speed, this particulate is delivered in exhaust gas at a rate of about 0.14 m^3/s (300 ft^3/min) with a mass loading of 7 x 10^{-5} kg/m^3 (0.03 gr/ft^3). The physical data for diesel particulate are summarized in Table 4. The properties of diesel fuel are given in Table 5.

TABLE 4. PHYSICAL CHARACTERISTICS OF DIESEL PARTICULATE

Parameter	Magnitude	Reference
Individual particle size	0.01 μm	3
Agglomerated particle size		
mmd	0.3 μm	4
% smaller than 1 μm	70	
Exhaust temperature		
Manifold	190-275°C	10
Muffler	164-210°C	10
Bulk density	120 kg/m^3	11
Gas flow rate (estimated for 200°C)	0.14 m^3/s	4
Mass loading	7 x 10^{-5} kg/m^3	11

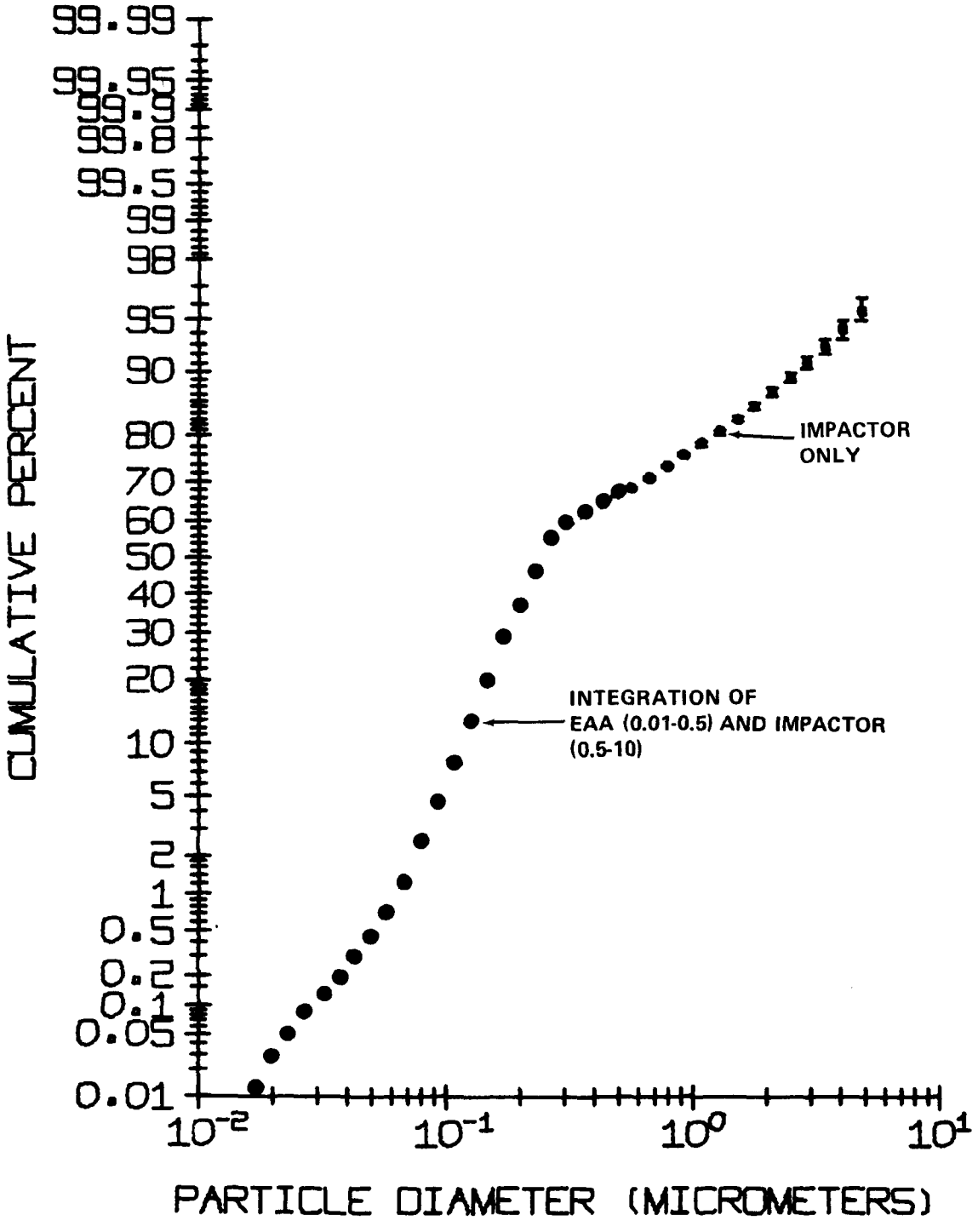

Figure 2. Size distribution of diesel particulate.[4]

TABLE 5. CHEMICAL AND PHYSICAL PROPERTIES OF DIESEL FUEL[11]

Flash point, °F minimum	125
Pour point, °F maximum	-5
Water and sediment, percent by volume, maximum	0.05
Carbon residue on 10% residuum, percent maximum	0.35
Distillation temperature, °F	
90% point, maximum	650
End point, maximum	700
Distillation recovery, percent by volume, minimum	97.0
Viscosity at 100°F, SSU	
Minimum	32
Maximum	45
Sulfur, percent by weight, maximum	0.75
Cetane Number, minimum	45
Gravity, degrees API	38

The characteristic oiliness of diesel particulate is due to condensed hydrocarbons adsorbed onto the agglomerated soot. An analysis of the collected particulate indicates that 33 to 50% is composed of organic substances.[11] Table 6 lists some of the compounds extracted from diesel particulate. The class of polynuclear aromatics, in particular, is associated with health problems, especially with lung cancer. Table 7 shows the relative carcinogenicity of some of these polynuclear aromatics. Detailed vapor pressure data for these and other compounds found in diesel exhausts are found in Appendix II.

The concentration of benzo(a)pyrene, one of the more potent carcinogens of the polynuclear aromatics, is often used as an indication of the potential health danger of exhaust products. Although the benzo(a)pyrene concentration of light duty diesel engines is equivalent to that of noncatalyst gasoline engines, it is an order of magnitude greater than the levels found in catalyst-equipped gasoline engines. In addition, there is some evidence that the high particulate level of diesel exhaust can increase the pulmonary retention time of substances such as benzo(a)pyrene, thereby increasing the chance of absorption by the body.

TABLE 6. A SUMMARY OF COMPOUNDS EXTRACTED FROM DIESEL PARTICULATE MATTER[1,2]

Acidic Compounds	Paraffinic Compounds	Aromatic Compounds
Phenol	Pentane	Benzene
Cresol	Hexane	Toluene
Dinitro-o-cresol	Octane	Diphenyl
Benzoic acid	n-Tetradecane	Anthracene
o,m,p-Phenylphenols	n-Pentadecane	Styrene
	n-Hexadecane	Xylene
Basic Compounds	n-Octadecane	Pyrene
Pyridine	n-Nonadecane	Chrysene
Aniline	n-Eicosane	Benzo(a)pyrene
Benzacridene	n-Heneicosane	Benzo(j)fluoranthene
o-Toluidine	Cyclohexane	Benzo(b)fluoranthene
	Methylcylohexane	Trimethylnaphthalene
Transitional Compounds		Ethylfluorene
Dioxane	Oxygenated Compounds	Dimethylphenanthrene
Methoxyphenanthrene	Hydroquinone	
	9,10-Anthraquinone	
	Furfuryl alcohol	
	Cyclohexanol	
	2-Hexanone	
	Methylacetate	
	Crotonaldehyde	
	2-Pentanone	

TABLE 7. CARCINOGENIC COMPOUNDS FOUND IN DIESEL EXHAUST PARTICULATE EMISSIONS[13]

Formula	Carcinogenic compound with corresponding formula	Carcinogenicity*	Molecular weight
$C_{18}H_{12}$	Chrysene	±	228.0936
	Benzo(c)phenanthrene	+++	
	Benz(a)anthracene	+	
$C_{20}H_{12}$	Benzo(a)pyrene	+++	252.0936
	Benzo(b)fluoranthene	++	
	Benzo(j)fluoranthene	++	
$C_{20}H_{14}$	Benz(j)aceanthrylene	++	254.1092
$C_{20}H_{16}$	7,12-Dimethylbenz(a)anthracene	++++	256.1248
$C_{21}H_{14}$	Dibenzo(a,g)fluorene	+	266.1092
$C_{20}H_{13}N$	Dibenzo(c,g)carbazole	+++	267.1045
$C_{21}H_{16}$	3-Methylcholanthrene	++++	268.1248
$C_{22}H_{16}$	Indeno(1,2,3-cd)pyrene	+	276.0936
$C_{22}H_{14}$	Dibenz(a,h)anthracene	+++	278.1092
	Dibenz)a,j)anthracene	+	
	Dibenz(a,c)anthracene	+	
$C_{21}H_{13}N$	Dibenz(a,h)acridine	++	279.1045
	Dibenz(a,j)acridine	++	
$C_{24}H_{14}$	Dibenzo(a,h)pyrene	+++	302.1092
	Dibenzo(a,i)pyrene	+++	
	Dibenzo(a,l)pyrene	+	

* The carcinogenicities are given in "Particulate Polycyclic Organic Matter," National Academy of Science, Washington, D.C., 1972, according to the following code:

± uncertain or weakly carcinogenic

+ carcinogenic

++, +++, ++++, strongly carcinogenic.

Consideration of the particle characteristics yields some insight into the problems associated with adapting control devices for stationary sources to mobile sources. The ultrafine particle size places the particulates in a region where collection devices are least efficient. Increasing the efficiency by increasing the device size is limited by the space available. On the other hand, increasing the efficiency by increasing the air stream blockage is limited by the allowable backpressure on the engine. Assuming a suitable efficiency is achieved, the next problem is storage of the collected particulate. At 90% collection, a treatment device for the Oldsmobile 350 diesel will have to store 0.019 m^3 (5 gal.) of particulate in 4,800 km (3,000 mi), assuming no compaction. The collected particulate is then subject to reentrainment by the relatively high 0.14-m^3/s (300-ft^3/min) flow rate.

SECTION 3

FILTRATION

FILTRATION FUNDAMENTALS

Introduction

Filtration is a commonly used particle removal process with applications ranging from dust removal from household heating and ventilation systems to high efficiency removal of radioactive particles in the nuclear industry. At a fundamental level, filtration is a complex process involving several particle collection mechanisms for which theoretical models are not entirely adequate. Filter design often relies on emiprical studies.

The following sections review the fundamental particle collection mechanisms which affect particle removal in filters, either separately or in combination depending on the characteristics of the aerosol, filter, and application. Available quantitative methods for predicting particle collection in fibrous filters and granular bed filters are then reviewed.

Fundamental Particle Collection Mechanisms

Filtration theory attempts to predict overall particle removal in a filter based on an understanding of the interaction of particles with a single filter element, i.e., a fiber, granule or previously collected particles. This requires an understanding of the flow field around single collectors including the manner in which the single collectors influence each other in the assembly, and the mechanisms by which particles are transferred from the gas stream to the collector element.

The single element efficiency, η, is defined as the number of particles collected by a filter element divided by the number of particles whose centers pass through the element's projected area as the particles approach it. The major mechanisms by which particles collect on a filter element are listed below and described in the following sections:

1. diffusion
2. interception

3. inertial impaction

4. gravity settling

5. electrostatic deposition

6. thermophoresis

7. flux forces

A single element efficiency due to any one mechanism, η_i, can be estimated for each of the fundamental collection mechanisms; however, it is frequently the case that one mechanism does not dominate. In this case it is necessary to combine two or more mechanisms when predicting the overall single element efficiency, η. As a first approximation, it is often assumed that particles not collected by one mechanism may be collected by others such that

$$\eta = 1 - \pi_i (1 - \eta_i) \tag{3.1}$$

where η_i is the computed single element efficiency for each collection mechanism.

Diffusion--

For particles in the submicron size range, Brownian motion enhances the probability of the particle hitting a collector element as the particle passes the collector. Diffusional deposition has been found to be inversely proportional to the dimensionless Peclet number, Pe, which is the ratio of transport by convective forces to transport by diffusional forces:

$$Pe = \frac{Vd_c}{D_p} \tag{3.2}$$

where: V = superficial velocity (m/s)

d_c = collector diameter (m)

D_p = particle diffusivity (m^2/s)

Particle diffusivity, D_p, can be determined from:

$$D_p = \frac{C_c kT}{3\pi\mu d_p} \tag{3.3}$$

where: C_c = Cunningham slip correction factor (dimensionless)

k = Boltzmann constant (joule/K)

T = absolute temperature (K)

μ = gas viscosity (Pa-s)

d_p = particle diameter (m)

As indicated by the inverse relationship with Peclet number, the single element efficiency factor for diffusional deposition, η_D, increases with decreasing velocity, particle diameter, and collector diameter.

Interception--

When a streamline passes within one particle radius of a collector element, a particle on that streamline can be removed by grazing contact with the collector surface. This removal process is dependent on particle size and is characterized by the dimensionless interception number, R:

$$R = \frac{d_p}{d_c} \tag{3.4}$$

where d_p = particle diameter (m)

d_c = collector diameter (m)

Interception is not directly dependent on velocity and can be effective even when diffusional, inertial, or other mechanisms are ineffective.

Inertial Impaction--

As the gas flows past a collector element, the streamlines curve around the collector. Near the collector surface, inertia will cause particles to deviate from the streamlines. Particles with sufficient inertia can cross streamlines and hit the collector. Inertial impaction has been found to be proportional to the dimessionless impaction parameter ψ:

$$\psi = \frac{\rho_p d_p^2 V C_c}{18 \mu d_c}$$

where: ρ_p = particle density (kg/m^3)

d_p = particle diameter (m)

V = superficial velocity (m/s)

C_c = Cunningham correction factor

μ = gas viscosity (Pa-s)

d_c = collector diameter (m)

The impaction parameter is the ratio of particle stopping distance (a measure of the deviation from the streamline) to the collector diameter. Single element impaction collection efficiency, η_I, is directly proportional to velocity and the square of particle diameter, and inversely proportional to collector diameter.

Gravity Settling--

Due to gravitational force, particles will have settling velocities which can cause deviations from flow streamlines around collectors. The single element efficiency for gravity settling, η_G, is proportional to the ratio of the particle settling velocity to the superficial gas velocity. Thus, the effect of gravity settling increases as the bulk gas velocity decreases, in effect allowing greater residence time in the filter for settling to occur. Terminal particle velocity is directly proportional to particle diameter squared and density; gravity settling will thus be enhanced when larger, denser particles are present.

Electrostatic Deposition--

The presence of charges on the particles or the collector elements can enhance particle collection. Theories for prediction of electrostatic deposition require estimates of particle and collector charge and dielectric properties which are not generally available in practice. Theoretical derivations of other collection mechanisms generally neglect electrostatic effects, and experiments are conducted so as to minimize electrostatic effects. Thus, in the absence of an applied electrical field, it is assumed that filter efficiencies predicted by other mechanisms will tend to underestimate overall efficiency to the extent electrostatic forces exist and electrostatic collection occurs.

Thermophoresis--

If a temperature gradient exists such that particle-laden gas entering a filter is hotter than the filter elements themselves, particle deviation towards the collector elements will occur. This is caused by more energetic molecular bombardment on the hotter side of the particle than on the side away from the colder collector surface. This tends to kick the particle

toward the collector surface. The thermal force causing particle deviation is proportional to the thermal gradient; therefore, if filters equilibrate to gas temperatures, thermophoresis does not occur.

Molecular Flux Forces--

Near condensing water droplets, the flux of gas molecules toward the droplet surface can cause particle deviation toward the droplet and collection on the droplet. Because droplets are larger than the particles, and are more easily removed in some cases, overall particle removal efficiency may be enhanced.

Fibrous Filters

Collection Efficiency--

Prediction of overall efficiency of a bed of fibers requires estimation of the single fiber efficiency resulting from the mechanisms described previously. Overall efficiency of a fibrous filter can be predicted by the following equation:[14]

$$E_{FT} = 1 - \exp\left\{-\frac{4}{\pi}\frac{L}{d_F}\frac{(1-\varepsilon)}{\varepsilon}\eta\right\} \qquad (3.6)$$

where: E_{FT} = overall efficiency of fibrous filter (fraction)

L = filter thickness (m)

d_F = fiber diameter (m)

ε = filter porosity (fraction)

η = single fiber efficiency (fraction)

The fiber diameter is the cross-sectional diameter for a filter of uniform fibers. For filters of nonuniform fibers, Chen[15] suggests $d = (\overline{d_F})_s^2/\overline{d_F}$, where $(\overline{d_F})_s^2$ is the surface average fiber diameter and $\overline{d_F}$ is the arithmetic average fiber diameter.

The porosity of fibrous filters is large, generally greater than 0.90, with 0.99 taken here as a typical value. Porosity is defined as:

$$\varepsilon = 1 - \alpha = 1 - \frac{\rho_B}{\rho_F} \qquad (3.7)$$

where: α = solidity (fraction)

$$= \frac{\text{fiber volume}}{\text{total filter volume}}$$

ρ_B = bulk density of filter (kg/m^3)

ρ_F = density of fiber (kg/m^3)

The single fiber efficiency factor, η_F, is for the dominant collection mechanism or combination of collection mechanisms calculated by equation 3.1. Theoretical and empirical methods are available to provide quantitative estimates of the single fiber efficiency resulting from diffusion, interception, impaction, and gravity settling.

The single fiber efficiency factor for particle collection by diffusion, η_D, in a fibrous filter is estimated by Fuchs and Strechkina:[16]

$$\eta_D = \frac{2.9}{[-\frac{1}{2} \ln(1-\epsilon) - 0.5]} Pe^{-2/3} \qquad (3.8)$$

where: ϵ = filter porosity (fraction)

Pe = Peclet number

The single fiber efficiency factor for interception is given by Davies[17] as:

$$\eta_R = (1+R) \ln(1+R) - \frac{1}{2}(1+R) + \frac{1}{2}(1+R)^{-1} \qquad (3.9)$$

where: R = interception parameter

$$= d_p/d_F$$

The single fiber efficiency factor for impaction in fibrous filters, η_I, has been expressed by Davies[17] as a function of the impaction parameter ψ as:

$$\eta_I = H\psi \qquad (3.10)$$

where: H = complicated function of porosity and d_p/d_F (See Table 8)

ψ = impaction parameter

The values of H and, thus, η_I increase as the fiber diameter decreases and as porosity decreases. Also, the impaction parameter, ψ, increases as the fiber diameter decreases and as gas velocity and particle diameter increase.

TABLE 8. VALUES OF H FOR USE IN EQUATION 3.10

α*	d_F (μm)	d_p/d_F †	H
0.02	20	0.01	0.0011
	10	0.02	0.0041
	4	0.05	0.0255
	2	0.10	0.0926
0.01	20	0.01	0.0009
	10	0.02	0.0034
	4	0.05	0.0208
	2	0.10	0.0755

* $\alpha = 1 - \epsilon$

† Particle diameter, $d_p = 0.20$ μm

The single fiber efficiency for gravity settling, η_G, in fibrous filters can be estimated by:

$$\eta_G = \frac{(d_p + d_F)}{d_F} \frac{V_{TS}}{V} \qquad (3.11)$$

where: d_p = particle diameter (m)

d_F = fiber diameter (m)

V_{TS} = particle settling velocity (m/s)

$$= \frac{\rho_p d_p^2 C_c g}{18\mu}$$

g = acceleration due to gravity (m/s^2)

ρ_p = particle density (kg/m^3)

μ = gas viscosity (Pa-s)

C_c = Cunningham correction factor (dimensionless)

V = superficial gas velocity (m/s)

Generally, the effect of gravity settling is small because when a particle is large enough to have a significant settling velocity it will be collected by impaction. However, at low superficial gas velocities where impaction is limited, gravity settling can be significant for particles too large to be removed by diffusion.

Pressure Drop--

For clean, unloaded fibrous filters, Davies[14] has suggested the following expression for prediction of pressure drop:

$$\Delta P = \frac{\mu L V F(\alpha)}{d_{Fe}^2} \qquad (3.12)$$

where ΔP = total pressure drop (Pa)

μ = gas viscosity (Pa-s)

L = filter thickness (m)

V = superficial velocity (m/s)

$d_{Fe} = (\overline{d_F^2})/\overline{d_F}$

$\alpha = 1 - \varepsilon$ (fraction)

$F(\alpha) = 64\alpha^{1.5}(1+56\alpha^3)$ for $\alpha < 0.02$

$F(\alpha) = 70\alpha^{1.5}(1+52\alpha^3)$ for $\alpha > 0.02$

For fibrous filters of low solidity, $\alpha < 0.02$, equation 3.12 can be approximated by:

$$\Delta P = \frac{64\mu L\alpha^{1.5}V}{d_{Fe}^2} \qquad (3.13)$$

Pressure drop is seen to be directly proportional to velocity. At practical operating conditions for fibrous filters, the flow around fibers is always laminar. Also, pressure drop increases rapidly as fiber diameter is decreased (at a constant α) indicating that attempts to increase filter efficiency by using smaller fibers will result in a pressure drop penalty.

Other Important Factors--

Temperature--Fundamental particle collection mechanisms are influenced by operating temperature. Although recent interest in high temperature filtration has increased experimentation in that area, filter performance at temperatures above

ambient conditions can be estimated by inspection of the temperature dependent factors in the filtration equations. The base-case conditions indicate that exhaust gas entering the filter would be 200°C (392°F).

Also, it should be noted that the volume of exhaust gas to be treated is a function of temperature. For example, the volume of gas at 20°C is only 62% of the volume at 200°C. Thus, as temperature and gas volume increase, the superficial gas velocity entering a filter of fixed cross-sectional area will also increase. Higher superficial gas velocity improves particle collection by inertial impaction and reduces collection by gravity settling and diffusion.

The collection efficiency of a filter due to inertial impaction is proportional to the Stokes number. The temperature dependence of the Stokes number is contained in the ratio of the Cunningham correction factor to gas viscosity, C_c/μ.

Gas viscosity increases as temperature increases. Viscosity can be adequately predicted as a function of temperature, e.g., the viscosity of air is 1.81×10^{-5} Pa-s at 20°C and 2.56×10^{-5} Pa-s at 200°C.

The Cunningham slip correction factor, which is significant for submicron particles, increases as the mean free path of the gas increases. At pressures near atmospheric, increases in absolute temperature will produce proportional increases in the mean free path of air molecules, e.g., λ_{air} is 0.069 μm at 20°C and 0.117 μm at 200°C. For a 0.2-μm diameter particle, the Cunningham correction factor will increase from 1.92 at 20°C to 2.65 at 200°C.

The increase in C_c counterbalances the decrease in C_c/μ due to viscosity increase. Thus, at 200°C the ratio C_c/μ is 97.2% of its value at 20°C. This indicates that collection of 0.2-μm diameter particles by inertial impaction at 200°C will be only slightly reduced when compared to filter performance at 20°C.

Collecton efficiency by <u>gravity settling</u> is also proportional to the ratio C_c/μ. Therefore, gravity settling can be expected to be slightly diminished at 200°C compared to performance at 20°C.

Collection efficiency by <u>interception</u> is shown to be only a function of the dimensionless interception parameter, d_p/d_c, which is not affected by temperature. Other expressions which have been proposed for interception show a weak dependence on temperature through the inclusion of Reynolds number, which results in a decrease in η_I as temperature increases.[18]

Due to the strong influence of temperature on particle diffusivity, D_p, particle collection efficiency by diffusion increases as temperature increases. Particle diffusivity is proportional to the ratio $(C_cT)/\mu$, which increases by 63% between 20°C and 200°C.

Thus, considering the only slightly diminished collection by inertial impaction, gravity settling, and interception and the significantly improved collection by diffusion, the base-case temperature of 200°C appears to improve collection efficiency somewhat, compared to operation at room temperature, at least for particles small enough to be collected by diffusion.

Filter compression--Equations 3.12 and 3.13 predict a linear change in pressure drop with velocity. However, fibrous filters tend to compress under high velocity, so that filter solidity, α, may increase with increasing velocity. The result is a nonlinear increase in pressure drop as filtration velocity increases.

Dust loading--The accumulation of dust within a filter has two basic effects: 1) a decrease in filter porosity, ε, and 2) a change in fiber diameter, d_F. These changes influence collection efficiency and pressure drop as dust loading occurs, and the equations for prediction of clean filter efficiency and pressure drop are no longer appropriate.

Although loaded filters often show increased efficiency, which is generally attributed to the presence of new collector sites, there is presently no adequate theory for the prediction of the efficiency of loaded filters. We will use clean bed performance models to estimate overall filter collection efficiency as a first, conservative estimate.

The change in the distribution of fiber diameters due to loading is difficult to estimate. However, if the particles and fibers are about the same diameter, the effect on pressure drop may be negligible. Davies[17] reviewed the theoretical literature and concluded that "the increase in pressure drop is almost independent of fiber radius." Therefore, the effect of dust loading on pressure drop is primarily due to the change in filter porosity.

The change in filter porosity with dust loading can occur either uniformly throughout the fiber filter or nonuniformly as a dust cake on the surface of the filter. Uniform deposition throughout the filter is more desirable in terms of filter storage capacity, i.e., useful life, and pressure drop buildup; however, one cannot be sure that surface cake will not form. There is no adequate general theory to explain pressure drop increase with dust load.

Condensation effects--Condensation of water or hydrocarbons within the filter can have advantages and disadvantages. The flux forces described previously can enhance particle collection on condensing droplets. The coating of fibers with condensate may increase adhesion of particles, thereby reducing reentrainment and bounce (discussed below). Also, condensation of hydrocarbons and subsequent droplet removal would reduce overall hydrocarbon emission. However, these positive effects may be negated if clogging of the filter occurs too rapidly, resulting in filter blinding or excessive pressure drop. Experimentation will be required to determine the significance of condensation on filter performance.

Fault processes--The particle collection models discussed assume that contact between particles and fibers results in complete particle retention. However, particles may fail to stick on contact, i.e., bounce, or be reentrained after contact, either as individual particles or as agglomerates. Such fault processes can reduce overall filter efficiency below that predicted by fundamental collection mechanisms. Important factors are particle and fiber size, shape and surface properties, and gas velocity and temperature.

Reentrainment--Theoretical and experimental studies have shown that, once a particle is collected on a fiber, a velocity much higher than the deposition velocity is needed to blow the particle off the fiber. Thus, it is reasonable to assume that once a particle is collected in a filter it will not reentrain unless specific efforts to clean the filter are made.

Once collected, particles act as collection sites and additional particles strike them. Over time, therefore, agglomerates of particles build up; the collection efficiency of a fiber bed may increase above its initial value due to the presence of collected particles.

However, under high loading conditions, the particle agglomerates may become sufficiently large so that the drag force exerted by the filtration velocity itself is sufficient to break agglomerates loose. Stenhouse[20] has stated that the amount of agglomerate blow-off is strongly dependent on the level of the particle-fiber and particle-particle adhesion forces. If the adhesion forces are high, collection efficiency will increase with dust loading; if the forces are low, collection efficiency may decrease as agglomerates are reentrained.

It is difficult to make definite statements about dust penetration as a function of loading. Davies[17] has noted the lack of experimental data in this area. Penetration may stay constant, increase, or decrease, depending on the nature of the

dust and fiber and the filtration conditions. Since it is not possible to predict filter performance in advance, the performance of a particular filter design under high loading conditions should be determined experimentally.

Bounce--Classical filtration theory assumes that all particles which hit a collecting body stick and are not removed. However, when particles with high inertia strike a collecting body, they may bounce off and thus not be collected. In order for a particle to stick to a fiber, the energy of adhesion must be greater than the elastic energy available from the impact.

An accurate analysis of the probability of particle adhesion requires a detailed calculation of the energies involved. These calculations require knowledge of the elastic-inelastic properties of the fiber and particle and are beyond the scope of this report. However, general trends can be presented here.

The energy of adhesion between particle and fiber is principally due to the van der Waal's attractive force, which is inversely proportional to the particle diameter. The energy needed to overcome adhesion is provided by the particle kinetic energy, which is proportional to the square of particle velocity and cube of the particle diameter. Thus, as particle inertia increases, the ratio of kinetic to binding energy will increase rapidly, until at some point particle bounce will become significant.

For a given particle size, collection due to inertia will be a strong function of velocity. At low velocities, the inertial collection will be negligible; as velocity is increased, the amount of inertial impaction will increase until the theoretical single fiber collection efficiency from impaction reaches 100%. At some point, however, the velocity will be high enough so that particle bounce becomes significant, and further increases in velocity will cause decreases in collection efficiency.

Experiments by Loffler[21] and Stenhouse[22] have shown that, for typical combinations of particles and fibers, particle bounce may become significant when the inertial impaction parameter approaches 10. Thus, when designing a fiber filter, this value of impaction parameter can be used to give an indication of operating regions where particle bounce may become significant and degrade performance. Exact calculation of adhesion probabilities is difficult and filled with uncertainties, and experiments are necessary to obtain good quantitative information.

Granular Filters

Collection Efficiency--

The methodology for prediction of the total efficiency for a bed of granules is analogous to that for fibrous filters. The major differences between fibrous filters and granular filters are the collector element geometry and filter porosity. Assuming spherical collectors packed in a bed with porosity, ϵ, the following equation is appropriate for prediction of total bed efficiency:[23,24]

$$E_{BT} = 1 - \exp\left\{-1.5 \frac{(1-\epsilon)}{\epsilon} \frac{L\eta}{d_g}\right\} \qquad (3.14)$$

where: E_{BT} = total bed efficiency (fraction)

L = bed depth (m)

d_g = granule diameter (m)

ϵ = bed porosity (fraction)

η = single granule efficiency (fraction)

The granule diameter used in equation 3.14 is the physical diameter, assuming uniform, spherical collectors.

The porosity of granular beds generally ranges from 0.26 for closest packing of spheres to 0.44 for loose, random packing.[25] A typical porosity value for fixed bed granular filters is 0.40, and this value will be used here to characterize a prototype granular filter.

As for fibrous filters, the single granule efficiency factor, η, represents the dominant collection mechanism or combination of collection mechanisms for a single collector located in an assembly of collectors. Empirical and theoretical methods have been proposed for estimating the single granule efficiency corresponding to each of the fundamental collection mechanisms. The equations for estimating η presented below have been selected as reasonable for calculation purposes, but are by no means the only possible choices.

The single granule efficiency for particle collection by diffusion, η_D, in a granular bed is estimated by:

$$\eta_D = \frac{5.224}{\epsilon} Pe^{-2/3} \qquad (3.15)$$

where: ε = bed porosity (fraction)

Pe = Peclet number (dimensionless)

This expression for η_D results from an approximation proposed by Tardos et al.[24] for conditions where Re < 10, Pe > 1000, and $0.35 \leq \varepsilon < 0.70$, based on the hydrodynamic model of Neale and Nader.

The single granule efficiency for particle collection by interception, η_R, is estimated by:

$$\eta_R = \frac{3}{2}\left(\frac{1-\alpha}{1-9(\alpha)^{1/3}+\alpha-1/5(\alpha)^2}\right)\frac{R^2}{(1+R)^2} \qquad (3.16)$$

where α = bed solidity = $1 - \varepsilon$ (fraction)

R = interception parameter = $\frac{d_p}{d_g}$ (dimensionless)

Equation 3.16 is an approximate solution proposed by Lee and Gieseke[26] based on the Kuwabara Flow Field where solidity, α, approaches 5/8. For porosity, ε, of 0.4 (α = 0.6), equation 3.16, reduces to:

$$\eta_I = 61.6\,\frac{R^2}{(1+R)^2} \text{ at } \varepsilon = 0.4 \qquad (3.17)$$

There are no generally accepted models for prediction of the single granule efficiency factor for particle collection by impaction, η_I, and an empirical relationship must be used. Schmidt et al.[27] suggests the following empirical expression for η_I based on an analysis by Jackson and Calvert:[28]

$$\eta_I = K_I Stk \qquad (3.18)$$

where: $K_I = \frac{\pi}{1.5(1-\varepsilon)}$

K_I = 3.49 @ ε = 0.4

Stk = Stokes number

$$= \frac{\rho_p d_p^2 V C_c}{9\mu d_g}$$

ρ_p = particle density (kg/m^3)

d_p = particle diameter (m)

V = superficial velocity (m/s)

μ = gas viscosity (Pa-s)

d_g = granule diameter (m)

C_c = Cunningham correction factor (dimensionless)

It should be noted that the Stokes number, Stk, is essentially the same as the impaction parameter, ψ, described previously except that, by defining convention, the impaction parameter is smaller than the Stokes number of a factor of 2.

The single granule efficiency factor for particle collection by gravity settling, η_G, is:

$$\eta_G = \frac{V_{ts}}{V} K_G \qquad (3.19)$$

where: V_{ts} = particle terminal settling velocity (m/s)

V = superficial velocity (m/s)

K_G = fraction of projected area of single collector available for particle capture

Paretsky et al. give $K_G = 0.0377$ for triangular packing and 0.0871 for square packing and suggest using an average value of 0.0624 for K_G.[23] Paretsky found that gravity settling decreases penetration when gas flow is downward through a packed bed and increases penetration for upward flow.

Pressure drop--

The pressure drop across a clean bed of granules can be predicted by the Ergun equation:[29]

$$\Delta P = \frac{150\mu VL}{d_g^2}\left[\frac{(1-\varepsilon)^2}{\varepsilon^3}\right] + \frac{1.75\rho_F V^2 L}{d_g}\left[\frac{(1-\varepsilon)}{\varepsilon^3}\right] \qquad (3.20)$$

where: ΔP = pressure drop (Pa)

μ = gas viscosity (Pa-s)

L = bed depth (m)

V = superficial velocity (m/s)

d_g = granule diameter (m)

ε = bed porosity (fraction)

ρ_F = gas density (kg/m^3)

Other Important Factors--

Temperature--Because the fundamental collection mechanisms in granular filters are the same as in fibrous filters, the effects of temperature should be similar. Operation of a granular filter at 200°C should not present any problems with respect to fundamental collection mechanisms. However, recent tests of granular (sand) bed filters at 150°C for removal of fly ash suggest that adhesion properties may be reduced, thus increasing the significance of fault processes.[30]

Dust loading--Accumulation of dust within a granular filter will reduce the porosity of the bed and provide new sites for additional particle collection. Pressure drop and collection should increase with dust loading in a granular bed. However, there appear to be granule sizes and gas velocity conditions at which saturation of the bed is possible, i.e., efficiency falls to zero at a high dust loading within the bed.[31]

As is true for fibrous filters, there are no adequate, general theories for prediction of collection efficiency and pressure drop in loaded granular bed filters. Loaded filter performance requires experimental verification.

Condensation effects--The effects of condensation within a granular bed are similar to those described for fibrous filters.

Fault processes--As mentioned, bed saturation at high loading and adhesion problems at high temperature may reduce filter performance through reentrainment and bounce. Goren[32] found reentrainment to decrease efficiency for 1- to 3-μm diameter particles at superficial velocities greater than 0.35 m/s in a bed of 2-mm diameter alumina spheres. Lee et al.[30] found 0.22 m/s to be the approximate velocity at which reentrainment became significant in a bed of 40-50 mesh sand at 150°C.

In general, granular material, such as sand or alumina, should be suitable for the base-case application. For best results, granule diameter should be 1 to 2 mm. Smaller granules would provide better initial particle collection but would have poorer dust storage characteristics and high pressure drop.

PREVIOUS USES OF FILTRATION FOR DIESEL EXHAUST

Several authors have reported on the use of filtration to trap diesel particulate. Springer and Stahman[10] utilized available lead-trap technology in their study. From a total of 48 combinations of devices, a best system for particulate removal was identified. This system, which consisted of two alumina-coated, steel wool-packed filters, initially reduced the exhaust

particulate by 64%. However, as shown in Figure 3, the collection efficiency decreased rapidly with distance travelled, accompanied by a sharp increase in the system backpressure. The high backpressure of this system had no great effect on the fuel economy of the test vehicle but the acceleration rate, already a weak point on diesels, was reduced by 20%.

Sullivan, Tissier, Hermance, and Bragg[33] examined six different filter materials in a study concerned with emission of underground diesel engines. Their results are summarized in Table 9. Although the collection efficiencies were quite good, the backpressures were very high. The first five materials formed a cake of particulate on the face of the filter, effectively sealing off the filter. The stainless steel-fiberglass material appeared to collect particulate matter throughout the entire filter without forming a cake. This resulted in a much slower rise in backpressure than the other materials tested, although it is still too rapid for automotive use.

TABLE 9. PERFORMANCE RESULTS OF FILTER MATERIALS[33]

Filter material	Collection efficiency	Time required to backpressure of 2.5×10^3 Pa. (Hours)
Teflon felt	99.9	0.25
Nomex felt	99 +	0.25
Woven fiberglass - graphite treated	98 +	0.25
Fiberglas batt	98 +	3
Fiberglas Aerocor	97 +	1
Knitted stainless steel fiberglas matrix	80	12

The Eikosha Company[34] in Japan has been conducting developmental work on a particulate collection device called an Aut-Ainer intended for use on both gasoline and diesel vehicles. Figure 4 shows one of these. The initial concept for this device was to collect emissions by condensation growth on a mesh material. The original system consisted of a number of expansion chambers followed by regions filled with metal mesh to serve as a collection medium. A ram air cooling tube was also provided down the center on the device. This device has been carried through a number of stages of development using fundamentally an experimental approach.

At the current stage of development, the device develops a collection efficiency of about 70% for diesel particulate when the system is clean. However, it is necessary to provide for

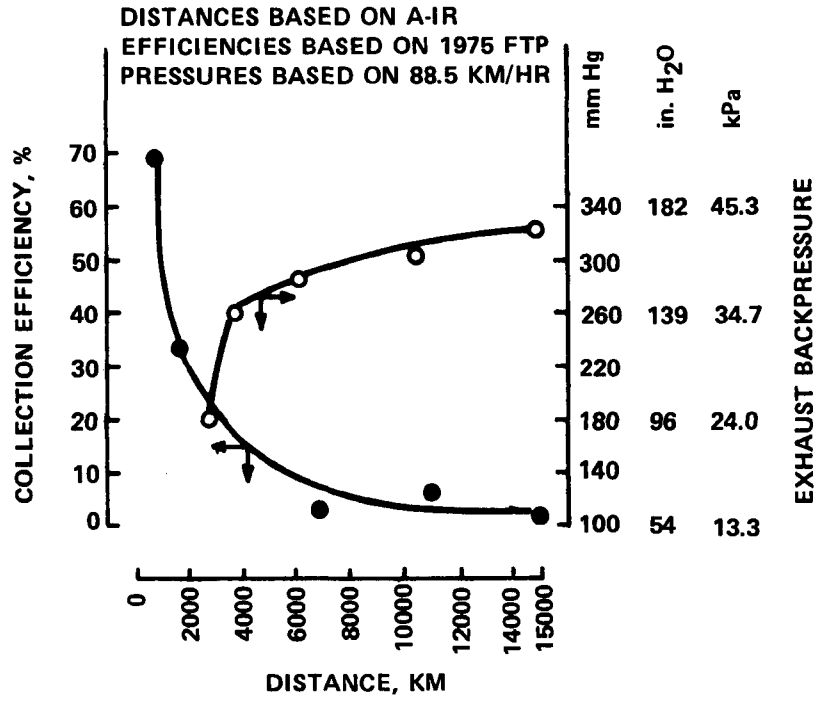

Figure 3. System efficiency and exhaust restrictions as functions of distance traveled.[10]

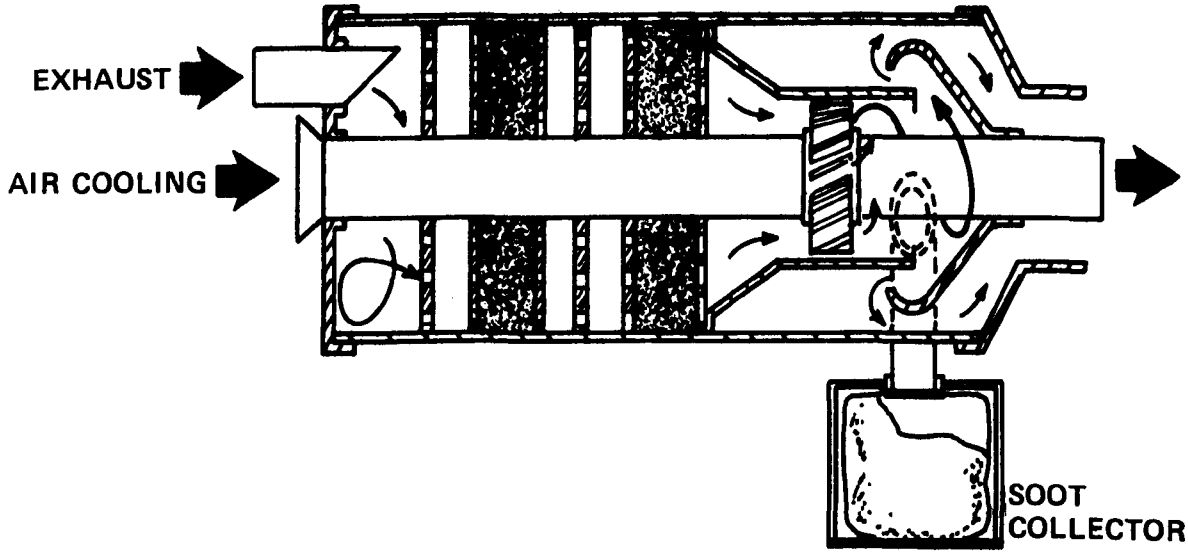

Figure 4. Aut-Ainer filter with cyclone soot collector.

cleaning at intervals of 2,000 kilometers of operation. In the absence of cleaning, the collection sites become covered with the very low density soot particles after which reentrainment occurs. Therefore, the device initially acts as a collection device until reentrainment occurs, at which time the characteristic behavior changes to that of an agglomerator.

The recognition of this fact led the developers to investigate adding a post-collection device as a means for collecting this reentrained material. Two methods are currently under investigation, each of which involves the use of a collector operating on a side stream consisting of about 10 to 15% of the total flow through the system. The method shown in Figure 4 uses a cyclone to divert the particulate to a collection bag. The other method uses a rotating particle catching wheel which passes through a backflow of air where the particulate is blown into the collection bag. This portion of the system still needs a lot of work, but the approach does show promise. Further study is needed to devise a more reliable method for diverting the reentrained material into the post-collection device.

General Motors Corporation[9] has tested a number of filter materials on diesel automobiles. One material tested was pleated paper. Each paper cartridge has a total volume of about 0.011 m^3 (3 gal.) with a surface area of 3.2 m^2 (5,000 $in.^2$). Collection efficiency was in the 80 to 90% range. However, after 1,100 km (700 mi) of Federal Test Procedure driving on an Oldsmobile test vehicle, the system backpressure had risen to 2.0×10^4 Pa (80 in. of water) from the 5.0×10^3 Pa (20 in. of water) from the standard exhaust system. Also, on several occasions the paper element caught fire.

General Motors also tested metal mesh filters, which showed efficiencies as high as 60%. Results of a 19,300-km (12,000-mi) test under very mild driving conditions showed efficiency degradation from 55% to 36% during the test. There was evidence that particulate blow-off and incineration had occurred during the course of the test. In other tests, filter destruction from incineration was observed. Table 10 summarizes the tests of filtration materials performed at General Motors.

TABLE 10. SUMMARY OF FILTRATION MATERIALS TESTED BY GENERAL MOTORS[9]

Trap material	Efficiency, %	Remarks
Opel 2.1 Liter Engine		
Corrugated foil fecralloy	36	High temperature resistance - good oxide adhesion
Chopped fecralloy	29	

(continued)

TABLE 10 (continued)

Trap material	Efficiency, %	Remarks
Chromium alloy ribbon	37	Low efficiency - high temperature resistance
Glass fiber fabric	34	Quick loadup
	65	Good efficiency - rapid loadup
Fiberfrax fiber fabric	46	Fair efficiency - fast loadup
Alumina fiber material	61	Good efficiency
	32	Low endurance
Catalyst Beads		
- Quadralobe	46	2- and 4-in. diameter cartridge - good efficiency
	62	Catalytic converter - good efficiency Rapid loadup time
- Trilobe	39	Moderate efficiency
- Low density spheres	43	Moderate efficiency
- Large Quadralobe	50	Moderate efficiency
- Porous ceramic	41	Moderate efficiency
- Small bead	47	Moderate efficiency
- Production catalyst	52	Moderate efficiency
Catalyst beads	<10	Low efficiency
	<10	Low efficiency
Ceramic monolith extruded	<10	Low efficiency
- Low density -	52	Fair efficiency
Torturous path ceramic	49	Fair efficiency
	39	Thermal failure
Ceramic bobbin	42	High temperature resistance Low capacity

(continued)

TABLE 10 (concluded)

Trap material	Efficiency, %	Remarks
Alumina coated metal mesh	63	Good efficiency - oxidation resistance to 1500°F
Metal mesh	28	Poor efficiency
	44	Effectiveness at start - poor; fair after buildup
	Olds 5.7 Liter Engine	
Catalyst beads -Quadralobe-	56	FTP-4 Series Converters
Production catalyst	40	FTP-4 Series Converters
Ceramic monolith extruded -low density-	30	
Metal wool	60	Fine grade promising
Corrugated fecralloy	30	
Alumina coated mesh	65	High efficiency trap material
Paper element	90	Excellent efficiency - not heat resistant
Fiberglas element	76	Temperature resistance to 750°C

FILTER CHARACTERISTICS FOR DIESEL PARTICULATE EMISSIONS

Introduction

The preceeding reports were based on the experimental approach to filter design utilizing existing filter materials. In contrast to that, this discussion uses the equations described previously for prediction of collection efficiency and pressure drop in clean fibrous and granular filters to estimate the performance of various filter designs.

Characteristics of the filters investigated in this section are given in Table 11. The approach used is to select a reasonable filter volume and path length and then to examine the performance of filters varying in both volume and path length. Both fiber bed and granular bed filters are considered. Porosity

TABLE 11. ESTIMATED FILTER PERFORMANCE FOR BASE-CASE CONDITIONS

Configuration	Volume (m^3)	Length (m)	Velocity (m/s)	Mass removal efficiency (%)		Pressure Drop (Pa)		Maximum lifetime (mi)	
				F*	G†	F*	G†	F*	G†
1	0.0113	0.10	1.26	76.1	84.0	1,860	4,370	3,500	1,300
2	0.0113	0.30	3.78	90.6	97.1	16,700	74,000	3,000	1,100
3	0.0113	0.90	11.3	94.6	100	150,000	1,590,000	2,800	1,100
4	0.0225	0.10	0.630	78.5	81.3	927	1,700	6,800	2,700
5	0.0225	0.30	1.89	93.5	95.8	8,350	24,000	5,700	2,300
6	0.0225	0.90	5.67	97.6	100	75,100	450,000	5,500	2,200
7	0.0450	0.10	0.315	82.2	79.8	464	732	13,000	5,400
8	0.0450	0.30	0.944	95.0	96.5	4,170	8,740	11,300	4,500
9	0.0450	0.90	2.83	99.3	99.9	37,500	137,000	10,800	4,300

*F - fibrous filter: $d_F = 1 \times 10^{-5}$ m (10 μm), $\epsilon = 0.99$.

†G - granular filter: $d_g = 1 \times 10^{-3}$ m (1 mm), $\epsilon = 0.40$.

of both fiber and granular bed filters is fixed at a "reasonable" value, respectively, for all cases. Fiber and granule diameters are also fixed. All variables concerning the properties of the gas stream and aerosol were fixed at the values listed in Table 12 for all cases. A specific filter configuration, which appears acceptable on the basis of predicted initial efficiency, pressure drop, and lifetime (mileage), is selected for more detailed investigation later.

TABLE 12. DIESEL PARTICULATE EMISSION PROPERTIES: BASE CONDITIONS USED FOR FILTER DESIGN

Gas stream conditions	
Temperature	200°C
Flow rate	0.14 m^3/s (300 ft^3/min)
Viscosity	2.3×10^{-5} Pa-s
Density	0.74 kg/m^3 (7.4×10^{-4} g/cm^3)
Particle Properties	
Concentration	7×10^{-5} kg/m^3 (0.03 gr/ft^3)
Density	1,100 kg/m^3 (1.1 g/cm^3)
Bulk density	120 kg/m^3 (0.12 g/cm^3)
Emission rate	0.5 g/mi
Size distribution	mmd = 0.2 μm, 70% smaller than 1 μm by mass

It is most important to point out the limitations of the analysis. Filtration fundamentals are not understood well enough to permit confident calculations of filter efficiency and pressure drop, even for beds of clean, new fibers or granules. Comparatively little work, either experimental or theoretical, has been done on filters loaded with collected dust so that the performance of dust-conditioned filters is not well known or understood.

In general, it is to be expected that the collection efficiency of a conditioned filter will exceed that of a clean filter. However, no acceptable theory to allow calculation of filter efficiency with increasing filter loading currently exists. The approach used here is to identify from theory the efficiency of a clean bed and assume that this is the lowest efficiency expected in practice.

The pressure drop across a conditioned filter should exceed that across a clean filter. Ideally, it should be possible to predict the increase in pressure drop with filter loading. However, no acceptable theory currently exists to allow making this calculation. The best that current understanding allows is calculation of the pressure drop across a clean filter, and the assumption that subsequent pressure drop will be higher once the filter is conditioned.

The presence of water vapor and condensible hydrocarbons in the exhaust gas suggests that particle collection by flux forces such as condensation/particle growth, diffusiophoresis, and Stephan flow may occur if the temperature of the gas stream is sufficiently low. Also, adhesion to the filter material may be increased. These effects might increase collection efficiency for small diesel exhaust particles. However, condensation might also affect the performance of the filter adversely by filling it with materials other than the particles it is designed to collect or by interfering with in situ cleaning mechanisms, thereby decreasing the lifetime. Such uncertainties point out the necessity of thorough empirical testing over all operating parameters before the design can be optimized.

Filter Configuration

Size--

A fundamental constraint on filter selection is the allowable volume of the filter container. The initial assumption is that the filter can be approximately the size of a muffler, assumed to be 1.0 m long by 0.30 m in diameter for total volume of 0.0225 m^3. To investigate the effect of filter size, filter volumes half that and twice that of our typical muffler size are also used.

Within a given filter volume, the gas flow can be oriented many ways, e.g., parallel or perpendicular to the long dimension or distributed through baffles or an annulus. Thus, in addition to filter volume, a characteristic length, L, or filter depth was selected. The lengths considered are 0.10, 0.30, and 0.90 m.

Selection of filter volume and length fixes the cross-sectional area, A, available for filtration as:

$$A = v/L \tag{3.21}$$

where: A = area (m^2)

v = volume (m^3)

L = length (m)

Therefore, for given volumetric flow rate, Q (m^3/s), through the filter, the superficial gas velocity, V (m/s), can be calculated as:

$$V = Q/A = QL/v \qquad (3.22)$$

The velocities which result for the base case volumetric flow rate of 0.14 m^3/s (300 ft^3/min) and the assumed filter volumes and lengths are shown in Table 11.

Filter Media--

The fibrous filter calculations are based on a filter packing of uniform 10-μm diameter fibers at a porosity of 99% (α = 0.01). Fibrous filter packing of this type is currently available and is considered typical with respect to filtration and pressure drop characteristics. The fibers could be stainless steel.

The granular bed filter calculations are based on a filter packing of uniform 1-mm diameter spheres at a porosity of 40% (ϵ = 0.40). Sand or ceramic granules in this size range are available and are considered typical granular filter media.

Estimated Filter Performance

Collection Efficiency--

The estimated mass removal efficiencies of the representative fibrous and granular filters over the range of filter configurations are listed in Table 11 and shown in Figure 5. The mass removal efficiencies are calculated from estimated filter fractional efficiency, i.e., efficiency as a function of particle size, and the base case particle mass size distribution. Filter efficiency was determined for four particle sizes (0.01 μm, 0.074 μm, 0.52 μm, and 6.5 μm), each of which is the midpoint of a quartile on the particle mass size distribution, i.e., each size represents 25% of the mass entering the filter. The overall mass removal efficiency listed in Table 11 is, thus, the average of the efficiencies found at each of the four quartile sizes.

In general, the fractional efficiency calculations show 99 to 100% collection of the smallest and largest quartile particle sizes, the former by diffusion as the dominant collection mechanism and the latter by inertial impaction. At the middle of the particle size distribution, characterized by particle sizes of 0.074 μm and 0.52 μm, collection efficiencies were generally less. The lowest calculated fractional efficiency was 46.1% for 0.074 μm particles in the granular filter under configuration 1.

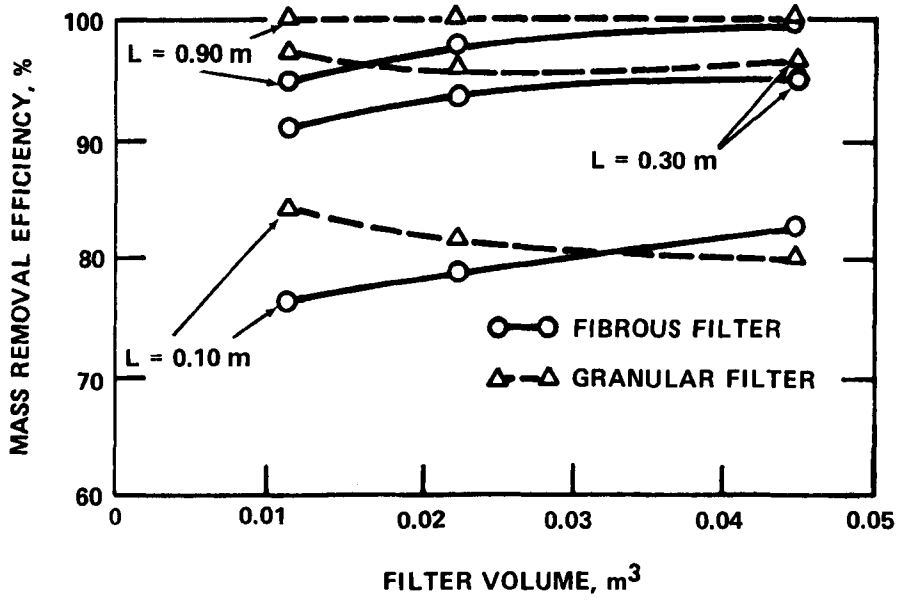

Figure 5. Filter efficiency versus volume.

Because the base-case particle mass size distribution is extrapolated from two points, it is important to note the influence of particle size on predicted efficiency. If more of the particle mass is associated with particle sizes between 0.07 to 0.5 μm than indicated by the base-case distribution, the overall mass removal efficiencies can be expected to be less than the values listed in Table 11.

By inspection of Figure 5, it appears that the typical fibrous and granular filters give similar overall clean filter efficiency at a given characteristic length. At a bed depth of 0.10 m, overall mass removal efficiencies of roughly 80 percent are predicted. Increased depth enhances particle removal, but it should be noted that these predicted efficiencies are for unloaded filters. As filter load increases, efficiency will generally increase assuming reentrainment does not become significant. It is likely that filters showing nearly perfect initial collection efficiency will quickly load and blind, providing reduced lifetime.

Pressure Drop--

Pressure drop is plotted against filter volume in Figure 6 for both granular bed filters and fiber bed filters. Assuming a maximum allowable pressure drop of 2,500 Pa (10 in. of water) for proper engine performance, the pressure drop data presented in Table 11 reveal impracticable pressure drops for all configurations with filter lengths greater than or equal to 0.30 m and associated superficial velocity greater than roughly 1.0 m/s.

The fiber bed pressure drops listed in Table 11 are optimistic, since a fiber bed will compress under flow and thus decrease in porosity. This effect probably only becomes significant at velocities greater than 1.0 m/s, however, and the pressure drops at these velocities are excessive even without considering compression.

Only configurations 4 and 7 show reasonable pressure drops for both fibrous and granular filters, and configuration 1 is possible for a fibrous filter only on the basis of pressure drop. Overall mass efficiencies for these configurations are approximately 80%. For all remaining configurations (showing initial efficiencies greater than 90%), the pressure drops are excessive.

Lifetime--

Filter lifetime is plotted against filter volume for both fiber bed filters and granular bed filters in Figure 7. The useful lifetime of a filter measured in terms of mileage between changes is impossible to predict accurately due to the uncertainties of pressure drop increase in loaded filters. However,

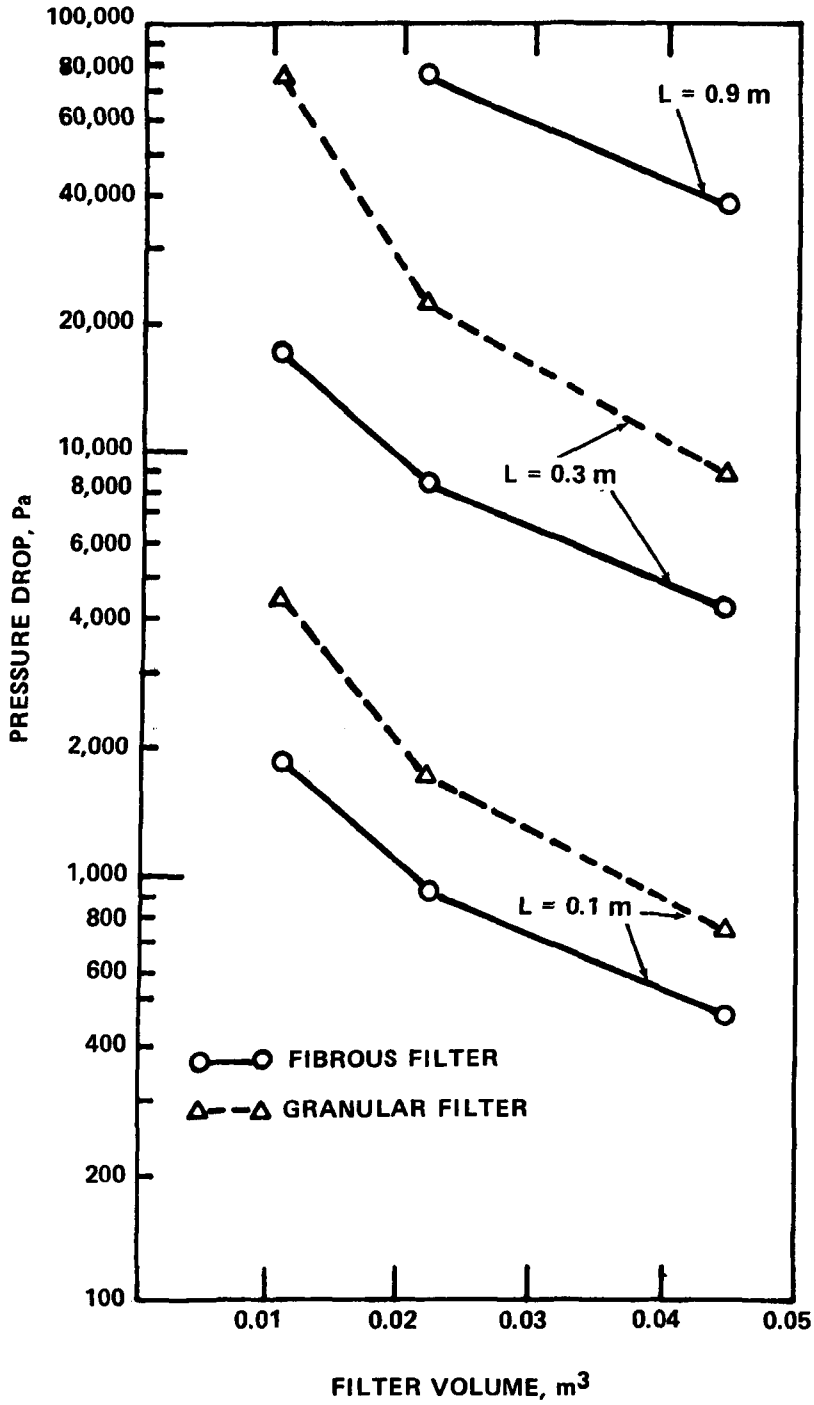

Figure 6. Pressure drop versus filter volume.

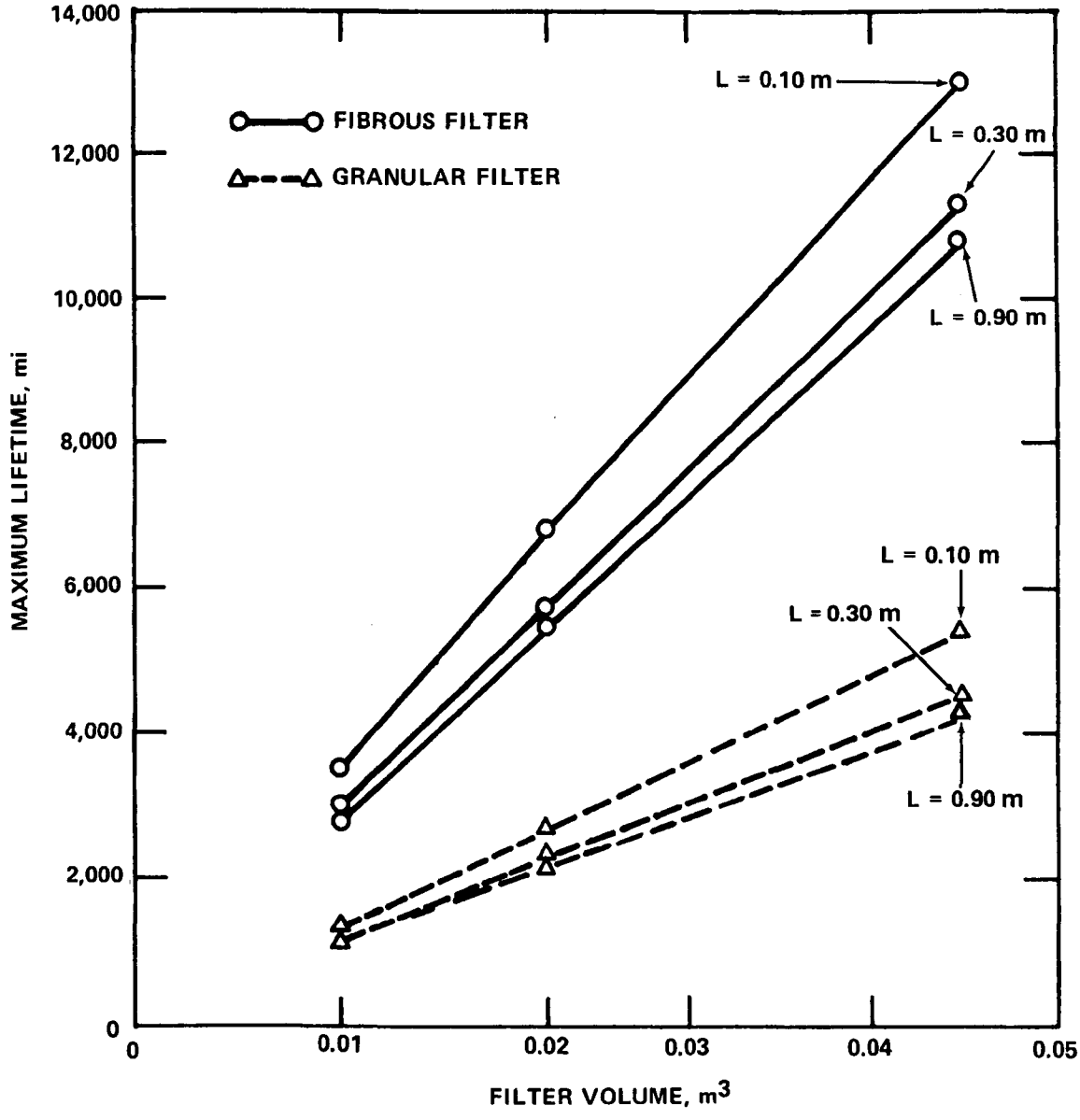

Figure 7. Maximum lifetime (mi) versus filter volume.

a simplistic approach to predict maximum possible lifetime involves estimating how long it would take to fill the void volume of a given filter with collected particles. This approach, of course, ignores the increase in pressure drop as porosity decreases; pressure drop may become unacceptably high long before bed voids are completely filled with collected particles. The lifetimes calculated using the void-filling approach are, therefore, much longer than would be expected in practice.

Using the simple model of filling void volume, maximum possible lifetime (as mileage) can be predicted by:

$$\text{lifetime (mi)} = \frac{v\epsilon\rho_B}{WE} \qquad (3.23)$$

where: v = filter volume (m^3)

ϵ = filter porosity (fraction)

W = particle mass emission rate (kg/mi)

E = overall filter efficiency

ρ_B = bulk packing density of collected dust (kg/m^3)

Using the base case emission rate of 5×10^{-4} kg/mi and bulk density of 120 kg/m^3, the maximum lifetime of each configuration can be estimated as shown in Table 11.

Assuming a maximum possible lifetime of at least 12,000 km (7,500 mi) (approximately one oil change), the granular filter is deficient in terms of storage capacity of collected dust for all configurations shown in Table 11. For fibrous filters, only configuration 7 meets the 12,000-km (7,500-mi) criterion, although configuration 4 may be acceptable if slightly different emission rates or bulk densities are used.

Summary

Granular filters can offer high efficiency and utilize cheap materials such as sand, which has good thermal and chemical resistance. However, because of inherently lower porosity, granular filters have a greater pressure drop, less dust storage capacity, and a greater weight than a fibrous filter of the same volume.

From the data presented in Table 11, the allowable pressure drop of 2,500 Pa and desired lifetime of 12,000 km (7,500 mi), only configuration 7 for a fibrous filter appears practicable; its efficiency is 82%. Configuration 7 is a large filter (0.045 m^3) oriented or baffled so as to provide a large cross-sectional area (0.45 m^2) for filtration across a depth of 0.1 m.

The major uncertainties in these calculations, beyond the accuracy of the predictive equations themselves, include the effects of 1) condensation of hydrocarbons or water, especially during cold starts, 2) reentrainment and bounce of "collected" particles which reduce overall efficiency, and 3) dust load. As discussed throughout this study, uncertainties regarding the effects of dust load make empirical verification of filter practicability necessary.

Also, the theoretical filter performance curves presented are based on the data set given in Table 12 to describe emissions from a diesel engine. Actual emissions deviate about these data as the engine is used in practice; to the extent that these aerosols are dissimilar to that described in Table 12, the analysis presented in this report is incomplete. Conclusions and recommendations based on this report must, therefore, be regarded as tentative. A prototype design based on this analysis must be considered preliminary.

PROTOTYPE FILTER FOR DIESEL EXHAUST

Description of Prototype Filter

Based on the screening of alternative configurations developed earlier in this section, a fibrous filter approximately the size of a conventional muffler or larger would provide acceptable particle removal efficiency and pressure drop for the base-case diesel emission conditions. In particular, configuration 7 would provide 82% efficiency at a pressure drop of 460 Pa (less than 2 in. of water) when new. Configuration 7, hereinafter referred to as the prototype fibrous filter, has a total volume of 0.045 m^3 with a nominal thickness, L, of 0.10 m and a cross-sectional area of 0.45 m^2 at an exhaust gas volumetric flowrate of 0.14 m^3/s (300 ft^3/min at 200°C).

This size device is considered a probable maximum size which provides large safety margins with respect to allowable pressure drop and desirable dust storage capacity. As shown in Figures 5, 6 and 7, total filter volume could be reduced to roughly 0.025 m^3 without violating the arbitrary lifetime criterion of 12,000 km (7,500 mi) while maintaining an efficiency of approximately 80%. Allowance of extra filter volume at this level of screening is appropriate considering the uncertainties concerning the effects of dust loading on filter pressure drop and lifetime.

There are many possible orientations of the fibrous filter media with respect to gas flow which maintain the required thickness and total cross-sectional area. The gas flow could be radially outward or inward with an annular filter element in a cylindrical container. A baffle arrangement could provide

the flow splitting required for a series of rectangular or oval filter panels within the filter container. The simplest design is a single rectangular filter element within a container oriented perpendicular or parallel to the exhaust pipe, the latter being shown in Figure 8.

The design shown in Figure 8 appears simple to construct. A single filter element could be inserted into the container from one end. Of course, specific applications may require other designs which are better left to automotive engineers.

Sensitivity Analysis

The equations used to calculate clean filter efficiency and pressure drop require values for superficial velocity, filter thickness, particle diameter, fiber diameter, filter porosity, and physical constants for gas stream conditions. The following sections discuss the impact on predicted filter performance of variations in these parameters. The results of the sensitivity analysis are listed in Table 13. Case 1 is the prototype design.

Filter Thickness--

Cases 2 and 3 in Table 13 show the effect of reducing the prototype filter thickness to 0.05 m and increasing it to 0.20 m, respectively, while maintaining all other parameters at the design condition. Efficiency decreases to 73% for the 0.05-m thick filter and increases to 91% for the 0.20-m thick filter. The pressure drop is directly proportional to filter thickness and, thus, doubles when the filter thickness is doubled.

Volumetric Flow Rate--

The base case specifies an exhaust gas volumetric flow rate of 0.14 m^3/s (300 ft^3/min) at 200°C. Cases 4 and 5 in Table 13 show the effect of reducing the flow rate to 0.094 m^3/s (200 ft^3/min) and increasing it to 0.212 m^3/s (450 ft^3/min), respectively. For a fixed filter geometry, the superficial gas velocity is proportional to exhaust gas flow rate. Efficiency improves slightly at the lower flow rate, but exhaust gas flow rates between 0.094 and 0.212 m^3/s appear to have little effect on the efficiency of the prototype filter. Clean filter pressure drop is proportional to the exhaust gas flow rate.

Fiber Diameter--

Cases 6 and 7 in Table 13 show the significance of fiber diameter. For the prototype filter design and exhaust gas flow rate, significant improvement in efficiency can be attained by reducing fiber diameter to 5 μm. Overall mass removal efficiency for the base-case aerosol increases to 99.7%, but the pressure drop penalty is great.

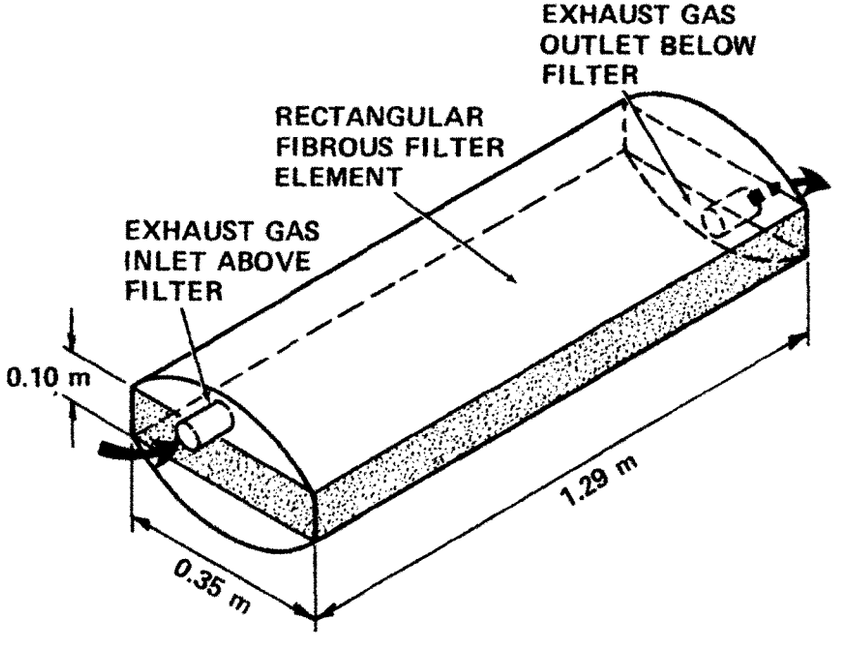

Figure 8. Prototype fibrous filter.

TABLE 13. PROTOTYPE FILTER SENSITIVITY ANALYSIS

Case	Q_g (m^3/s)	V (m/s)	L (m)	d_p (μm)	d_F (μm)	ε	Eff. (%)	ΔP (Pa)
1	0.142	0.315	0.10	*	10	0.99	92.2	464
2	0.142		0.05				73.4	232
3	0.142		0.20				91.1	927
4	0.094	0.210	0.10				84.5	309
5	0.212	0.472					80.0	695
6	0.142	0.315			5		99.7	1,850
7	0.142				20		63.1	116
8	0.142				10	0.98	93.5	1,310
9	0.142					0.995	69.1	164
10	0.142			0.01		0.99	100.0	464
11				0.02			99.9	
12				0.04			97.7	
13				0.074			82.2	
14				0.10			69.7	
15				0.20			43.8	
16				0.30			37.2	
17				0.40			38.9	
18				0.52			46.7	
19				0.80			74.5	
20				1.00			90.7	
21				1.50			99.9	
22				2.0			100.0	
23				6.5			100.0	

Q_g = exhaust gas flow rate; V = superficial velcoity; L = filter thickness..

d_p = particle diameter; d_F = fiber diameter; ε = porosity; Eff. = overall mass removal efficiency; ΔP = pressure drop.

* Base-case particle size distribution represented by four quartile diameters.

Increasing the fiber diameter to 20 μm reduces overall efficiency to 63%, but pressure drop is very low at approximately 120 Pa. The larger fiber diameter, particularly if it is stainless steel, will generally cost less per unit filter volume, and the low pressure drop may be desirable. Therefore, use of a fiber diameter greater than 10 μm may be advantageous, particularly if efficiency is found to increase with dust load.

Porosity--

A porosity of 0.99 for the prototype filter was selected as a typical value. However, porosity of fibrous filter material generally ranges between 0.98 and 0.995. Cases 8 and 9 show the effect on filter performance for this range of porosity. Efficiency and pressure drop are significantly affected by changes in porosity, and porosity is, therefore, a key design parameter.

Particle Size--

Cases 10 through 23 and Figure 9 show the variation in efficiency of the prototype filter as a function of particle size entering the filter. Figure 9 is the calculated fractional efficiency curve for the prototype fibrous filter operating at base-case conditions. The variation reflects the effect of particle size on the fundamental collection mechanisms. Diffusion appears to dominate below 0.05 μm, and impaction appears to dominate above 1.0 μm. A minimum efficiency occurs near 0.3 μm where all mechanisms are inadequate.

From the fractional efficiency curve, the overall mass efficiency of the prototype filter can be calculated for any inlet particle size distribution. The use of only four quartile particle sizes from the base-case particle size distribution can be seen to be a crude estimate of overall mass efficiency. If the actual diesel exhaust particle size distribution is less polydisperse than the base case but the mmd is still about 0.2 μm, overall mass efficiency of the prototype filter will be significantly less than predicted.

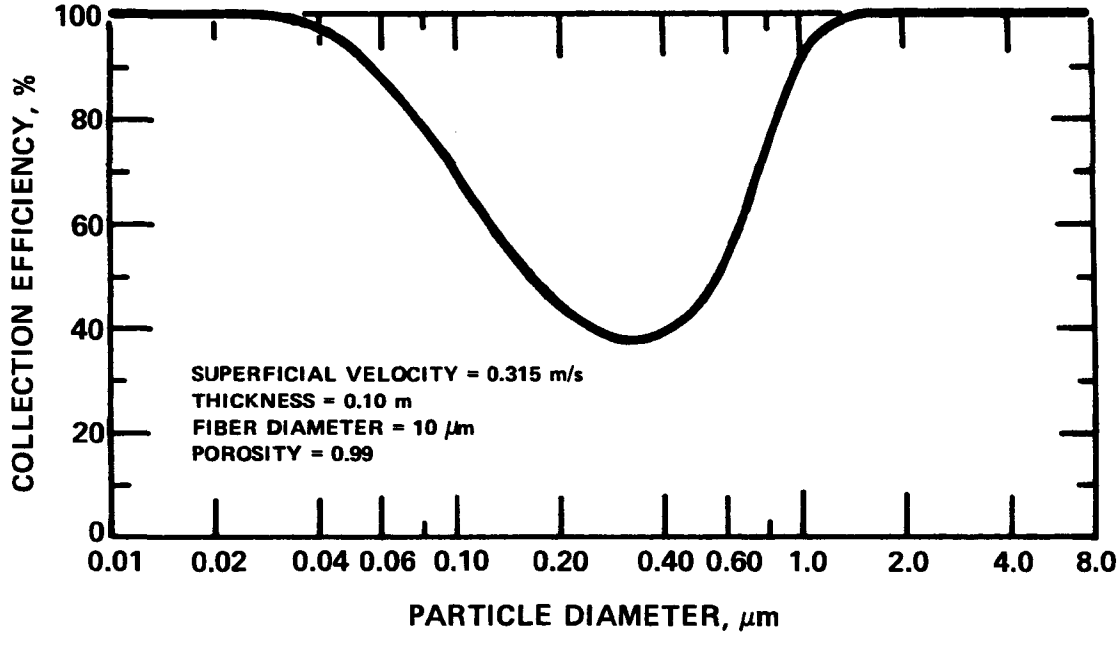

Figure 9. Fibrous filter efficiency versus particle diameter.

SECTION 4

ELECTROSTATIC DEVICES

FUNDAMENTAL STEPS IN THE ELECTROSTATIC PRECIPITATION PROCESS

Creation of an Electric Field and Corona Current

The first step in the precipitation process is the creation of an electric field and corona current. This is accomplished by applying a large potential difference between a small-radius electrode and a much larger radius electrode, where the two electrodes are separated by a region of space containing an insulating gas. For industrial applications, a large negative potential is applied at the small-radius electrode and the large-radius electrode is grounded.

At any applied voltage, an electric field exists in the interelectrode space. For applied voltages less than a value referred to as the "corona starting voltage", a purely electrostatic field is present. At applied voltages above the corona starting voltage, the electric field in the vicinity of the small-radius electrode is large enough to produce ionization by electron impact. Between collisions with neutral molecules, free electrons are accelerated to high velocities and, upon collision with a neutral molecule, their energies are sufficiencly high to cause an electron to be separated from a neutral molecule. Then, as the increased number of electrons moves out from the vicinity of the small-radius electrode, further collisions between electrons and neutral molecules occur. In a limited high electric field region near the small-radius electrode, each collision between an electron and a neutral molecule has a certain probability of forming a positive molecular ion and another electron, and an electron avalanche is established. The positive ions migrate to the small-radius electrode and the electrons migrate into the lower electric field regions toward the large-radius electrode. These electrons quickly lose much of their energy and, when one of them collides with a neutral electronegative molecule, there is a probability that attachment will occur and a negative ion will be formed. Thus, negative ions, along with any electrons which do not attach to a neutral molecule, migrate under the influence of the electric field to the large-radius electrode and provide the current necessary for the precipitation process.

Figure 10 is a schematic diagram showing the region very near the small-radius electrode where the current-carrying negative ions are formed. As these negative ions migrate to the large-radius electrode, they constitute a steady-state charge distribution in the interelectrode space which is referred to as an "ionic space charge." This "ionic space charge" establishes an electric field which adds to the electrostatic field to give the total electric field. As the applied voltage is increased, more ionizing sequences result and the "ionic space charge" increases. This leads to a higher average electric field and current density in the interelectrode space.

Figure 11 gives a qualitative representation of the electric field distribution and equipotential surfaces in a wire-plate geometry, which is most commonly used. Although the electric field is very nonuniform near the wire, it becomes essentially uniform near the collection plates. The current density is very nonuniform throughout the interelectrode space and is maximum along a line from the wire to the plate.

In order to maximize the collection efficiency obtainable from the electrostatic precipitation process, the highest possible values of applied voltage and current density should be employed. In practice, the highest useful values of applied voltage and current density are limited by either electrical breakdown of the gas throughout the interelectrode space or of the gas in the collected particulate layer. High values of applied voltage and current density are desirable because of their beneficial effect on particle charging and particle transport to the collection electrode. In general, the voltage-current characteristics of a precipitator depend on the geometry of the electrodes, the gas composition, temperature and pressure, the particulate mass loading and size distribution, and the resistivity of the collected particulate layer. Thus, maximum values of voltage and current can vary widely from one precipitator to another and from one application to another.

Particle Charging

Once an electric field and current density are established, particle charging can take place. Particle charging is essential to the precipitation process because the electrical force which causes a particle to migrate toward the collection electrode is directly proportional to the charge on the particle. The most significant factors influencing particle charging are particle diameter, applied electric field, current density, and exposure time.

The particle charging process can be attributed mainly to two physical mechanisms, field charging and thermal charging.[35,36,3] These two mechanisms are discussed below.

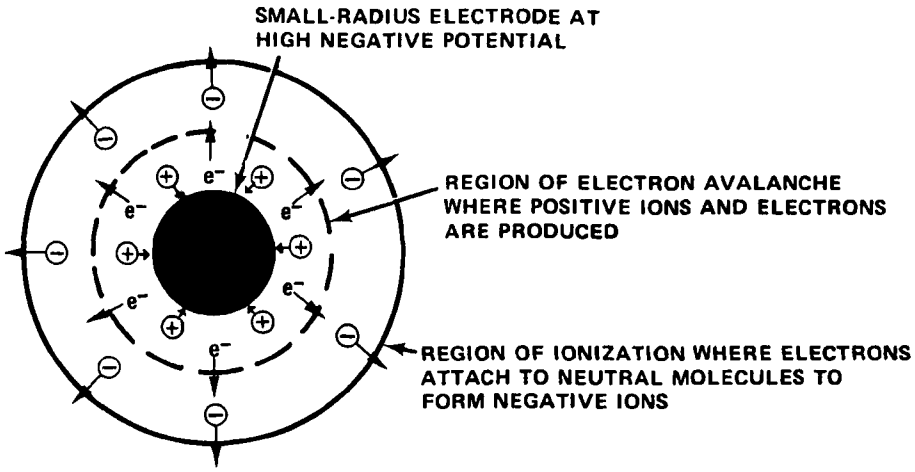

Figure 10. Region near small-radius electrode.

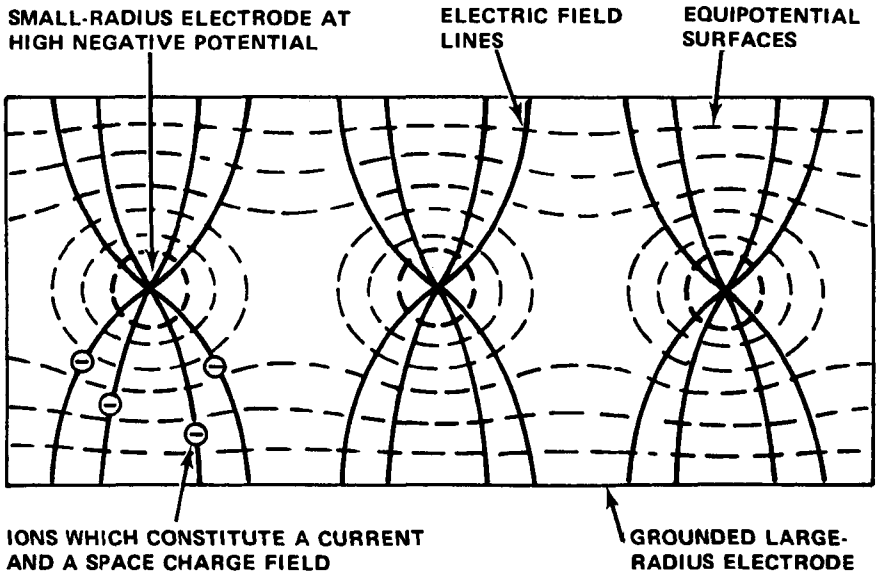

Figure 11. Electric field configuration for wire-plate geometry.

(1) At any instant in time and location in space near a particle, the total electric field is the sum of the electric field due to the charge on the particle and the applied electric field. In the field charging mechanism, molecular ions are visualized as drifting along electric field lines. Those ions moving toward the particle along electric field lines which intersect the particle surface impinge upon the particle surface and place charge on the particle.

Figure 12 depicts the field charging mechanism during the time it is effective in charging a particle. In this mechanism, only a limited portion of the particle surface (0 to $\theta<\pi/2$) can suffer an impact with an ion, and collisions of ions with other portions of the particle surface are neglected. Field charging takes place very rapidly and terminates when sufficient charge (the saturation charge) is accumulated to repel additional ions. Figure 13 depicts the electric field configuration once the particle has attained the saturation charge. In this case, the electric field lines circumvent the particle, and the ions move along them around the particle.

Theories based on the mechanism of field charging agree reasonably well with experiments whenever particle diameters exceed about 0.5 μm and the applied electric field is moderate to high. In these theories, the amount of charge accumulated by a particle depends on the particle diameter, applied electric field, ion density, exposure time, ion mobility, and dielectric constant of the particle.

(2) The thermal charging mechanism depends on collisions between particles and ions which have random motion due to their thermal kinetic energy. In this mechanism, the particle charging rate is determined by the probability of collisions between a particle and ions. If a supply of ions is available, particle charging occurs even in the absence of an applied electric field. Although the charging rate becomes negligible after a long period of time, it never has a zero value as is the case with the field charging mechanism. Charging by this mechanism takes place over the entire surface of the particle and requires a relatively long time to produce a limiting value of charge.

Figure 14 depicts the thermal charging process in the absence of an applied electric field. In this case, the ion distribution is uniform around the surface of the particle, and each element of surface area has an equal probability of experiencing an ion collision. Thermal charging theories that neglect the effect of the applied electric field adequately describe the charging rate over a fairly broad range of particle sizes where the applied electric field is low or equal to zero. In addition, they work well for particles smaller than 0.2 μm in diameter regardless of the magnitude of the applied electric field.

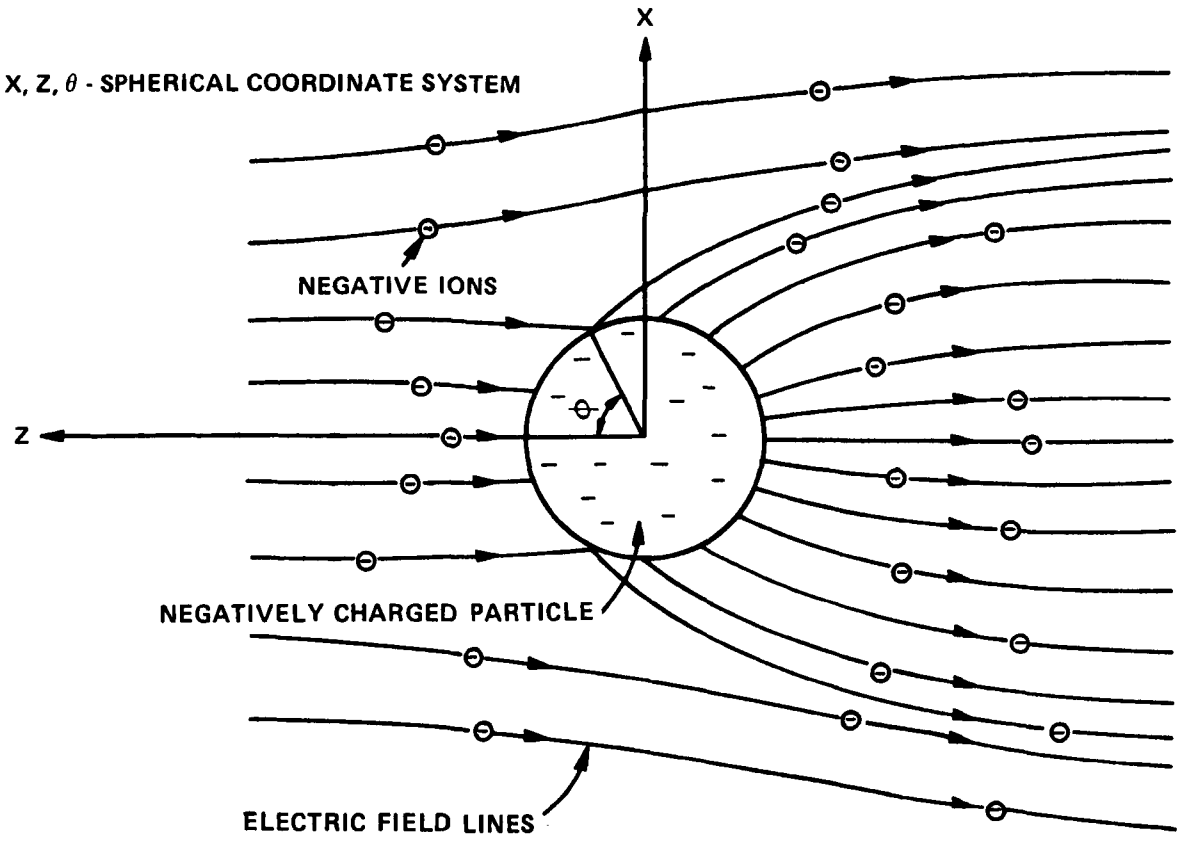

Figure 12. Electric field configuration during field charging.

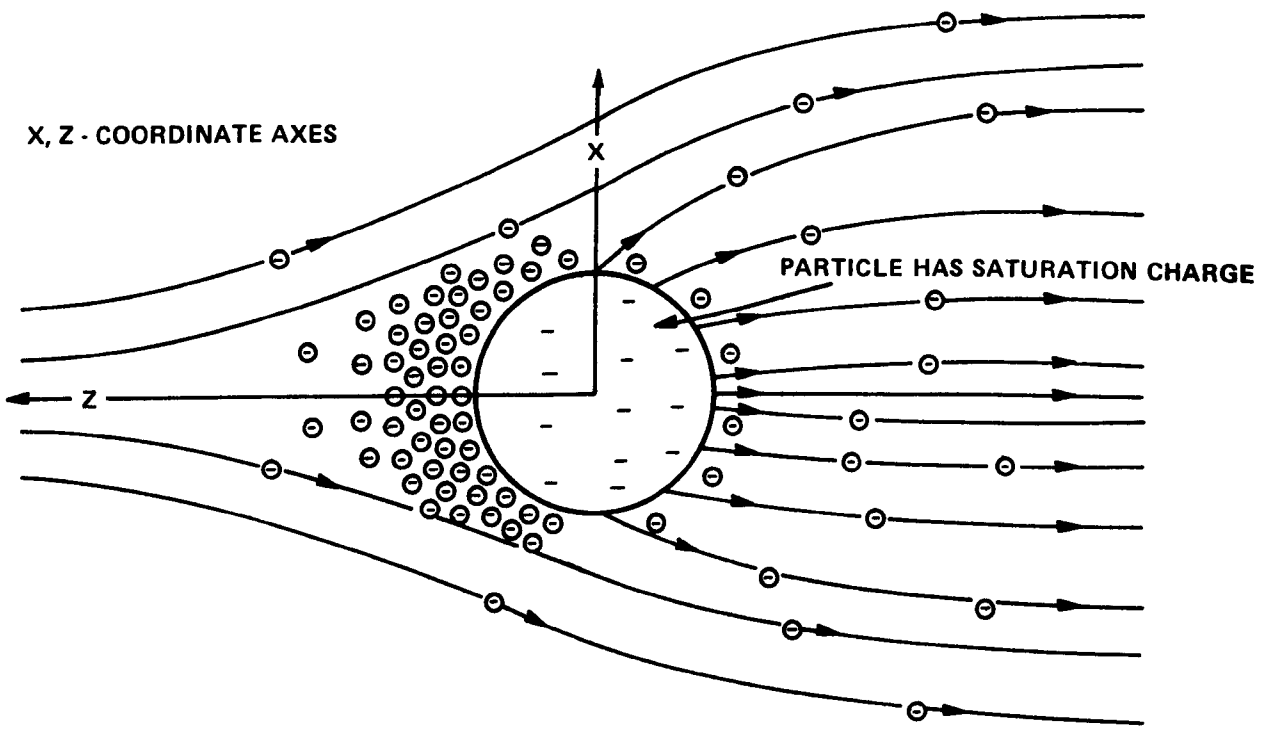

Figure 13. Electric field configuration and ion distribution for particle charging in an applied field after saturation charge is reached.

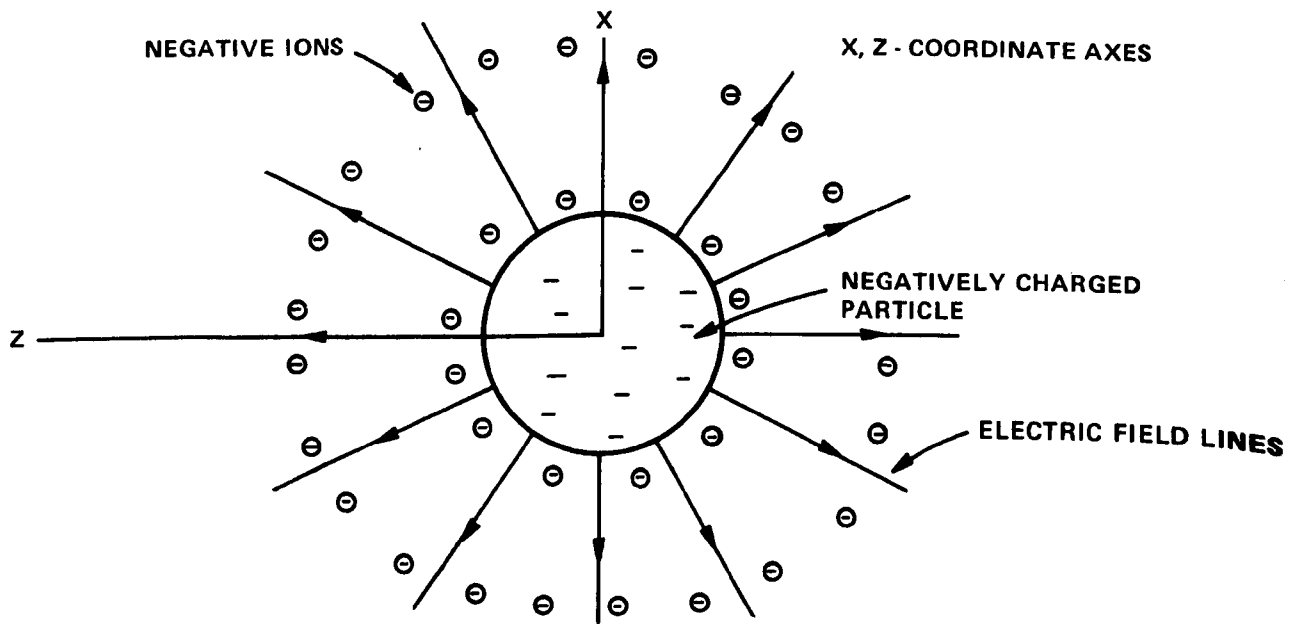

Figure 14. Electric field configuration and ion distribution for particle charging with no applied field.

Figure 13 depicts the thermal charging process in the presence of an applied electric field after the particle has attained the saturation charge determined from field charging theory. The effect of the applied electric field is to cause a large increase in ion concentration on one side of the particle while causing only a relatively small decrease on the other side. Although the ion concentration near the surface of the particle becomes very nonuniform, the net effect is to increase the average ion concentration, the probability of collisions between ions and the particle, and the particle charging rate.

In thermal charging theories, the amount of charge accumulated by a particle depends on the particle diameter, ion density, mean thermal velocity of the ions, absolute temperature of the gas, particle dielectric constant, residence time, and the applied electric field. The effect of the applied electric field on the thermal charging process must be taken into account for fine particles having diameters between 0.1 and 2.0 μm. Depending most importantly on the applied electric field and to a lesser extent on certain other variables, particles in this size range can acquire values of charge which are two to three times larger than that predicted from either the field or the thermal charging theories. For these particles, neither field nor thermal charging predominates and both mechanisms must be taken into account simultaneously.

In most cases, particle charging has a noticeable effect on the electrical conditions in a precipitator. The introduction of a significant number of fine particles or a heavy concentration of large particles into an electrostatic precipitator significantly influences the voltage-current characteristics. Qualitatively, the effect is seen by an increased voltage for a given current compared to the particle-free situation. As the particles acquire charge, they must carry part of the current, but they are much less mobile than the ions. This results in a lower "effective mobility" for the charge carriers and, in order to obtain a given particle-free current, higher voltages must be applied to increase the drift velocities of the charge carriers and the ion densities.

The charged particles, which move very slowly, establish a "particulate space charge" in the interelectrode space. The distribution of the "particulate space charge" results in an electric field distribution which adds to those due to the electrostatic field and the ionic field to give the total electric field distribution. It is desirable to determine the space charge resulting from particles because of its influence on the electric field distribution, especially near the collection plate, where, for the same current, the electric field is raised above the particle-free situation. In addition, the "particulate space charge" is a function of position along the length of the precipitator since particle charging and collection are a function of length.

Particle Collection

As the particle-laden gas moves through a precipitator, each charged particle has a component of velocity directed towards the collection electrode. This component of velocity is called the electrical drift velocity, or migration velocity, and results from the electrical and viscous drag forces acting upon a suspended charged particle. For the particle sizes of practical interest, the time required for a particle to achieve a steady-state value of migration velocity is negligible and, near the collection electrode, the magnitude of this quantity is given by[38]

$$w_p = \frac{qE_pC_c}{6\pi a\mu} \tag{4.1}$$

where w_p = migration velocity near the collection electrode of a particle of radius a (m/s),

q = charge on particle (coul),

E_p = electric field near the collection electrode (volt/m),

a = particle radius (m),

μ = gas viscosity (Pa-s),

C_c = Cunningham correction factor, or slip correction factor[39] = $(1 + A\lambda/a)$,

where $A = 1.257 + 0.400 \exp(-1.10\ a/\lambda)$, and

λ = mean free path of gas molecules (m).

In industrial precipitators, laminar flow never occurs and the effect of turbulent gas flow must be considered. The turbulence is due to the complex motion of the gas itself, electric wind effects of the corona, and transfer of momentum to the gas by the movement of the particles. Average gas flow velocities in most cases of practical interest are between 0.6 and 2.0 m/s. Due to eddy formation, electric wind, and other possible effects, the instantaneous velocity of a small volume of gas surrounding a particle may reach peak values which are much higher than the average gas velocity. In contrast, migration velocities for particles smaller than 0.6 μm in diameter are usually less than 0.3 m/s. Therefore, the motion of these smaller particles tends to be dominated by the turbulent motion of the gas stream. Under these conditions, the paths taken by the particles are random and the determination of the collection efficiency of a given

particle becomes, in effect, the problem of determining the probability that a particle will enter a laminar boundary zone adjacent to the collection electrode in which capture is assured.

Using probability concepts and the statistical nature of the large number of particles in a precipitator, White[40] derived an expression for the collection efficiency in the form

$$\eta = 1 - \exp\left(-A_p w_p / Q\right) \quad , \tag{4.2}$$

where η = collection fraction for a monodisperse aerosol,

A_p = collection area (m^2)

w_p = migration velocity near the collection electrode of the particles in the monodisperse aerosol (m/s), and

Q = gas volume flow rate (m^3/s).

The simplifying assumptions on which the derivation of equation 4.2 is based are:

(1) The gas is flowing in a turbulent pattern at a constant, mean forward-velocity.

(2) Turbulence is small scale (eddies are small compared to the dimensions of the duct), fully developed, and completely random.

(3) The particle migration velocity near the collecting surface is constant for all particles and is small compared with the average gas velocity.

(4) There is an absence of disturbing effects, such as particle reentrainment, back corona, particle agglomeration, or uneven corona.

Experimental data[41] under conditions which are consistent with the above assumptions demonstrate that equation 4.2 adequately describes the collection of monodisperse aerosols in an electrostatic precipitator under certain idealized conditions.

In industrial precipitators, the above assumptions are never completely satisfied but they can be approached closely. With proper design, the ratio of the standard deviation of the gas velocity distribution to the average gas velocity can be made to be 0.25 or less so that an essentially uniform, mean forward-velocity would exist. Although turbulence is not generally a completely random process, a theoretical determination of the

degree of correlation between successive states of flow and between adjacent regions of the flow pattern is a difficult problem and simple descriptive equations do not presently exist for typical precipitator geometries. At the present, for purposes of modeling, it appears practical and plausible to assume that the turbulence is highly random. For particles larger than 10 μm in diameter, the turbulence does not dominate the motion of these particles due to their relatively high migration velocities. Under these conditions, equation 4.2 would be expected to underpredict collection efficiencies. The practical effect in modeling precipitator performance will be slight, however, since even equation 4.2 predicts collection efficiencies greater than 99.6% for 10-μm diameter particles at relatively low values of current density and collection area [i.e., a current density of 1×10^{-4} A/m^2 and a collection area to volume flow ratio of 39.4 $m^2/(m^3/s)$].

Removal of Collected Material

In dry collection, the removal of the precipitated material from the collection plates and subsequent conveyance of the material away from the precipitator represent fundamental steps in the collection process. These steps are fundamental because collected material must be removed from the precipitator and because the buildup of excessively thick layers on the plates must be prevented in order to ensure optimum electrical operating conditions. Material which has been precipitated on the collection plates is usually dislodged by mechanical jarring or vibration of the plates, a process called rapping. The dislodged material falls under the influence of gravity into hoppers located below the plates and is subsequently removed from the precipitator.

The effect of rapping on the collection process is determined primarily by the intensity and frequency of the force applied to the plates. Ideally, the rapping intensity must be large enough to remove a significant fraction of the collected material but not so large as to propel material back into the main gas stream. The rapping frequency must be adjusted so that a larger thickness which is easy to remove and does not significantly degrade the electrical conditions is reached between raps. In practice, the optimum rapping intensity and frequency must be determined by experimentation. With perfect rapping, the sheet of collected material would not reentrain, but would migrate down the collection plate in a stick-slip mode, sticking by the electrical holding forces and slipping when released by the rapping forces.

LIMITING FACTORS AFFECTING PRECIPITATOR PERFORMANCE

Allowable Voltage and Current Density

The performance of a precipitator which has good mechanical and structural features will be determined primarily by the electrical operating conditions. Any limitations on applied

voltage and current density will be reflected in the optimum collection efficiency which can be obtained. A precipitator should be operated at the highest useful values of applied voltage and current density for the following reasons:

(1) high applied voltages produce high electric fields;

(2) high electric fields produce high values of the saturation and limiting charge that a particle may obtain;

(3) high current densities produce high rates at which particles charge to the saturation or limiting values of charge;

(4) high current densities produce an increased electric field near the collection electrode due to the "ionic space charge" contribution to the field; and

(5) high values of electric field and particle charge produce high migration velocities and increased transport of particles to the collection electrode.

Electrical conditions in a precipitator are limited by either electrical breakdown of the gas in the interelectrode space or by electrical breakdown of the gas in the collected particulate layer. In a clean-gas, clean-plate environment, gas breakdown can originate at the collection electrode due to surface irregularities and edge effects which result in localized regions of high electric field. If the electric field in the interelectrode space is high enough, the gas breakdown will be evidenced by a spark that propagates across the interelectrode space. The operating applied voltage and current density will be limited by these sparking conditions.

If a particulate layer is deposited on the collection electrode, then the corona current must pass through the particulate layer to the grounded, collection electrode. The voltage drop across the particulate layer is

$$V_p = j\rho t, \tag{4.3}$$

where V_p = voltage drop (volt),

j = current density (A/m^2),

ρ = resistivity of particulate layer (ohm-m), and

t = thickness of the layer (m).

The average electric field in the particulate layer, E_p(volt/m), is given by

$$E_p = j\rho. \tag{4.4}$$

The average electric field in the particulate layer can be increased to the point that the gas in the interstitial space breaks down electrically. This breakdown results from the acceleration of free electrons to ionization velocity to produce an avalanche condition similar to that at the corona electrode. When this breakdown occurs, one of two possible situations will ensue. If the electrical resistivity of the particulate layer is moderate ($\sim$0.1-1.0 x 10^9 ohm-m), then the applied voltage may be sufficiently high so that a spark will propagate across the interelectrode space. The rate of sparking for a given precipitator geometry will determine the operating electrical conditions in such a circumstance. If the electrical resistivity of the particulate layer is high (>1 x 10^9 ohm-m), then the applied voltage may not be high enough to cause a spark to propagate across the interelectrode space. In this case, the particulate layer will be continuously broken down electrically and will discharge positive ions into the interelectrode space. This condition is called back corona. The effect of these positive ions is to reduce the amount of negative charge on a particle due to bipolar charging and reduce the electric field associated with the "ionic space charge". Both the magnitude of particle charge and rate of particle charging are affected by back corona. Useful precipitator current is therefore limited to values which occur prior to electrical breakdown whether the breakdown occurs as sparkover or back corona.

Field experience shows that current densities for precipitators operating at about 150°C are limited to approximately 5 to 7 x 10^{-4} A/m^2 due to electrical breakdown of the gases in the interelectrode space. Consequently, this constitutes a current limit under conditions where breakdown of the particulate layer does not occur.

Electrical breakdown of the particulate layer has been studied extensively by Penney and Craig[42] and Pottinger[43] and can be influenced by many factors. Experimental measurements show that particulate layers experience electrical breakdown at average electric field strengths across the layers of approximately 5 x 10^5 V/m. Since it takes an electric field strength of approximately 3 x 10^5 V/m to cause electrical breakdown of air, this suggests that high localized fields exist in the particulate layer and produce the breakdown of the gas in the layer. The presence of dielectric or conducting particles can cause localized regions of high electric field which constitute a negligible contribution to the average electric field across

the layer. The size distribution of the collected particles also influences the electrical breakdown strength by changing the volume of interstices. It has also been found that breakdown strength varies with particulate resistivity with the higher breakdown strength being associated with the higher resistivity.

Particle Reentrainment

Particle reentrainment occurs when collected material reenters the main gas stream. This can be caused by several different effects and, in certain cases, can severely reduce the collection efficiency of a precipitator. Causes of particle reentrainment include (1) rapping which propels collected material into the interelectrode space, (2) action of the flowing gas stream on the collected particulate layer, (3) sweepage of material from hoppers due to poor gas flow conditions, air inleakage into the hoppers, or the boiling effect of rapped material falling into the hoppers, and (4) excessive sparking which dislodges collected material by electrical impulses and disruptions in the current which is necessary to provide the electrical force which holds the material to the collection plates.

Recent studies[44,45] have been made to determine the effect of particle reentrainment on precipitator performance. In studies where the rappers were not employed, real-time measurements of outlet emissions at some installations showed that significant reentrainment of mass was occurring due to factors other than rapping. These studies also showed that for high-efficiency, full-scale precipitators approximately 30 to 85% of the outlet particulate emissions could be attributed to rapping reentrainment. The results of these studies show that particle reentrainment is a significant factor in limiting precipitator performance.

PREVIOUS USES OF ELECTROSTATIC DEVICES FOR DIESEL EXHAUST

Only two reports of the use of electrostatic devices on diesel particulate have been located. One of these was a study performed by Battelle Columbus Laboratories for General Motors, in which an electric field was used to concentrate the particulate into a portion of the exhaust.[9] This work resulted in the device shown in Figure 15. The device concentrated 50% of the particulate into 16% of the exhaust gas. According to General Motors, the insulators quickly became coated with particulate, resulting in erratic operation and several failures.

In the other instance, Southwest Research Institute reported testing an electrostatic precipitator built by Gordine Systems, Inc.[46] Although this device was designed to operate in the 1.2 to 1.6 x 10^4-V region, continuous discharge was observed at 1.0 x 10^4 V, which was taken as the maximum operating voltage. After 11 min of exposure to diesel exhaust, the device showed

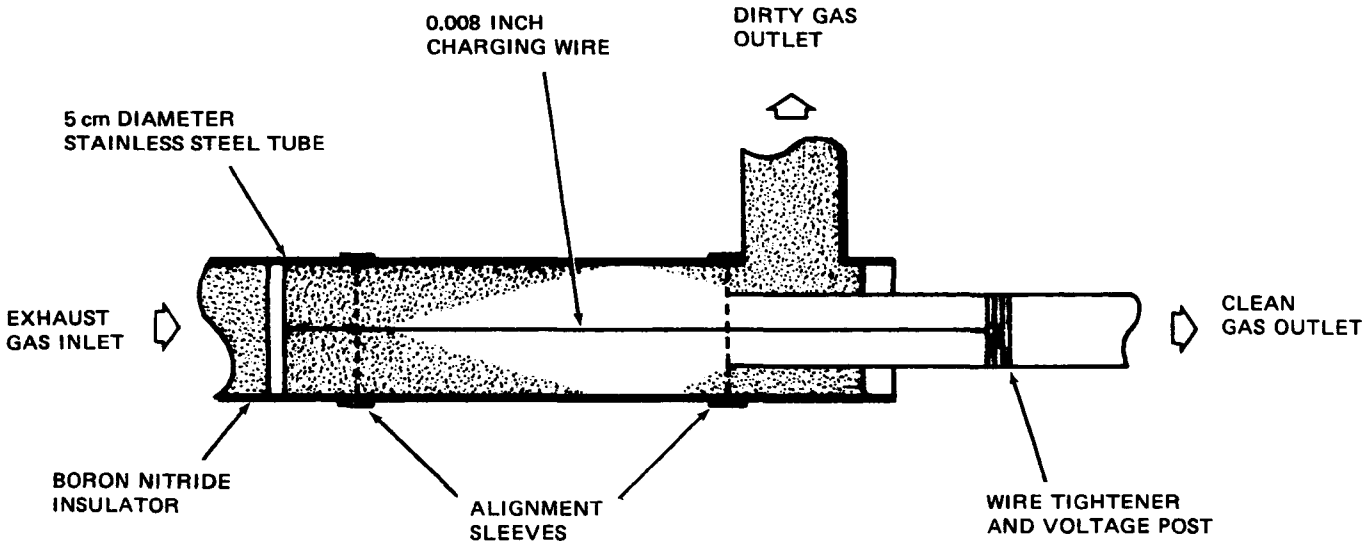

Figure 15. Electrostatic particulate remover.[9]

a dramatic increase in ionizer current indicating current leakage through conduction paths of particulate. Measurements of the collection efficiency were limited to smokemeter measurements, which indicated that the device had no effect at all on the exhaust.

APPLICATION OF ELECTROSTATIC FUNDAMENTALS TO DIESEL EXHAUST

Introduction

The chief advantage in the use of an electrostatic device to control diesel particulate lies in the high efficiency which can be achieved at low backpressure. However, there are several problem areas associated with this type of device. One of these problems is reentrainment. Because the particles are primarily carbon, they are expected to have a relatively low resistivity. This implies that they would loose their charge readily when attached to a conductive surface such as the collection plates of a precipitator. Without electrostatic attraction between the collected particles and the collection plates, the particles have to depend on their stickiness due to adsorbed hydrocarbons for adhesion to the collection surface. This may prove inadequate when subjected to a high velocity gas flow which pulsates with the opening and closing of the exhaust valves and to the mechanical vibration that occurs on a moving vehicle.

The water content of the gas presents another problem area due to the fact that, at starting, the collection device will pass through a temperature range which includes the dew point temperature. The presence of condensed water films in conjunction with a conductive particulate may cause conductive paths to accumulate on the insulator surfaces, which will in time short out the device. After the device has reached operating temperature, all of the water will be in the vapor form and no further accumulation should take place. Several possibilities exist for dealing with the problem:

(1) Only electrically activate the device after it has reached operating temperature. This would leave only the mechanical collection forces active during the starting cycle. This solution does not appear very attractive because the emissions are particularly bad during start up.

(2) Bypass the device altogether during starting by diverting the exhaust through a regular muffler until the control device has exceeded the dew point temperature. This has the same drawback as solution 1.

(3) Use internal heating elements within the critical insulators to keep the insulators above the dew point. This would present problems due to the fact that the

temperature would have to be above the dew point prior to starting.

(4) Use insulators that are hydrophobic so that there would be minimum chance of the water film forming on the surface. This seems somewhat impractical due to the fact that there is bound to be surface contamination from the conductive particles alone.

(5) Design the insulators with sufficient surface path length and dead air zones to minimize the effect of tracking. This solution will not eliminate the problem, but it may lengthen the time period sufficiently so that the insulators may be cleaned during regular device maintenance.

Efficiency of an Electrostatic Precipitator

For a calculation of the size and efficiency of an electrostatic precipitator for collecting diesel exhaust particulate, it is necessary to make several assumptions. First, assume a two stage geometry in which the particle charging process preceeds and is separate from the particle collection process. After particles are charged to saturation, we can find the numbers of charges on each particle by making some approximations. If we assume a 0.20-m cylinder with a 0.25-cm wire, then from an example in White[47] we can achieve a charging field E_c of 1.0×10^6 V/m with a current density $j = 2.0 \times 10^{-2}$ A/m^2. Assuming a 200°C operating temperature, we have a value for the ion mobility b of 3.1×10^{-4} m^2/V-s. Then using the expression for the ion density

$$N_o = \frac{j}{beE_c} \qquad (4/5)$$

we obtain $N_o = 4.0 \times 10^{14}$ ions/m^3.

If we assume a 0.14-m/s flow rate through the 0.20-m pipe, we get a gas velocity of 4.32 m/s. If the charging is done by a 0.15-m long rod, we find that the particles are in the charging region for a time t = 0.035 s. Smith and McDonald[48] have plotted the number of charges on a particle as a function of $N_o t$, E_c, and particle size. From this, we can estimate a value of 40 electron charges for a 0.30-μm particle.

We can now calculate the ion drift velocity as given by equation 4.1:

$$w_p = \frac{qE_p C_c}{6\pi a\mu} \qquad (4.1)$$

For this example assume the following values:

q = 40 electron charges

$E_p = 1 \times 10^6$ V/m

$C_c = 1.7$

$a = 0.15 \times 10^{-6}$ m (1/2 of particle mmd)

$\mu = 2.5 \times 10^{-5}$ Pa-s

to obtain a drift velocity of $w_p = 0.15$ m/s. We can now solve equation 4.2 for the collection efficiency in terms of the collection area. Table 14 shows the plate area required for a given collection efficiency.

TABLE 14. REQUIRED COLLECTION AREA FOR A DESIRED COLLECTION EFFICIENCY FOR AN ELECTROSTATIC PRECIPITATOR

Efficiency, η	Area, A_p (m^2)
0.5	0.66
0.6	0.87
0.7	1.14
0.8	1.52
0.9	2.18
0.95	2.84

DESCRIPTION OF PROTOTYPE ELECTROSTATIC DEVICES

An electrostatic precipitator has been proposed to control diesel particulate. This device features a periodic wet flushing scheme to thoroughly clean the collected particulate from all internal surfaces of the system.

A vertically oriented, cylindrical geometry appears best suited to such a cleaning method and optimum from the standpoint of structural strength. A conceptual sketch indicating the basic features of such a system is shown in Figure 16. A two-stage device was selected to provide a maximum collecting surface within the space limitations of a vehicular installation. The exhaust gas from the engine enters the precipitator tangentially

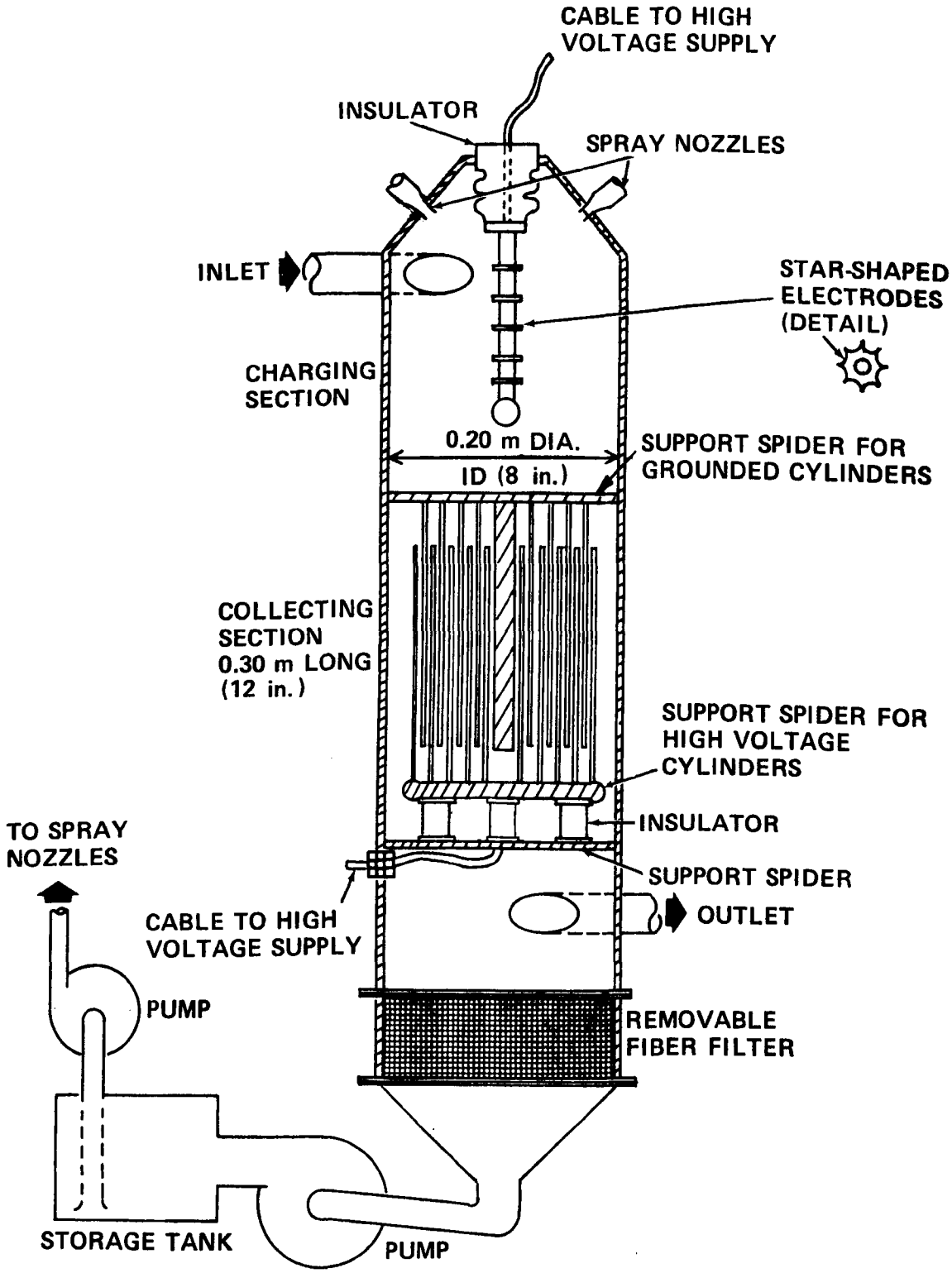

Figure 16. First prototype electrostatic precipitator for collecting diesel particulate.

so as to avoid immediate impaction on the high voltage insulators. The cyclonic motion of the gas in the first stage (upper half) of the precipitator has little effect on particulate collection by impaction because most of the particles are very fine; however, the circular path allows for adequate charging time for the particles before they enter the collecting stage.

Particle charging is achieved by means of an electrical corona discharge from flat, star-shaped electrodes mounted on the axial rod extending downward from the insulator at the top of the device. A corona ball on the end of the rod suppresses discharges to the grounded plates in the collecting stage. This structure is preferred over a more conventional fine-wire corona discharge electrode because of its ruggedness.

The collecting stage consists of a set of concentric cylinders. In sequence of decreasing diameter, the odd-numbered cylinders are connected to electrical ground and the even-numbered cylinders are connected to the output of a high voltage power supply. The high voltage cylinders are connected together by a metal bus bar and nested between the grounded insulators. Insulating spacers between cylinders are avoided in order to minimize leakage current due to fouling by low resistivity material. Three stand-off insulators are used to support the entire array of high voltage cylinders.

The precipitator is to be cleaned periodically by spraying a nonvolatile liquid through the nozzles at the top of the device. The liquid is pulled through a fiber filter at the bottom of the precipitator and then pumped into a storage tank for the next cleaning cycle. The period between flushing operations would probably be governed by the length of time required for the particulate buildup on the insulators to develop a significant currant leakage path between high voltage components and ground. Provisions would be required to bypass the precipitator during the cleaning operation, which might take 30 to 60 s.

The 0.20-m diameter and 0.15-m long charging region of this device allow an estimation of collection efficiency using the numbers obtained earlier in this section. From the detailed drawings, the plate area can be calculated to be 1.46 m^2. According to Table 14, 1.52 m^2 is required for the 80% efficiency, which leads to an estimated 79% efficiency for this device. In practice, the efficiency should be somewhat higher due to the star-shaped electrodes on the charging rod.

A second electrostatic device which has been proposed for diesel exhaust is a radial flow device which uses dielectric filter material in the collection region. This device, shown in Figure 17, has the following features:

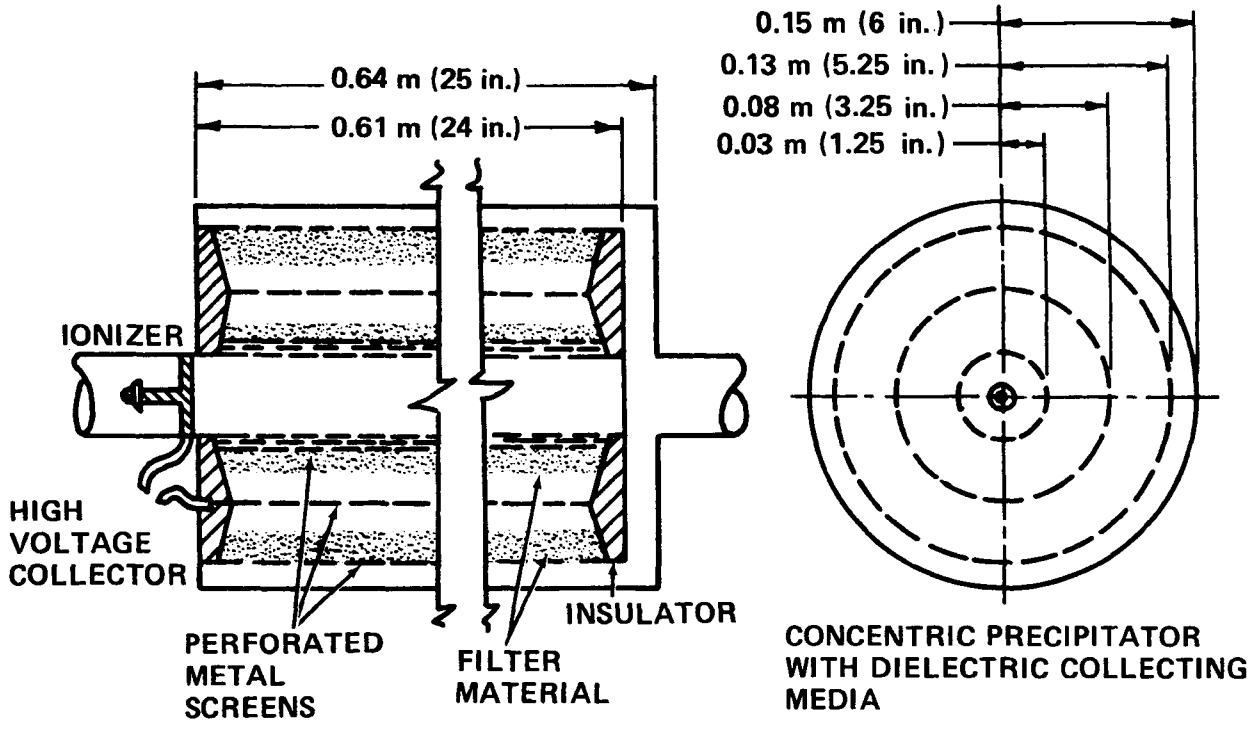

Figure 17. Second prototype electrostatic precipitator for collecting diesel particulate.

(a) two stage operation, thus minimizing ozone generation and power consumption,

(b) adaptation of high velocity gas throughput in small diameter ducts to low radial velocities for collection, thereby reducing reentrainment,

(c) high efficiency for the submicron particle size range,

(d) utilization of a combination of mechanical collection forces as well as coulombic, dielectrophoretic, and image electrical forces,

(e) convenient geometry for using electrified media in the collection stage and ready adaptation to removable cartridge form.

It is believed that the most effective form of collector would involve a gradation using three collection zones. The first would be a mechanical impaction collector utilizing the high velocity jets of gas produced by the inner perforated screen that changes the gas flow from the axial to the radial direction. The second zone could be a relatively coarse fibrous bed of collection media with superimposed electrostatic field. The final zone would be a finer graded bed of fibrous media with superimposed electrostatic field.

The efficiency of this device is harder to predict than that shown in Figure 16. If the effects of the dielectric material are neglected and the particles are assumed to have acquired the same charge as in the wire-cylinder example earlier in this section (admittedly a bad assumption), then for the metal collection plate area of 1.2 m^2 an efficiency of 0.7 (70%) can be obtained from Table 14. The effects of the dielectric material will be to increase the collection efficiency. Figure 18 shows the results of using various geometries of dielectric material in a similar device. Note that the collection efficiency for the device was improved for any choice of dielectric geometry and that the most efficient case was for a fibrous bed similar to that proposed here.

This device does have two possible design drawbacks. The first of these is the susceptibility to conductive contamination on the insulators. This will probably be worse on the ionizer and may necessitate the use of a different type of ionizer. The second is the increase in backpressure that will result when the dielectric fiber bed becomes loaded with particles. The magnitude of this problem can only be determined experimentally.

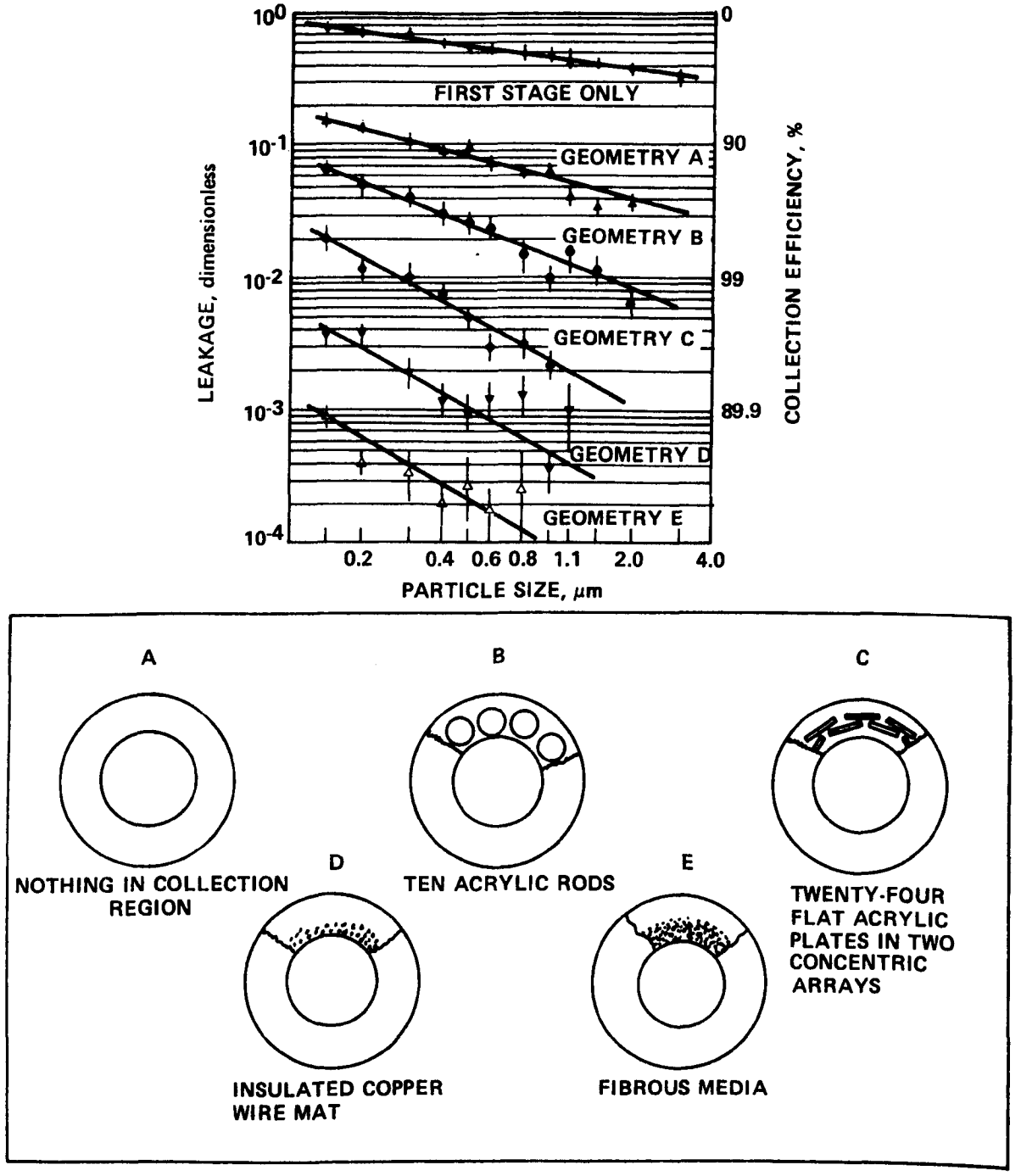

Figure 18. Collection efficiency of a concentric precipitator with dielectric collection media.[49]

SECTION 5

WET SCRUBBERS

DESCRIPTION OF SCRUBBER PROCESSES FOR COLLECTION OF PARTICULATE MATTER

Mechanisms

General--

There are a number of particle collection mechanisms utilized in wet scrubbers. Inertial impaction is the primary collection mechanism for particles of aerodynamic diameter larger than about 0.5 μm. The particle aerodynamic diameter is the diameter of a sphere of unit density which has the same gravity settling velocity as the real particle.

Inertial Impaction--

A gas stream approaching an object such as a scrubbing liquid droplet has fluid streamlines curved around the droplet. The inertial force causes migration of the particle across the curved fluid streamlines to the droplet surface resulting in particle collection. The collection of the particles on the droplet by inertial impaction is dependent upon three factors: (1) the velocity distribution of the gas flowing around the droplet, (2) the particle trajectory (which is dependent upon factors such as the air resistance on the particle, the particle mass, the droplet diameter, and the gas velocity with respect to the droplet), and (3) the adhesion of particles to the droplet once impacted on the droplet surface.

The velocity of the particle with respect to the droplet is characterized by the collecting body Reynolds number, Re_c:

$$Re_c = U_G \rho_G d_d / \mu_G \qquad (5.1)$$

where: U_G = undisturbed gas stream velocity with respect to the obstacle (m/s)

ρ_G = gas stream density (kg/m^3)

d_p = diameter of the droplet (m)

μ_G = gas stream viscosity (Pa-s)

At low gas velocities, viscosity factors govern the streamlines, so they smoothly spread around the object at a relatively large distance upstream of the object. At high Reynolds numbers, the streamlines abruptly diverge immediately upstream of the obstacle. The effect of sudden spreading of the streamlines at a high Reynolds number (high velocity) is to reduce the ability of the particles to make the sudden change of direction required to stay with the streamlines, thereby increasing inertial impaction and particle collection.

The dimensionless Stokes parameter, K_p, characterizes the motion of the particle around a collecting droplet:

$$K_p = \frac{\rho_p d_p^2 U_G C_c}{9 \mu_G d_c} \qquad (5.2)$$

where: ρ_p = particle density (kg/m^3)

d_p = particle diameter (m)

U_G = gas stream velocity (m/s)

μ_G = gas stream viscosity (Pa-s)

d_c = droplet diameter (m)

C_c = Cunningham correction factor (dimensionless)

The physical meaning of the Stokes parameter is the ratio of the particle's "stopping distance" to the radius of the collector. The stopping distance is the distance it would take the particle to stop in a still fluid. For spherical obstacles the critical value of K_p, the value at which smaller values result in no inertial deposition, is 0.083. Similarly, for cylindrical obstacles, the critical K_p is 0.125. In reality, even below the critical K_p values, some collection is made at the back of the obstable because of turbulent eddies.

Gravitational Collection--

With gravitational collection, the collection obstacle settles under free-fall through gas stationary with respect to the velocity of the obstacle. The collection made by this method is similar to that of the gas moving around a stationary obstacle.

Brownian Diffusion--

Very small particles (diameter <0.1 μm) can easily follow the streamlines when they diverge around an obstacle, and are thus rarely collected by inertial impaction. In gas streams

with low velocities, small particles can move across the streamlines due to Brownian motion. If the particles diffuse into the collection obstacles, they are collected and removed from the gas stream.

The values for particle diffusivities are several orders of magnitude smaller than that of gases and are close to those values of solutes in liquid. Using the Einstein equation, the particle diffusion coefficient can be calculated for particles larger than 0.062 μm:

$$D_p = \frac{C_c kT}{3\pi\mu_G d_p} \qquad (5.3)$$

where: C_c = Cunningham correction factor (dimensionless)

k = Boltzmann constant (joule/K)

T = absolute temperature

μ_G = gas stream viscosity (Pa-s)

d_p = particle diameter (m)

One major assumption in using this equation is that the particle concentration remains constant at a large distance from the collecting obstacle, and that near the collection surface the particle concentration is zero.

Electrostatic Collection--

There are five aspects of electrical forces that affect the particle near the collecting obstacle; these are dependent on particle and collector charging.

a. When both particle and collector are oppositely charged, the coulombic force K_{e_1} dominates.

b. When only the collector is charged and this induces an image charge of opposite polarity to the particle, the force K_{e_2} dominates.

c. When only the particle is charged and it induces an image charge of opposite polarity to the collector, the force K_{e_3} has an influence on particle collection.

d. The repulsive force on the particle due to similarly charged particles on the collector's surface, K_{e_4}, has an influence on particle collection.

e. The attractive force, K_{e_5}, between a charged particle and a grounded collector that has an induced charge caused by the surrounding charged particles has an influence on particle collection.

Both the repulsive force (K_{e_4}) and the space charge attractive force (K_{e_5}) are dependent on particle concentration and in most cases can be considered negligible unless the scrubber uses bubbles as the collector. The image force K_{e_3} is small and in most cases will be negligible.

Thermophoresis and Diffusiophoresis--

Temperature or water vapor pressure gradients between the surface of the collection droplets and the surrounding gases can create a particle velocity toward the droplets, thereby increasing particle collection efficiency. The magnitude of the velocity, and its effect on collection efficiency, depends on characteristics of the gas and the gradient involved.

Thermophoresis--When the gas temperatures on opposite sides of a particle are different, gas molecules on the warmer side will have a higher kinetic energy, and will randomly strike the particle with more force than will molecules on the cooler side of the particle. This unbalanced striking force causes the particle to move away from the warmer temperature zone. The velocity at which the particle moves depends on the temperature gradient across the particle, the relative thermal conductivities of the gas and particle (which govern the rate at which thermal energy is conducted through the particle), and the density and viscosity of the gas (which govern the drag force on the particle at a given velocity). In general, thermophoresis does not have a significant effect on particle collection because a large temperature gradient is required to cause particle migration velocities of a reasonable magnitude.

Diffusiophoresis--When the partial vapor pressure of water in the bulk gas is greater than the water vapor pressure at the surface of the collection droplets, water vapor will condense from the gaseous state onto the droplets. A bulk motion of gas toward the droplets is thus created to replace the condensed vapor. This bulk motion of the gas toward the droplet and motion of the water vapor towards the droplet sweep the particle toward the droplet. In general, diffusiophoresis can have a significant effect for the collection of fine particles.

Effect of Thermo- and Diffusiophoresis on Collection Efficiency--The two phoretic forces can either increase or decrease collection efficiency, depending on the direction of the appropriate gradient. Thermophoresis will increase collection effi-

ciency when the collection droplets are cooler than the surrounding gases. Diffusiophoresis will increase collection efficiency when collection droplets are condensing, and will reduce collection efficiency when the droplets are evaporating.

Types of Scrubbers

General--

Wet scrubbers are generally classified by the geometry or physical configuration of the scrubber. Because there are many gas-liquid contacting geometries possible, there is a considerable number of scrubber types available. However, the scrubber types have design and operating parameters which can be compared, as shown in Table 15.

Spray Towers--

A spray towers is the simplest type of scrubber. A spray of liquid droplets is produced by nozzles and allowed to fall through a rising stream of dirty gases. The simplest of spray scrubbers produce droplets that are sufficiently large so that the settling velocity is greater than the upward velocity of the gas stream. To increase the residence time of the droplets, the spray droplets are formed at such a size that the settling velocity is less than the vertical gas velocity, entraining the spray droplets in the gas stream. This will decrease the relative velocity between the particles and the droplet, resulting in a smaller inertial impaction parameter, but it will increase those collection mechanisms that require a longer residence time. The predominant collection mechanism most spray scrubbers are designed for is inertial impaction; thus the collection efficiency for small particles is low.

Venturi Scrubbers--

In the venturi scrubber, the relative velocity between the gas and the injected liquid causes the formation of the droplets. The gas is accelerated through a mechanical constriction, causing any water that is injected in the venturi throat to be sheared off and atomized. The droplet diameters formed can range from 10 to 300 μm, depending upon the gas velocity. Within the venturi throat the turbulence due to the gas acceleration enhances impingement collection. The particle removal efficiency is mainly a function of the pressure drop, liquid-to-gas flow rate ratio, and velocity of the gas through the venturi throat. The velocity and liquid-to-gas ratio have this effect by controlling the relative throat velocity and the degree of collection by the droplets. The gas pressure drop and the gas velocity in the venturi throat are related. It is necessary to have some means

TABLE 15. OPERATING AND DESIGN PARAMETERS OF SCRUBBERS

Type	Liquid-to-gas flow ratio (m^3/1000 m^3)	Gas velocity (m/s)	Gas pressure drop (Pa)	Gas residence time (s)	Capability of collecting 0.2-μm particles
Spray	0.27-4.0	0.60-3.0	<250	5-20	low
Venturi	0.13-2.7	30-120	2500-37300	0.1	possible with high gas velocity
Impingement plate	0.13-0.27 per plate	15-30 through jets	250-1000 per plate	2-4	low
Sieve plate	0.13-0.27 per plate	15-30 through jets	250-1000 per plate	2-4	low-medium
Charged droplet	0.13-2.7	0.60-3.0	250	5-20	high
Floating bed	1.3-6.7	3.0-6.0	1000-1250 per stage	1-5	low-medium
Induced draft	0.53-1.3	1.2-6.0	500-2000	1-2	low

of collection of the droplets entrained in the gas stream by the venturi. Mist droplet collectors include cyclone separators, wire mesh filters, sieve plate scrubbers, and impingement baffle vanes.

Impingement Plate Scrubbers--

Impingement plate scrubbers are generally towers with horizontal plates placed at regular intervals. These plates have a pattern of holes in them (0.1 to 1.0 cm and 6,400 to 32,000 holes/m^2) to allow the gas to pass through. Impingement baffles are located directly above the holes in the tray. As the gas accelerates through the orifices in the tray, the entrained particles are also accelerated; many of these particles will impact onto the baffle and be washed away by the liquid flowing over the top of the trays. Due to the gas flow through the orifices at a high velocity, some of the water flowing over the plates and baffles is torn away creating water droplets. These droplets have a low velocity compared to the gas stream, which allows for the impaction of the particles onto the droplets. This allows for two means of impaction for collecting the particles, impaction on the droplets and impaction on the baffles. The liquid flow is controlled by weirs. In most cases a mist eliminator is needed; either vane axial cyclones or impingement baffle vanes are effective for the size of droplets produced.

Sieve Plate Bubble Scrubbers--

Sieve plate scrubbers are also known as foam scrubbers. The particles are collected on the inside surfaces of the foam bubbles. In appearance these scrubbers look like an impingement plate scrubber, without the impingement baffles. Generally, the foam scrubbers have a larger quantity of orifices and also a larger orifice diameter.

Collection by inertial impaction takes place during the formation of the bubble. A secondary impaction mechanism works as the bubble rises through the foam. This is due to gas and particulate circulation inside the bubble, causing centrifugal deposition of the particles on the bubble's wall. Because of the long residence time due to bubble rise through the foam, Brownian diffusion plays an important role in the collection of small particles. Particle collection by Brownian diffusion is also enhanced by gas circulation in the bubble during bubble rise through the liquid.

The kinetic energy from the gas up-flow prevents the liquid from weeping through the perforations. If the gas velocity decreases below the critical velocity for weeping, the liquid will seep through the orifices, causing a large decrease in particle

collection efficiency. On the other hand, if the gas velocity becomes too great, the pressure drop will become so large that the liquid will discontinue to flow, and flooding (build-up of liquid in the tower as it cannot flow downwards) occurs.

Charged Droplet Scrubbers--

Electrostatics can enhance the performance of wet scrubbers, making it a logical extension to any of the previously discussed scrubbers. Charging of the particles can be accomplished by passing the dust-laden gases through a high-voltage ionizing section where corona discharge ionizes the air; through interception with the air ions, the charge is transferred to the particles. These charged particles then enter the scrubber; if the particles are not collected by the typical mechanisms of the scrubber, collection may occur by the electrostatic attraction.

This particle-droplet attraction can be caused by the image charge induced onto the droplet by the charged particle. The droplet can be electrostatically charged to the polarity opposite to the particle charge, and the particle-droplets undergo coulombic attraction forces (which can be the largest electrostatic particle-droplet attractive forces available).

DISCUSSION OF THE LITERATURE ON WET SCRUBBERS

Very little literature appears to exist on the subject of wet scrubbers for diesel engines. Such literature as was located in the literature survey for this project provides little information on specific scrubber designs that would be applicable to particulate control in light-duty vehicles.

Lawson and Vergeer[50] reported on the results obtained with a diesel engine intended for operation in an underground environment. They described two wet scrubbers as "a single path water bath conditioner" and "a more sophisticated packed bed water scrubber." For the single pass device, the authors reported that particulate capture averaged only about 30%, which was considered unsatisfactory performance. For the packed bed device, the removal efficiency of particulates was, at best, only marginally better than that in the single pass device and under some operating conditions was virtually identical to that in the single pass device. Much of the authors' interest in the functioning of wet scrubbers was for the control of hydrocarbons and gases.

Wood and Colburn[51] also addressed scrubbers for use with diesel equipment in an underground environment. They, too, were concerned not only with the removal of particulates but with the removal of gases such as nitrogen oxides. The authors provided little specific information on scrubber design or scrubber

performance. Their general position seemed to be that the performance of wet scrubbers has not been systematically investigated but that such performance should be systematically studied in view of the many design options that are available and the large body of background information that has been accumulated for scrubbers in other applications. The authors made one specific recommendation: that water injection into the exhaust turbine of a turbocharger be investigated as a means of particulate control.

Sudar and Grantham[52] described the use of a molten alkaline carbonate scrubber on a diesel urban bus. This device was of primary interest for controlling nitrogen oxide emissions. The effect of the device on particulate emissions does not appear to have been quantified. It is not apparent that a fused salt scrubber would offer any advantages over a water scrubber for particulate removal.

CALCULATION OF SCRUBBER EFFICIENCIES FOR PARTICULATE CONTROL

General Approach

The characteristics of diesel particulate that were used in calculations of scrubber efficiencies were as follows:

Particle density - 2,000 kg/m^3 (2.0 g/cm^3)

Particle mass median diameter - 2 x 10^{-7} m (0.2 μm)

The assumption was made that the diesel exhaust gas would enter the scrubber at either of two temperatures, 52 or 200°C. The lower of these two temperatures is that prescribed by EPA for measuring condensible gases as particulate. The upper temperature is an estimated temperature of the exhaust gas as it enters the muffler. The volume flow rate of gas at the upper temperature was estimated as 0.14 m^3/s (300 ft^3/min) for an automobile at highway cruising speed. The corresponding volume flow rate at the lower temperature was estimated as 0.097 m^3/min (206 ft^3/min) for the same conditions.

Estimates of the operating temperature and water vapor concentration in a scrubber were made by assuming that adiabatic equilibration of the gas and water would be established with respect to both temperature and water vapor concentration. The operation of the water loop supplying the scrubber was assumed to be virtually isothermal, and the concentration of water vapor entering the scrubber was estimated as 3% by volume. The resulting estimates for the different operating conditions were then as follows:

Gas, water temperature, 52°C
Gas, water outlet temperatures, 30°C
Gas outlet water vapor concentration, 4.19%

Gas inlet temperature, 300°C
Gas, water outlet temperatures, 50°C
Gas outlet water vapor concentration, 12.17%

The calculations of scrubber efficiencies and related parameters followed the format presented in the Scrubber Handbook.[53] These calculations were related to the pressure drops in the scrubbers, which were assumed to be limited to a maximum of 2,500 Pa (25.4 cm or 10 in. of water head). In one type of approach, it was convenient to set the pressure drop at the maximum desired and then to calculate the related parameters and finally the efficiency. This approach was followed with the venturi scrubber. In another approach, various parameters were assigned reasonable values, and then the resulting efficiency and pressure drop were calculated. This approach was followed with the sieve plate bubble scrubber. In the calculations to follow, the SI system of units used heretofore in this report was abandoned because of the expression of equations in the Scrubber Handbook in cgs or English units.

Calculations for a Venturi Scrubber

Design Considerations--

Calculations were made for a venturi operating at the maximum allowable pressure drop of 25.4 cm (10 in.) of water. This was done even though a common pressure drop for a venturi is frequently much higher. A series of selected liquid-to-gas volume ratios was assumed, and then values of various parameters—ultimately the efficiency—were calculated.

Calculations*--

1. Assume the maximum pressure drop and calculate the velocity of the gas in the throat of the venturi for a series of liquid-to-gas ratios.

$$U_G = \left[\frac{\Delta P}{1.03 \times 10^{-3}(L/G)}\right]^{0.5} \qquad (5.4)$$

* Definition of symbols and numerical values of certain parameters are given in the following section, Notation.

2. Calculate the diameter of the droplets produced in the venturi.

$$d_d = \frac{50}{U_G} + 91.8(L/G)^{1.5} \tag{5.5}$$

3. Calculate the Stokes impaction parameter.

$$K_p = \frac{\rho_p d_p^2 U_G C_c}{9\mu_G d_d} \tag{5.2}$$

4. Calculate the function given below involving the Stokes impaction parameter and the wetting factor f, where f is assumed to be 0.25 for a hydrophobic particle.

$$F(K_p,f) = \left[-0.7 - K_p f + 1.4 \ln \left(\frac{K_p f + 0.7}{0.7} \right) + \frac{0.49}{0.7 + K_p f} \right] \frac{1}{K_p} \tag{5.6}$$

5. Calculate the penetration of diesel particulate through the venturi.

$$P_t = \exp \left[\frac{2U_G \rho_L d_d}{55\mu_G} (F(K_p,f))(L/G) \right] \tag{5.7}$$

6. Calculate the efficiency of particulate removal.

$$\eta = 100(1 - P_t) \tag{5.8}$$

Notation--

C_c = Cunningham correction factor

d_p = diameter of particle (2×10^{-5} cm)

d_d = diameter of droplet (cm)

f = wetting factor (0.25)

$F(K_p,f)$ = function of Stokes impaction parameter and wetting factor

K_p = Stokes impaction parameter

L/G = liquid-to-gas ratio (dimensionless)

ΔP = pressure drop (25.4 cm of water)

P_t = penetration

U_G = gas velocity in throat (cm/s)

η = efficiency, %

ρ_p = particle density (2.0 g/cm^3)

ρ_L = water density (g/cm^3)

μ_G = gas viscosity (g/(cm-s))

Results--

The results of the calculations are given in the following two tables. In Table 16, the assumed scrubber temperature is 30°C. In Table 17, the assumed temperature is 50°C. The results indicate that a maximum efficiency of 4 to 5% would occur at either temperature. The conclusion, therefore, is that a venturi would be too inefficient for particulate removal from diesel exhaust under the assumed constraint of pressure drop.

Calculations for a Sieve Plate Bubble Scrubber

Design Considerations--

The inefficiency of collecting 0.2-μm particles by impaction in a venturi scrubber led to consideration of a sieve plate bubble scrubber, in which collection by the combined mechanisms of impaction and diffusion was expected to give more promising results. Reasonable values were assigned to the appropriate operating parameters, and calculations were made of efficiency and pressure drop.

Calculations*--

1. Assume an orifice diameter of 0.5 cm and (a) calculate the minimum orifice velocity U_h to prevent weeping and (b) calculate the maximum superficial gas velocity U_s for a column to prevent flooding. The equations are:

$$U_h = [10g(\frac{\rho_L}{\rho_G})d_h \exp[-4(L/G')^{0.25}(\frac{\rho_G}{\rho_L})^{0.125}]^{0.5} \quad (5.9)$$

$$U_s = k(\frac{\rho_L - \rho_G}{\rho_G})^{0.5} \text{ where } k = 6 \quad (5.10)$$

2. For assumed values of the foam height h, calculate the efficiency of particle collection η (a percentage) by the combined mechanisms of impaction and diffusion. The equation is:

---

* Definition of symbols and numerical values of certain parameters are given in the following section, Notation.

TABLE 16. EFFICIENCY OF PARTICULATE REMOVAL IN A VENTURI AT 30°C*

$L/G^{\dagger}$	U_G, cm/s	d_d, cm	K_p	$F(K_p,f)$	η, %
3.342×10^{-5}	2.72×10^{4}	1.86×10^{-3}	13.26	-1.092×10^{-1}	3.53
6.684×10^{-5}	1.92×10^{4}	2.65×10^{-3}	6.572	-6.734×10^{-2}	4.36
1.337×10^{-4}	1.36×10^{4}	3.82×10^{-3}	3.229	-3.351×10^{-2}	4.43
2.674×10^{-4}	9.60×10^{3}	5.61×10^{-3}	1.552	-1.304×10^{-2}	3.59
4.010×10^{-4}	7.84×10^{3}	7.12×10^{-3}	9.998×10^{-1}	-6.657×10^{-3}	2.86
1.337×10^{-3}	4.29×10^{3}	1.61×10^{-2}	2.417×10^{-1}	-6.144×10^{-4}	1.10
2.674×10^{-3}	3.04×10^{3}	2.91×10^{-2}	9.476×10^{-2}	-9.080×10^{-5}	0.42

* Constants: $\rho_L = 0.99567$ g/cm^3; $\mu_G = 1.86 \times 10^{-4}$ g/(cm/s); $C_c = 1.898$.

† These are dimensionless quantities corresponding to L/G ratios ranging from 0.25 to 20 gal./1000 ft^3.

TABLE 17. EFFICIENCY OF PARTICULATE REMOVAL IN A VENTURI AT 50°C*

$L/G^{\dagger}$	U_G, cm/s	d_d, cm	K_p	$F(K_p,f)$	η, %
6.684×10^{-5}	1.92×10^{4}	2.65×10^{-3}	6.486	-6.667×10^{-2}	4.09
1.337×10^{-4}	1.36×10^{4}	3.82×10^{-3}	3.187	-3.308×10^{-2}	4.14
2.674×10^{-4}	9.60×10^{3}	5.61×10^{-3}	1.532	-1.278×10^{-2}	3.33
4.010×10^{-4}	7.84×10^{3}	7.12×10^{-3}	9.858×10^{-1}	-6.533×10^{-2}	2.66
5.347×10^{-4}	6.79×10^{3}	8.50×10^{-3}	7.152×10^{-1}	-3.805×10^{-3}	2.14
6.684×10^{-4}	6.07×10^{3}	9.82×10^{-3}	5.534×10^{-1}	-2.473×10^{-3}	1.80

* Constants: $\rho_L = 0.98807$ g/cm^3; $\mu_G = 1.95 \times 10^{-4}$ g/(cm-s); $C_c = 1.964$.

† These are dimensionless quantities corresponding to L/G ratios ranging from 0.50 to 5 gal./1000 ft^3.

$$\eta/100 = 1 - \exp[-40F^2K_p - 1.87h(\frac{D_p}{(r_b)^3V_b})^{0.5}] \quad (5.11)$$

The inertial impaction parameter K_p is given by the equation:

$$K_p = \frac{\rho_p d_p^2 U_h C_c}{9\mu_G d_d} \quad (5.12)$$

The foam density can be estimated by:

$$F = \exp[-(0.184U_s\rho_G^{0.5} + 0.45)] \quad (5.13)$$

The radius of bubbles formed, r_b, is computed from:

$$r_b = (0.355)(\frac{d_h U_h}{\nu_G})^{-0.05} \quad (5.14)$$

The rising velocity of the bubble V_b is calculated from:

$$V_b = 1.53[\frac{g(\rho_L - \rho_G)\delta}{\rho_L^2}]^{0.25} \quad (5.15)$$

The diffusion coefficient D_p can be estimated by:

$$D_p = \frac{C_c kT}{3\pi\mu_G d_d} \quad (5.3)$$

Finally, the Cunningham correction factor is estimated from the following:

$$C_c = [\frac{2 \times 10^{-8}T}{d_p}(2.79 + 0.894 \exp(\frac{-2.47 \times 10^7 d_p}{T}))] + 1 \quad (5.16)$$

3. Calculate the smallest allowable column diameter from the equation:

$$d_c = (\frac{4Q_G'}{\pi(0.8U_s)})^{0.5} \quad (5.17)$$

In this calculation, U_s is reduced to 80% of the value previously calculated to ensure against flooding.

4. Calculate the pressure drop for a sieve tray plate (expressed in inches of water):

$$h_t = h_w + h_{ow} + h_{dp} + h_r \quad (5.18)$$

where: $h_w = h'F$ (the pressure head up to the level of the weir) (5.19)

$$h_{ow} = 0.48\ F_w \left(\frac{Q_L}{W_T}\right)^{0.67}$$ (the pressure head above the level of the weir) (5.20)

$$h_{dp} = \frac{\rho_G U_h^2}{2C^2 \rho_L g(2.54)}$$ (the pressure head from the dry plate) (5.21)

$$\frac{1}{C^2} = 1.14[0.4(1.25 - f_h) + (1 - f_h)^2]$$

$$h_r = \frac{0.06\delta}{\rho_L d_h'}$$ (the residual pressure head) (5.22)

Notation--

Quantity	Value at 30°C	Value at 50°C
C_c = Cunningham correction factor	1.898	1.964
d_p = particle diameter (cm)	2×10^{-5}	2×10^{-5}
d_c = column diameter (cm)	28.50	28.85
d_h = perforation diameter (cm)	0.5	0.5
d_h' = perforation diameter (in.)	0.1968	0.1968
D_p = diffusion coefficient (cm^2/s)	2.252×10^{-6}	2.394×10^{-6}
f_h = fraction of tray area perforated	0.07	0.07
F_w = correction for column wall curvature	1.2	1.2
F = foam density	0.263	0.265
g = acceleration of gravity (cm/s^2)	981	981
h = foam height (cm)	5, 10	5, 10
h' = foam height (in.)	1.968, 3.937	1.968, 3.937
h_{dp} = dry plate pressure drop (in. of water)	-	-
h_r = residual pressure drop (in. of water)	-	-

Quantity	Value at 30°C	Value at 50°C
h_{ow} = pressure head due to water over weir height (in. of water)	-	-
h_w = pressure head due to water up to weir height (in. of water)	-	-
h_t = total pressure head (in. of water)	-	-
k = Boltzmann constant (ergs/K)	1.381×10^{-16}	1.381×10^{-16}
K_p = Stokes impaction parameter	-	-
L/G = liquid-to-gas ratio (gal./1000 ft^3)	-	-
L/G' = liquid-to-gas ratio (L/min^3)	-	-
Q_G = gas flow rate (gal./min)	-	-
Q_G' = gas flow rate (cm^3/s)	-	-
Q_L = liquid flow rate (gal./min)	-	-
r_b = bubble radius (cm)	-	-
T = temperature (K)	303	323
U_s = superficial gas velocity (cm/s)	-	-
U_h = orifice gas velocity (cm/s)	-	-
V_b = bubble velocity (cm/s)	24.891	24.648
W' = weir length (in.)*	9.25	9.25
μ_G = gas viscosity (g/(cm-s))	1.86×10^{-4}	1.95×10^{-4}
ν_G = gas kinematic viscosity (cm^2/s)	0.163	0.186
ρ_G = gas density (g/cm^3)	1.1468×10^{-3}	1.0428×10^{-3}

* See Figure 19.

Quantity	Value at 30°C	Value at 50°C
ρ_L = liquid density (g/cm^3)	0.99567	0.98807
ρ_L' = liquid density (lb/ft^3)	62.4	61.9
ρ_p = particle density (g/cm^3)	2.0	2.0
δ = liquid surface tension (dyne/cm)	71.18	67.91
η = single stage efficiency (%)	-	-
η_t = total efficiency (%)	-	-

Results--

The results of the calculations are given in the series of tables that follows. Table 18 presents the results of calculations of U_h and U_s for various assumed L/G values. Tables 19 and 20 give the results of efficiency calculations for a single-stage sieve tray operating at 30 and 50°C, respectively, with two assumed foam heights, 5 and 10 cm. Table 21 gives calculated column diameters, and Table 22 gives calculated pressure drops for a single-stage sieve tray, as visualized in Figure 19.

TABLE 18. MINIMUM ORIFICE VELOCITY AND MAXIMUM SUPERFICIAL VELOCITY IN A SIEVE PLATE BUBBLE SCRUBBER

Temp, °C	L/G, gal./1000 ft^3	L/G', L/m^3	U_h, cm/s	U_s, cm/s
30	1.5	0.2	1162	177
	3.0	0.4	1043	177
	4.5	0.6	969	177
	6.0	0.8	916	177
	7.5	1.0	875	177
50	1.5	0.2	1222	185
	3.0	0.4	1097	185
	4.5	0.6	1021	185
	6.0	0.8	966	185
	7.5	1.0	922	185

TABLE 19. SCRUBBER PARAMETERS AND SINGLE-STAGE EFFICIENCY IN A SIEVE PLATE BUBBLE SCRUBBER AT 30°C

h, cm	U_h, cm/s	r_b, cm	K_p	η, %
5	1100	0.236	0.001985	2.96
10	1100	0.236	0.001985	5.31
5	1500	0.233	0.002707	3.20
10	1500	0.233	0.002707	5.59
5	2000	0.229	0.003609	3.50
10	2000	0.229	0.003609	5.95
5	2500	0.227	0.004511	3.78
10	2500	0.227	0.004511	6.25
5	3000	0.225	0.005413	4.05
10	3000	0.225	0.005413	6.54
5	3500	0.223	0.006315	4.32
10	3500	0.223	0.006315	6.84
5	4000	0.222	0.007218	4.58
10	4000	0.222	0.007218	7.11

TABLE 20. SCRUBBER PARAMETERS AND SINGLE-STAGE EFFICIENCY IN A SIEVE PLATE BUBBLE SCRUBBER AT 50°C

h, cm	U_h, cm/s	r_b, cm	K_p	η, %
5	1100	0.238	0.001980	3.19
10	1100	0.238	0.001980	5.42
5	1500	0.234	0.002700	3.28
10	1500	0.234	0.002700	5.74
5	2000	0.231	0.003600	3.57
10	2000	0.231	0.003600	6.07
5	2500	0.228	0.004499	3.86
10	2500	0.228	0.004499	6.40
5	3000	0.226	0.005399	4.14
10	3000	0.226	0.005399	6.71
5	3500	0.224	0.006299	4.42
10	3500	0.224	0.006299	7.01
5	4000	0.223	0.007199	4.68
10	4000	0.223	0.007199	7.28

TABLE 21. COLUMN DIAMETERS OF A SIEVE PLATE BUBBLE SCRUBBER

Temp, °C	Q_G, ft³/min	Q_G', cm/s	U_s,[a] cm/s	h, cm	d_c, cm	d_c, ft
30	192	90,614	142	5	28.50	0.935
	192	90,614	142	10	28.50	0.935
50	205	96,749	148	5	28.85	0.947
	205	96,749	148	10	28.85	0.947

a. Taken as 80% of the values listed in Table 17.

TABLE 22. PRESSURE DROP VALUES IN A SINGLE STAGE OF A SIEVE PLATE BUBBLE SCRUBBER[a]

Temp, °C	F	h, cm	h_w	h_{ow}	h_{dp}	h_r	h_t
30	0.263	5	0.518	0.064	1.409	0.349	2.340
	0.263	10	1.035	0.064	1.409	0.349	2.857
50	0.265	5	0.522	0.066	1.291	0.332	2.211
	0.265	10	1.043	0.066	1.291	0.332	2.732

a. All values in inches of water. U_h was assumed to be 2000 cm/s. L/G was assumed to be 1.5 gal./1000 ft³ to assign a value to Q_L in the calculation of h_{ow}.

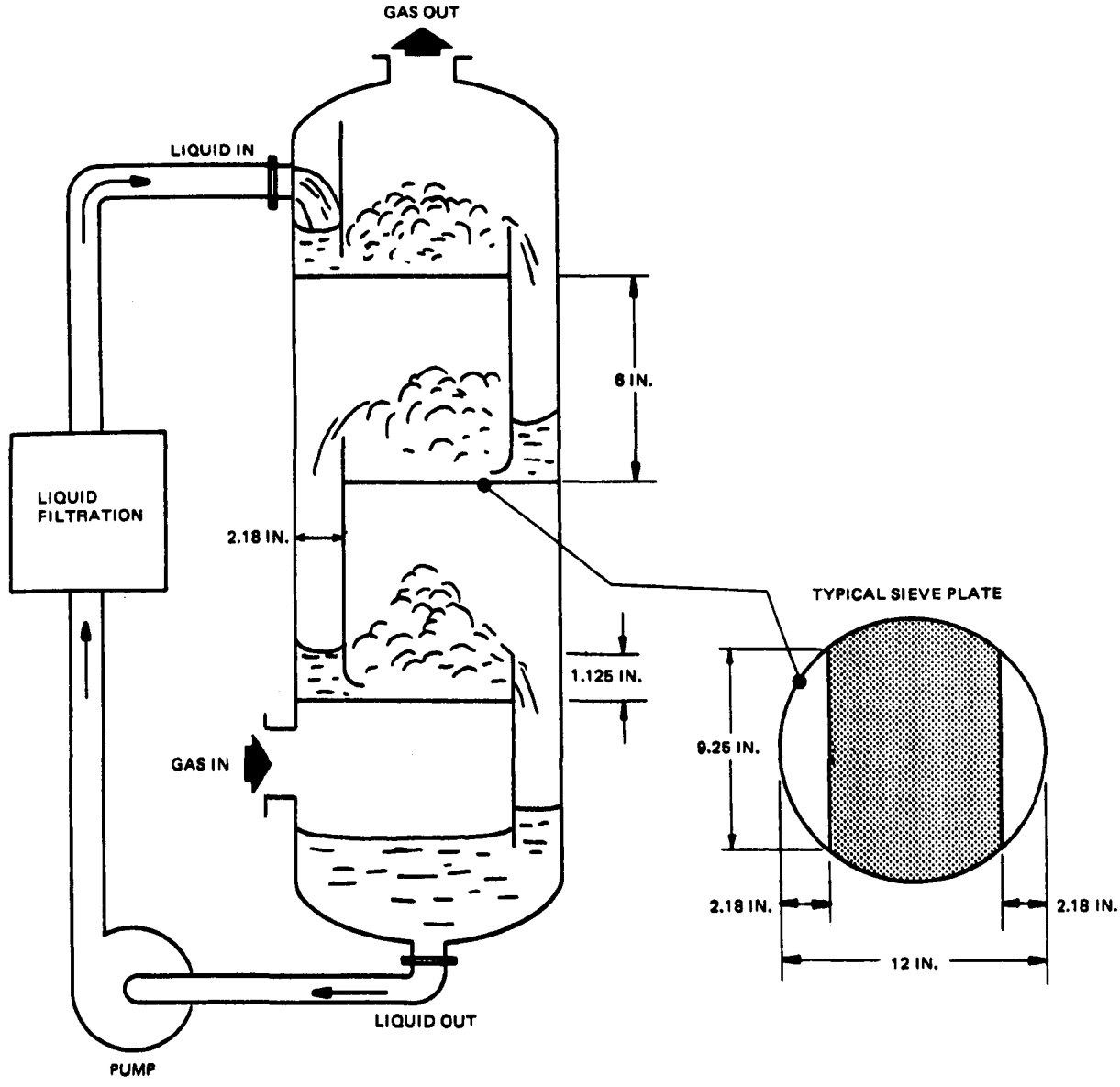

Figure 19. Diagram of a sieve plate bubble scrubber.

The results of the calculations are summarized in Table 23. This table is based on an assumed value of U_h of 2000 cm/s (which is safely above the value required to prevent weeping) and assumed values of U_s of 142 and 148 cm/s at temperatures of 30 and 50°C, respectively, which are 80% of the maximum values calculated to prevent flooding. The results are given for two conditions: (1) the number of stages allowable to give a pressure drop not exceeding 2,500 Pa and (2) the number of stages required to give a total efficiency greater than 50%. It is shown that with a pressure drop below 2,500 Pa, the maximum efficiency obtainable is about 17%. It is shown, on the other hand, that the pressure drop must reach at least 8,000 Pa to give an efficiency exceeding 50%. In the first instance, the estimated height of the scrubber is about 75 cm (2.5 ft); in the second instance, the estimated height is about 300 cm (10 ft). The conclusion, therefore, is that the sieve plate bubble scrubber is not a practical solution to the problem of removing diesel particulate.

Calculations for Other Scrubber Types

Approximate calculations were made for three scrubber types in addition to the venturi and the sieve plate bubble scrubber. The other three types were the impaction plate, the ordinary spray scrubber, and the electrostatic spray scrubber. The essential conclusions reached were as follows:

- The impaction plate with orifices of 0.1 cm would produce a maximum efficiency of about 20% if constrained to operate at a maximum pressure difference of 2,500 Pa.
- A spray tower would have to be roughly 275 cm (9 ft) tall to accomplish a particulate removal efficiency of 50% and would require an excessive volume flow of liquid.
- An electrostatic spray scrubber with a height not exceeding 90 cm (3 ft) might produce a removal efficiency of around 50%. However, this device would not offer design advantages over other electrostatic devices discussed in this report.

FURTHER CONSIDERATIONS

The general conclusion to be reached from the foregoing material is that wet scrubbers employing water are not, in general, suitable for removing particulate from diesel exhaust. Under the constraint of a 2,500-Pa pressure drop, they are not efficient enough in removing the fine particles present in diesel smoke. A possible exception is the charged droplet scrubber, but it is not clear that this device would be preferable to some other type of electrostatic device.

TABLE 23. SUMMARY OF CALCULATIONS FOR A SIEVE PLATE BUBBLE SCRUBBER[a]

Design limitation	Temp, °C	h, cm	d_c, cm	U_s, cm/s	No. of plates	η_t,[b] %	ΔP,[b] Pa
$\Delta P \leq$ 10 in. of H_2O	30	5	0.935	142	4	13.3	2,330
		10	0.935	142	3	16.8	2,130
	50	5	0.947	148	4	13.5	2.200
		10	0.947	148	3	17.1	2,040
$\eta \geq$ 50%	30	5	0.935	142	20	51.0	11,700
		10	0.935	142	12	52.1	8,540
	50	5	0.947	148	20	51.7	11,000
		10	0.947	148	12	52.8	8,160

a. Constant conditions: U_h = 2000 cm/s, L/G = 1.5 gal./1000 ft^3, number of holes per tray = 150.

b. Total efficiency and total pressure drop.

The above conclusion is reinforced by consideration of the rate of water loss by evaporation in a wet scrubber. The water loss by evaporation would obviously be more severe for diesel exhaust entering a wet scrubber at 200°C rather than at 52°C. Therefore, the first consideration will be made of the scrubber with inlet gas at 200°C and outlet gas and water at 50°C.

Diesel exhaust entering a scrubber at 200°C at a rate of 0.14 m^3/s (300 ft^3/min) will contain about 3% by volume water vapor as the result of fuel combustion in the engine. This rate corresponds to the flow of 1.97 g/s of water vapor. On leaving the scrubber at 50°C with water vapor at the saturation level (concentration, 12.17% by volume), the gas stream will carry water vapor away at the rate of 8.83 g/s. Thus, water will be lost at the rate of 6.86 g/s. This is equivalent to about 6.86×10^{-6} m^3/s. For comparison, the rate of fuel consumption may be calculated by assuming that the exhaust flow rate corresponds to a highway speed of 1.61 km/s (60 mi/h) and that the fuel consumption rate is 2.52×10^{-6} m^3/s (25 mi/gal. or 0.04 gal./min). The conclusion, therefore, is that water would be consumed at 2.7 times the rate of consumption of diesel fuel.

For diesel exhaust entering a scrubber at 52°C and leaving at 30°C with 4.19% water, the rate of water consumption will be 2.05 g/s or 2.05×10^{-6} m^3/s (roughly the same as the rate of diesel fuel consumption). However, even if this rate of water consumption were acceptable, it would not be clear that the exhaust gas could be economically cooled to 52°C before entering a scrubber.

The conclusion that a wet scrubber would not be a practical device is further reinforced by considerations of the freezing point of water. To avoid the freezing of water under normal climatic conditions, some anti-freeze substance would have to be added. The addition of such a substance would probably not have a beneficial effect on the already low efficiencies of various scrubber devices, and it might have a deleterious effect.

SECTION 6

CONCLUSION

From the preceeding discussion, it is possible to draw some conclusions regarding the applicability of scrubbers, electrostatic devices, and filters to the problem of controlling diesel particulate emissions. The first of these, scrubbers, can be eliminated from further consideration due to the large size required to obtain adequate efficiencies at reasonable backpressures, and to the high rate of water consumption.

Second, electrostatic devices merit further consideration for the important reasons that they present very little backpressure to the system and that they maintain a relatively high collection efficiency over the 0.1- to 0.8-μm particle size range over which, according to theory, a dip in filter efficiency occurs. To offset this, they have the severe disadvantage of dysfunction due to conductive particle contamination. Further research will have to be performed to design a system which can eliminate this difficulty. A lesser problem is that of disposal of the collected particulate. A method must be developed whereby the device may be cleaned and the collected particulate properly and safely disposed of as a matter of routine maintenance.

The third mechanism, filtration, demonstrates the same problem of disposal of the collected particulate. Another problem area is the possibility of high backpressure. Although it is possible to design a device of appropriately low backpressure when new, only experimentation will determine the amount of particulate the filter can collect without elevating the backpressure beyond allowable limits and adversely effecting engine performance. The problem of surface seal over can be avoided by utilizing a filter with a large face area such as the proposed prototype. The advantage of filtration is that it is a mechanically simpler concept. Filters, while not necessarily simple to design, are simpler to build and maintain in the field than electrostatic devices and as a consequence should be cheaper and more convenient in use.

Both electrostatic devices and filtration devices show promise of becoming workable solutions to the diesel exhaust problem. However, more research is needed on both types of devices. Prototypes need to be fabricated and tested on actual

diesel exhaust streams. Determinations of collection efficiency as a function of particle size would be useful in the study of the collection mechanisms involved, which should in turn lead to the development of improved collection devices. Testing of prototype devices will also yield additional insights into the particulate problems that affect each device.

Additional study is also needed on the effect of gas stream temperature on the hydrocarbon portion of the particulate. A study by Black and High[54] indicates that most of the condensation and subsequent adsorption of vaporous hydrocarbons occurs in the last few feet of the vehicle's tail pipe. This implies that a temperature reduction in the exhaust system would increase the amount of hydrocarbons which condense and can therefore be collected as particulate. Supportive evidence has been given by Masuda,[55] who reports that Eikosha has seen a 20% by volume increase in collected particulate occur when the cooling air flow on the Aut-Ainer filter was increased.

SECTION 7

REFERENCES

1. Springer, K.J., and T.M. Baines. Emissions from Diesel Versions of Production Passenger Cars. SAE paper # 770818, presented at the SAE Passenger Car Meeting, Detroit, Michigan, September 26-30, 1977.

2. Broome, D., and I. Khan. The Mechanism of Soot Release from Combustion of Hydrocarbon Fuels from Air Pollution Control in Transport Engines. Institution of Mechanical Engineering, London, England, 1971.

3. Lipkea, W.H., J.H. Johnson, and C.T. Vuk. The Physcial and Chemical Character of Diesel Particulate Emissions - Measurement Technique and Fundamental Considerations. SAE Paper # 780108, presented at the SAE Congress and Exposition, Detroit, Michigan, February 27-March 3, 1978.

4. McCain, J.D., and D. Drehmel. Particle Size Measurements of Automotive Diesel Emissions. Paper presented at the Second Symposium on the Transfer and Utilization of Particulate Control Technology, Denver, Colorado, July 23-27, 1979. (A reprint of this paper appears in this report as Appendix I.)

5. Stern, A.C., Editor. Air Pollution Vol. III: Sources of Air Pollution and Their Control. Academic Press, New York, New York, 1968.

6. Briggs, T., J. Throgmorton, and M. Karaffa. Air Quality Assessment of Particulate Emissions from Diesel-Powered Vehicles. Final Report prepared for the Environmental Protection Agency by PEDCo Environmental, Inc., under Contract No. 68-02-2515. EPA-450/3-78-038, U.S. Environmental Protection Agency, Research Triangle Park, North Carolina, March 1978.

7. Pitts, J.N., Jr., A.M. Winer, and K.A. Van Cauwenberghe. An Overview on Diesel Exhaust and Air Quality: Chemical Implications. In: Proceedings of the Workshop on Unregulated Diesel Emissions and Their Potential Health Effects, National Highway Traffic Safety Administration, Environmental Protection Agency and Dept. of Energy, April 27-28, 1978.

8. Federal Register, 44(33) February 1, 1979.

9. General Motors Response to EPA Notice of Proposed Rulemaking on Particulate Regulation for Light-Duty Diesel Vehicles, April 19, 1979.

10. Springer, K., and R. Stahman. Removal of Exhaust Particulate from a Mercedes 300D Diesel Car. SAE Paper # 770716, presented at the SAE Off-Highway Vehicle Meeting and Exhibition, Mecca, Milwaukee, Wisconsin, September 12-15, 1977.

11. Frey, J.W., and M. Corn. Physcial and Chemical Characteristics of Particulates in a Diesel Exhaust. American Industrial Hygiene Association Journal, September-October, 1967.

12. Funkenbusch, E.F., D.G. Leddy, and J.H. Johnson. The Characterization of the Soluble Organic Fraction of Diesel Particulate Matter. SAE Paper # 790418, presented at the Congress and Exposition Cobo Hall, Detroit, Michigan, February 26-March 2, 1979.

13. Mentser, M. and A.G. Sharky. Chemical Characterization of Diesel Exhaust Particulates. Publication No. PERC/RI-77/5, Pittsburgh Energy Research Center, Pittsburg, Pennsylvania, March 1977.

14. Davies, C.N. Aerosol Science. Academic Press, Chapters 8 and 9, 1966.

15. Chen, C.Y. Filtration of Aerosols by Fibrous Media. Chemical Review, 55:595, 1955.

16. Fuchs, N.A., and I.B. Strechkina. A Note on the Theory of Fibrous Aerosol Filters. Annals of Occupational Hygiene, 6(1):27-30, 1963.

17. Davies, C.N. Air Filtration. Academic Press, 1973.

18. Saxena, S.C., and W.M. Swift. Dust Removal from Hot and Compressed Gas Streams by Fibrous and Granular Bed Filters: A State of the Art Review. Argonne National Laboratory, May 1978.

19. Loffler, F. Collection of Particles by Fiber Filters. Air Pollution Control, Part 1, W. Strauss, Ed. Wiley-Interscience, New York, New York, 1971.

20. Stenhouse, J.I.T., G.P. Bloom, and N.T.J. Chard. Dust Loading Characteristics of High Inertial Fibrous Filters. American Industrial Hygiene Association Journal, 39(3):219, 1978.

21. Loffler, F. Adhesion Probability in Fiber Filters. Clean Air, 8(4), 1974.

22. Stenhouse, J.I.T., G.P. Bloom, and N.T.J. Chard. High Inertia Fibrous Filtration—Optimum Conditions. Filtration Separation, 15(2):128, 1978.

23. Paretsky, L., et al. Panel Bed Filter for Simultaneous Removal of Fly Ash and SO_2: II Filtration of Dilute Aerosol by Sand Beds. Journal of the Air Pollution Control Association, 21(4):204-209, April 1971.

24. Tardos, G.I., N. Abauf, and C. Gutfinger. Dust Deposition in Granular Bed Filters: Theories and Experiments. Journal of the Air Pollution Control Association, 28(4):354-363, April 1978.

25. Eastwood, J., et al. Random Loose Porosity of Packed Beds. British Chemical Engineering, 14(11):1542-1545, November 1969.

26. Lee, K.W., and J.A. Gieseke. Collection of Aerosol Particles by Packed Beds. Environmental Science and Technology, 13(4):466-470, April 1979.

27. Schmidt, E.W., et al. Filtration Theory for Granular Beds. Journal of the Air Pollution Control Association, 28(2):143-146, February 1978.

28. Jackson, S., and S. Calvert. Entrained Particle Collection in Packed Beds. A.I.Ch.E. Journal, 12:1075, November 1966.

29. Ergun, S. Fluid Flow Through Packed Columns. Chemical Engineering Progress, 48:89-94, 1952.

30. Lee, K.C., et al. The Panel Bed Filter. Electric Power Research Institute (EPRI AF-560), May 1977.

31. Taub, S.I. Filtration Phenomena in a Packed Bed Filter, Doctoral Thesis, Carnegie-Mellon University, 1971.

32. Goren, S.L. Aerosol Filtration by Granular Beds. Paper presented at the EPA Particulate Control Technology Symposium, Denver, Colorado, July 1978.

33. Sullivan, H., L. Tessier, C. Hermance, and G. Bragg. Reduction of Diesel Exhaust Emissions (Underground Mine Service). Prepared for the Department of Energy, Mines and Resources, Ottawa, by the Mechanical Engineering Department of the University of Waterloo, Waterloo, Ontario, May 1977.

34. Communication between Eikosha Company and Grady B. Nichols of Southern Research Institute.

35. Pauthenier, M., and M. Moreau-Hanot. Charging of Spherical Particles in an Ionizing Field. J. Phys. Radium, 3(7):590-613, 1932.

36. White, H.J. Particle Charging in Electrostatic Precipitation. Trans. Amer. Inst. Elec. Eng. Part 1, 70:1186-1191, 1951.

37. Murphy, A.T., F.T. Adler, and G.W. Penney. A Theoretical Analysis of the Effects of an Electric Field on the Charging of Fine Particles. Trans. Amer. Inst. Elec. Eng., 78:318-326, 1959.

38. White, H.J. Industrial Electrostatic Precipitation. Addison-Wesley, Reading, Massachusetts, 1963. p. 157.

39. Fuchs, N.A. The Mechanics of Aerosols, Chapter 2. Macmillan, New York, New York, 1964.

40. White, H.J. Reference 8, pp. 166-170.

41. White, H.J. Reference 8, pp. 185-190.

42. Penney, G.W., and S. Craig. Pulsed Discharges Preceding Sparkover at Low Voltage Gradients. AIEE Winter General Meeting, New York, New York, 1961.

43. Pottinger, J.F. The Collection of Difficult Materials by Electrostatic Precipitation. Australian Chem. Process Eng., 20(2):17-23, 1967.

44. Gooch, J.P., and G.H. Marchant, Jr. Electrostatic Precipitator Rapping Reentrainment and Computer Model Studies. Final Draft Report prepared for the Electric Power Research Institute by Southern Research Institute, 1977.

45. Spencer, H.W. A Study of Rapping Reentrainment in a Nearly Full Scale Pilot Electrostatic Precipitator. EPA-600/2-76-140, U.S. Environmental Protection Agency, Research Triangle Park, North Carolina, 1976.

46. Springer, K.I. An Investigation of Diesel-Powered Vehicle Odor and Smoke. Final Report to the National Air Pollution Control Administration, Department of Health, Education, and Welfare, October 1969. Publication No. AR-695.

47. White, H.J. Industrial Electrostatic Precipitation. Addison Wesley, Reading, Massachusetts, 1963.

48. Smith, W.B., and J.R. McDonald. Development of a Theory for the Charging of Particles by Unipolar Ions. J. Aerosol Sci., 7:151-166, 1976.

49. Inculet, I.I., and G.S.P. Castle. A Two-Stage Concentric Geometry Electrostatic Precipitator with Electrified Media. ASHRAE Journal, March 1971.

50. Lawson, A., and H. Vergeer. Analysis of Diesel Exhaust Emitted from Water Scrubbers and Catalytic Purifiers. Ontario Research Foundation, 1977.

51. Wood, C.D., and J.W. Colburn, Jr. Control Technology for Diesel Equipment in the Underground Mining Environment-A Review of Selected Topics. Final Report prepared by Southwest Research Institute for U.S. Department of the Interior, Bureau of Mines, Twin Cities, Minnesota, Purchase Order P3381399, January 1979.

52. Sudar, S., and L. Grantham. Diesel Exhaust Emission Control Program. Final Report prepared by Atomics International for Southern California Rapid Transit District, Los Angeles, California, January 1974.

53. Calvert, S., J. Goldschmid, D. Leith, and D.P. Mahta. Scrubber Handbook, Volume I. Report prepared by Ambient Purification Technology, Inc., for Environmental Protection Agency. Contract CPA-70-95. August 1972.

54. Black, F., and L. High. Diesel Hydrocarbon Emissions, Particulate and Gas Phase Symposium on Diesel Particulate Emission Measurement Characteristic. U.S. Environmental Protection Agency, Research Triangle Park, North Carolina.

55. Private Communication, S. Masuda with M.G. Faulkner of Southern Research Institute.

APPENDIX I

PARTICLE SIZE MEASUREMENTS OF AUTOMOTIVE DIESEL EMISSIONS

by

Joseph D. McCain
Southern Research Institute
2000 Ninth Avenue, South
Birmingham, Alabama 35205

and

Dennis C. Drehmel
Industrial Environmental Research Laboratory
Environmental Protection Agency
Research Triangle Park, North Carolina 27711

Presented at

The Second Symposium on the Transfer and Utilization of Particulate Control Technology, Denver, Colorado, July 23-27, 1979

Introduction

The federally mandated fuel economy standards for passenger automobiles have resulted in considerable impetus being given to the introduction of substantial numbers of diesel powered automobiles into the passenger car fleet. The diesel engine has long been acknowledged as being "dirtier" than the spark ignition gasoline engine (by factors of 30 to 50 in particulate emissions). The diesel particulate emissions are primarily carbonaceous, but 10 percent to 50 percent by weight of the material is adsorbed higher molecular weight organics, a significant portion of which may be polycyclic aromatics.[1] Preliminary results of Ames microbial mutagenicity bioassay tests have indicated the possibility that these particulates may be carcinogenic.

Possible solutions to the diesel particulate problem are combustion modification or the use of aftertreatment devices in the exhaust gas stream to collect and/or render the material innocuous. Such treatment may be mandatory if the emissions do prove to represent a significant carcinogenic risk. Selection of candidate aftertreatment devices requires knowledge of the chemical and physical properties of the particles. These include particle morphology, particle size distribution, bulk densities of the collected material, and particulate mass concentration and emission rates in the exhaust gas stream. Because the organic fraction of the particles appears to be adsorbed on the surfaces of graphitic carbon base particles, the temperature history of the gas stream may be important. If the sorption process takes place at elevated temperatures, then collection of the particulate at the normal, relatively hot, exhaust gas temperatures may be sufficient. However, if the sorption takes place only during and after cooling of the exhaust stream to near ambient conditions, the hot particle collection will not result in the removal of the organic fraction.

The study reported here represents the first of a planned series of experiments to characterize the exhaust emissions from the point of view of aftertreatment exhaust gas cleanup and to collect samples for bioassays to determine whether the biological effects of particles collected at exhaust line temperatures are the same as those collected after dilution and cooling by ambient air.

Test Program

The tests described here were performed November 27 through December 1, 1978, at a U. S. EPA facility located at Research Triangle Park, North Carolina. A 1979 Oldsmobile 88 with a 350 Cubic Inch Displacement (CID) diesel engine was operated on a

Burke E. Porter No. 1059 Chassis Dynamometer. The dynamometer was programmed to emulate the Clayton roadload curve for water-brake dynamometers used for vehicle certification. Test conditions included the 13 minute Fuel Economy Test (FET) combined city-highway test cycle, 97 kmph highway cruise, 56 kmph highway cruise, and 56 kmph no load conditions. However, conditions were not equivalent to those required by EPA for vehicle certification and the test results should not be compared to those acquired by official certification methods and conditions.

Sampling and measurement methods included Andersen cascade impactors, conventional filtration techniques followed by condensers and organic sorbent traps, optical single particle counters, electrical mobility methods, and diffusional methods. All samples were taken directly from a modified exhaust pipe which was run out from under the chassis and alongside the passenger side of the automobile to permit reasonable access to the exhaust stream.

Andersen Model III cascade impactors with glass fiber impaction substrates and backup filters were used to obtain total particulate loadings and particle size distributions on a mass basis over the size range from about 0.4 μmA to 5 μmA. The impactors were operated in an oven close-coupled to the exhaust pipe. During runs at a steady engine load (56 kmph and 97 kmph), the oven was maintained at the same temperature as the exhaust gas temperature at the sampling point. During the 13 minute FET cycle testing, the impactors and ovens were maintained at about the average exhaust gas temperature for the cycle, 175°C.

In addition to the cascade impactors, a Thermosystems Model 3030 Electrical Aerosol Analyzer (EAA) was used to determine concentrations and size distributions of particles in the size range of 0.01 μm to 0.5 μm. Particle concentrations ranging from 0.3 μm to 2.5 μm were monitored using a Royco Model 225 optical particle counter. The Southern Research Institute SEDS III sample extraction, conditioning, and dilution system was used as an interface between the exhaust system and the EAA and particle counter. This system provides a mechanism for the removal of condensible vapors from the sample gas stream at elevated temperatures followed by quantitative dilution to particle concentrations within the operating ranges of the measurement instruments.

Figure 1 is a diagrammatic sketch of the layout of the exhaust system and measurement instrumentation during the tests.

The vehicle operating conditions were selected to provide samples collected at elevated exhaust gas temperatures prior to cooling for the same engine cycle as the very large (10 kg) sample collected for bioassay work. This 10 kg bioassay sample was being collected using the FET test cycle using a standard "constant volume" automatic dilution tunnel. The hot samples collected were to be used for Ames tests to provide some indication

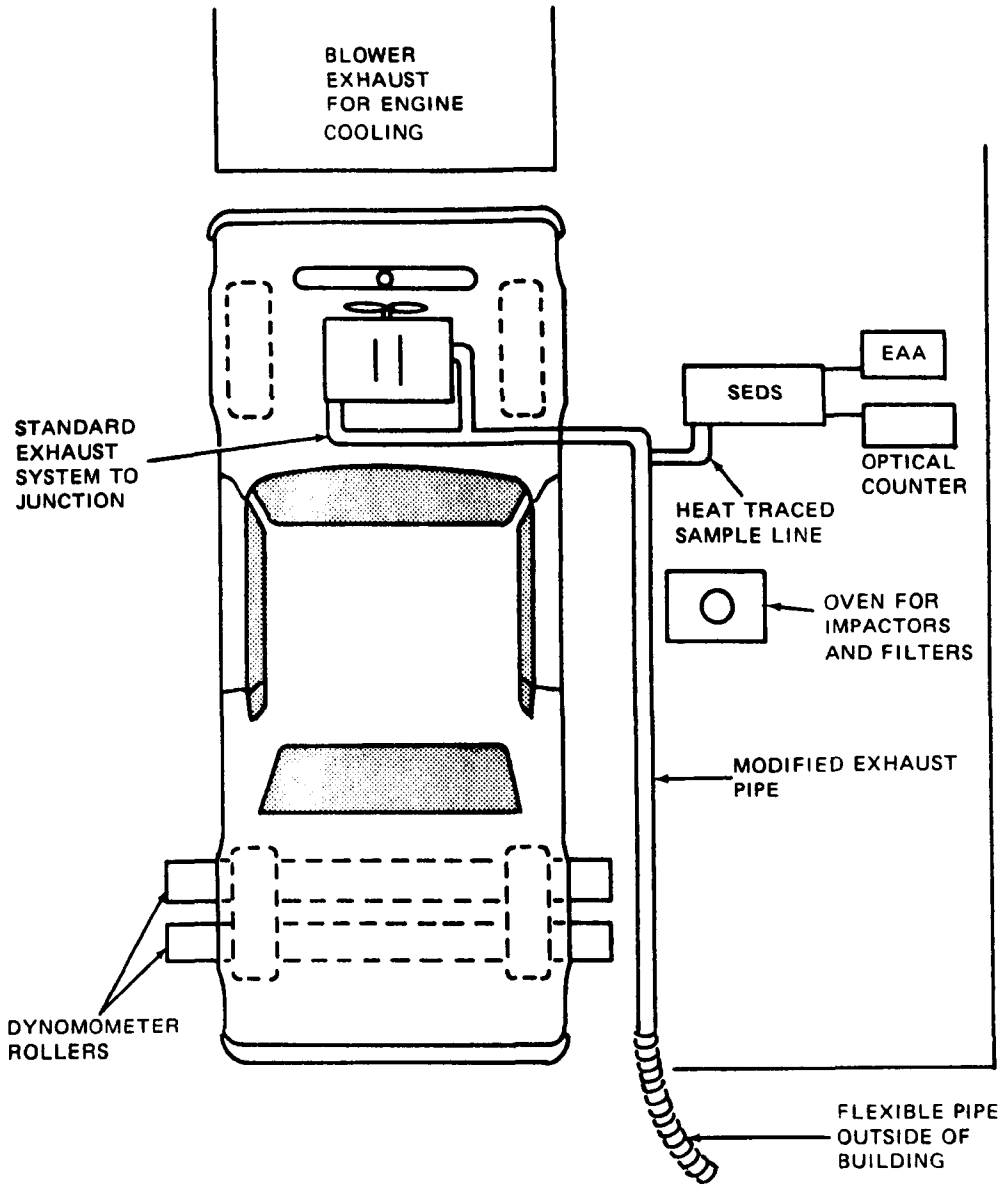

Figure 1. Modified exhaust pipe and test equipment layout for diesel emission testing.

of the relative mutagenicity of material collected at the exhaust line temperatures and material collected after cooling and dilution. This information is intended to provide some insight into whether hot collection of the particles will remove the carcinogenic component of the exhaust. In the program as originally conceived, samples were to be taken at a number of points between the exhaust manifold and the tailpipe to provide samples collected over a range of temperatures and engine loads. These would have provided information on changes in particle size distribution and composition as the exhasut gases were cooled. Time limitations in preparing for the tests rendered it impossible to carry out the proposed plan. However, it was found that a considerable swing in gas temperature did occur with changes in engine load. However it is not possible to differentiate between engine load/speed induced and temperature induced concentration and composition changes in the data obtained during this test.

Overall particulate loadings, engine gas flows, and sampling temperatures for the cascade impactor samples are given in Table I. Particle size distributions for the various conditions are given in Figures 2, 3, 4 and 5. Each figure in this series contains a plot of cumulative percentage smaller than the indicated diameter versus diameter from the impactor data alone and that obtained by integrating the distributions from the electrical aerosol analyzer up to 0.5 μm and continuing the integration from 0.5 μm to 10 μm with the impactor data. A particle density of 1.0 g/cm^3 was assumed for the integrations of the EAA data. The overall size distributions from 0.01 μm to 10 μm obtained in this fashion agree very well with those obtained from the impactors alone.

The variability in particulate concentrations through the FET cycle is illustrated in Figure 6. This shows particle concentrations versus time in three particle size intervals through several test cycles. These data were obtained using the optical particle counter.

The particulates collected at exhaust gas temperatures were found to be approximately 15 percent by mass organics. The results of the biotesting of the samples from the impactors, filters, and organic vapor traps will be reported elsewhere.

Conclusions

Typical particulate concentrations at exhaust line conditions for the Oldsmobile 350 CID diesel engine were found to be about 50 mg/NCM. Aerodynamic mass median diameters were about 0.3 to 0.5 μm with larger medium diameters being obtained from higher

TABLE I. RESULTS OF CASCADE IMPACTOR SAMPLING

Operating mode	Average exhaust volume flowrate (m^3/s)	Average exhaust temperature at sampling location (^oC)	Particulate loading (mg/NCM)	Aerodynamic mass median particle diameter (μmA)
FET cycle	0.051	177	68	0.26
97 kmph	0.057	218	55	0.54
56 kmph (with load)	0.033	149	45	0.46
56 kmph (no load)	(Not Available)	129	39	0.33

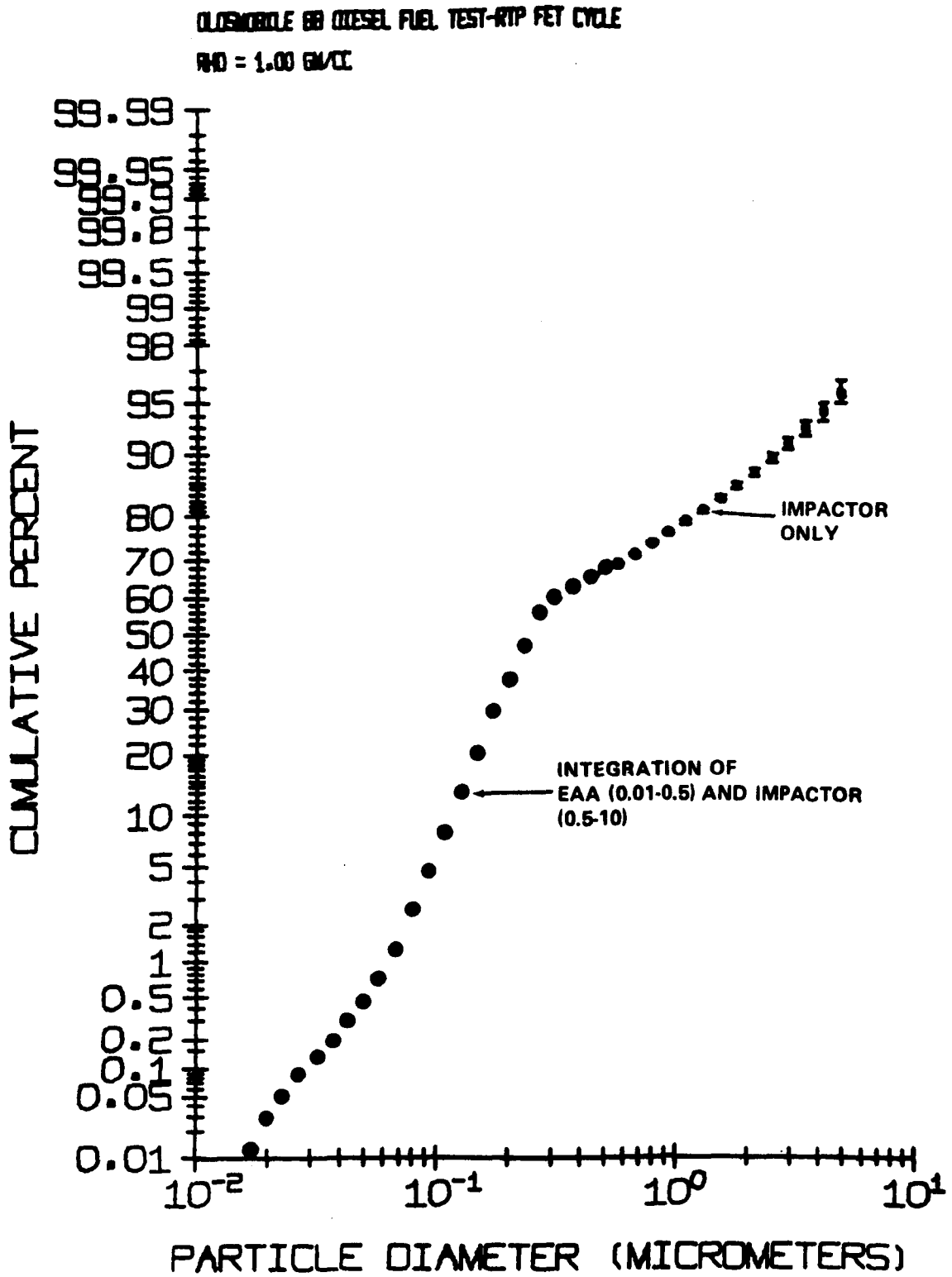

Figure 2. Particle size distribution for FET-cycle.

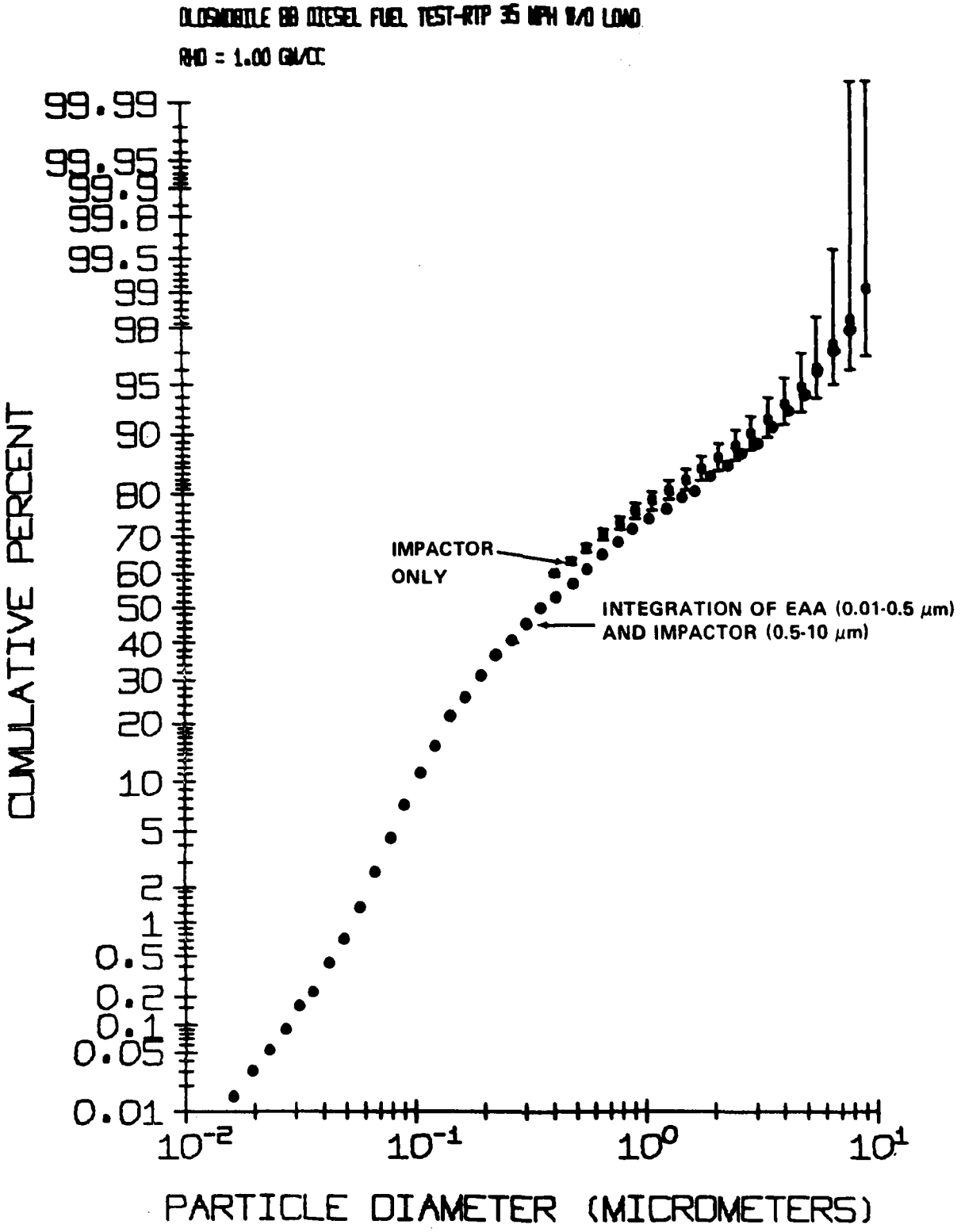

Figure 3. Particle size distribution for 35 mph no load condition.

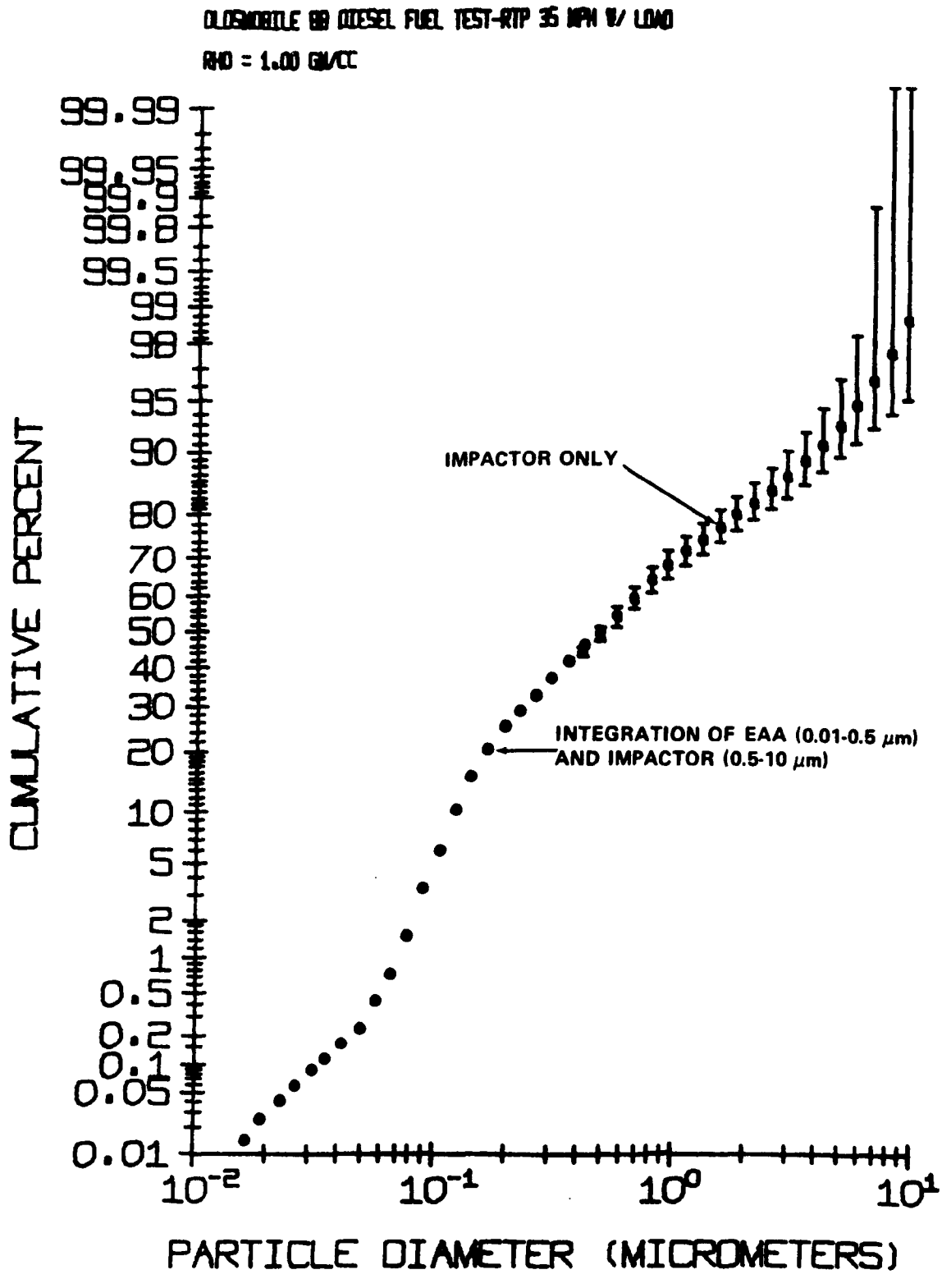

Figure 4. Particle size distribution for 35 mph with load condition.

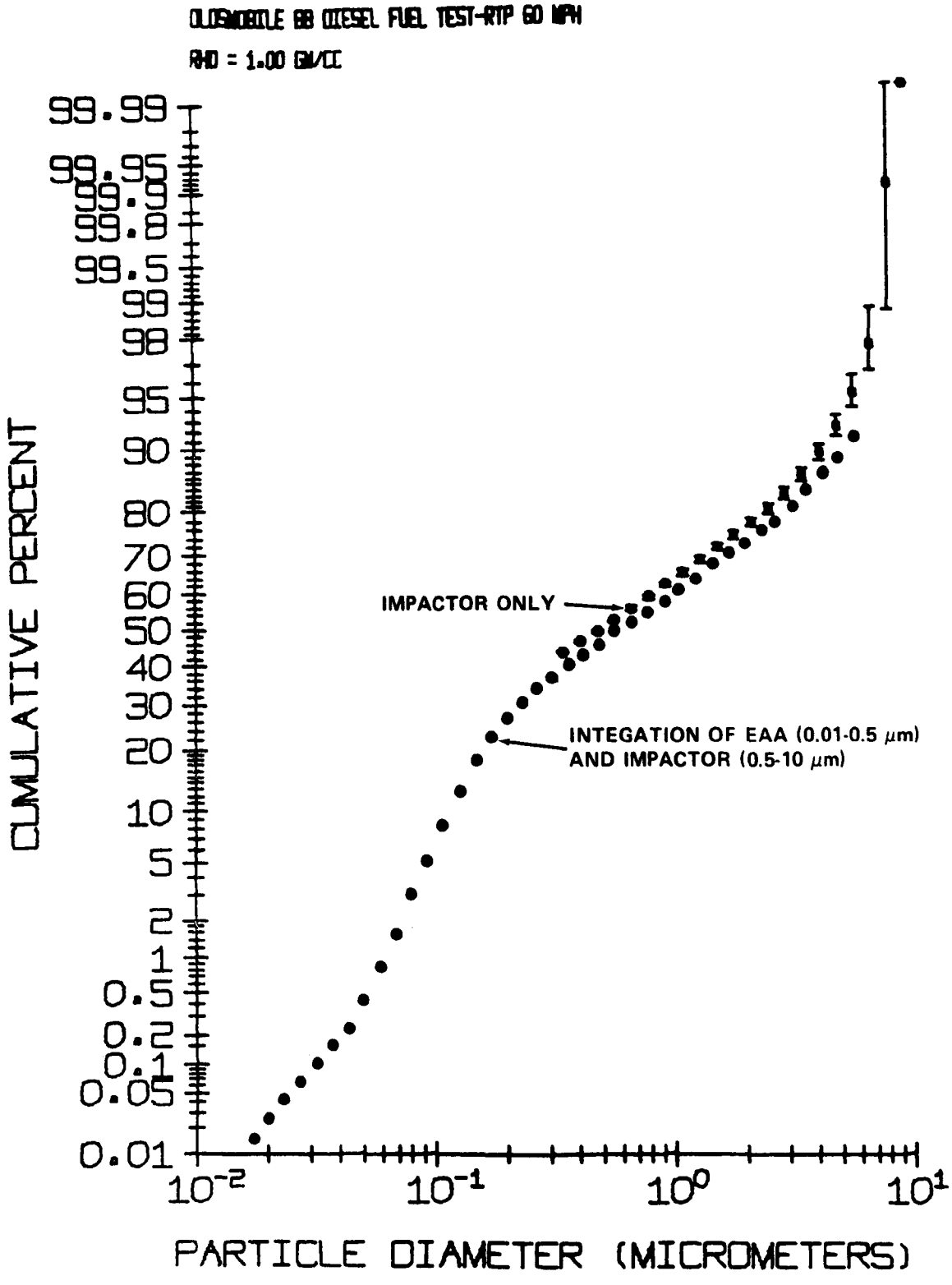

Figure 5. Particle size distribution for 60 mph condition.

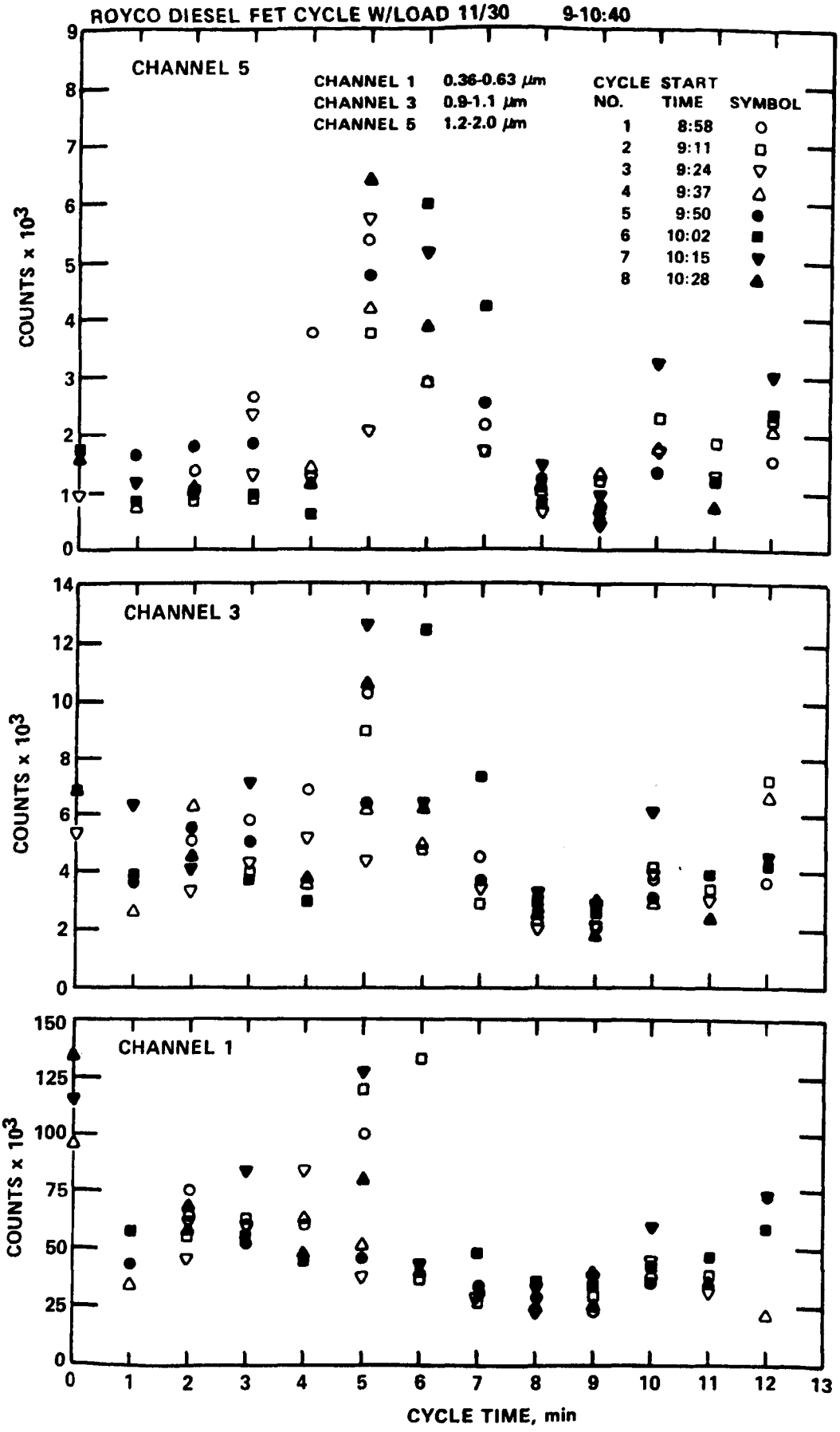

Figure 6. Relative concentration versus time for three particle size ranges during several FET cycles.

engine speed/load conditions under steady state operating conditions. The results reported here are qualitatively similar in size distribution to those found by other investigators in measurements of emissions from heavy duty diesel engines insofar as the impactor data are concerned.[2,3]

References

1. Blacker, S.M. EPA Program to Assess the Public Health Significance of Diesel Emissions. Journal of the Air Pollution Control Assoc. Vol 28, page 769, August 1978.

2. Lipkea, W.H., J.H. Johnson, and C.T. Vuk. The Physical and Chemical Character of Diesel Particulate Emissions - Measurement Technique and Fundamental Considerations. SAE Paper # 780108, presented at the SAE Congress and Exposition, Detroit, Michigan, February 27-March 3, 1978.

3. Springer, K., and R. Stahman. Removal of Exhaust Particulate from a Mercedes 300D Diesel Car. SAE Paper # 770716, presented at the SAE Off-Highway Vehicle Meeting and Exhibition, Mecca, Milwaukee, Wisconsin, September 12-15, 1977.

APPENDIX II

VAPOR PRESSURE VERSUS TEMPERATURE DATA ON ORGANIC COMPOUNDS LISTED BY MENTSER AND SHARKY[13] FOR DIESEL EXHAUST

APPENDIX II. VAPOR PRESSURE VS. TEMPERATURE DATA ON ORGANIC COMPOUNDS LISTED FOR DIESEL EXHAUST

	Possible compound	Molecular weight	Formula	Melting Point, °C	Boiling point, °C at 760 mm	Vapor pressure (mmHg) at various temperatures						Ref	Comments
						25°C	50°C	75°C	100°C	125°C	150°C		
1	Crotonaldehyde	70.0417	C_4H_6O	-74	104	25.1	88.4	260.1	662.0	1498.7	3080.4	CRC	Reported values based on only two P-T data points
2	β-Propiolactone	72.0210	$C_3H_4O_2$	-33.4	162 (decomp.)	2.4	10.4	36.1	106.2	272.9	627.4	CRC	Decomposes at bp (162°C)
3	2-Butanone	72.0573	C_4H_8O	-86.35	79.6	90.2	267.2	656.9	1400.8	2673.0	4669.7	Antoine	
	Tetrahydrofuran	72.0573	C_4H_8O	-108.5	66	166.5	439.4	1009.0	-	-	-	CRC	
4	Pentane	72.0936	C_5H_{12}	-129.72	36.07	512.5	1193.8	2423.0	4420.7	7414.0	11620.4	Antoine	
5	Ethyl Formate	74.0366	$C_3H_6O_2$	-80	54.3	258.1	652.2	1442.5	2868.4	5232.3	8889.9	CRC	
	Glycidol	74.0366	$C_3H_6O_2$	-	166.5	0.5	2.6	11.1	38.5	114.4	298.9	CRC	Reported values based on sketchy data. Linearity of plot of log P vs. I/T is poor.
	Methyl Acetate	74.0366	$C_3H_6O_2$	-98.7	57.8	224.4	582.2	1317.0	2670.6	4955.4	8547.2	CRC	
6	Carbon Disulfide	75.9442	CS_2	-110.8	46.5	358.4	852.1	1789.0	3400.7	5963.4	9786.0	CRC	
7	Benzene	78.0468	C_6H_6	+5.5	80.1	95.2	271.3	647.8	1350.5	2531.8	4360.8	Antoine	
8	Pyridine	79.0421	C_5H_5N	-42	115.4	21.4	70.0	193.6	467.2	1009.3	1990.7	CRC	
9	Cyclohexene	82.0780	C_6H_{10}	-103.5	83.0	88.8	250.6	594.3	1233.6	2306.4	3966.3	Antoine	
10	Cyclohexane	84.0936	C_6H_{12}	+6.6	80.7	97.6	271.8	637.4	1310.1	2427.8	4141.7	Antoine	
11	Methyl Acrylate	86.0366	$C_4H_6O_2$	<-75	80.5	87.8	255.5	637.5	Polymerizes at bp (80.5°)			CRC	Polymerizes
12	2-Pentanone	86.0729	$C_5H_{10}O$	-77.8	103.3	16.1	68.1	234.5	684.0	1744.1	3981.5	CRC	
13	Hexane	86.1092	C_6H_{14}	-95.3	68.7	151.3	405.3	921.3	1845.0	3345.5	5602.6	Antoine	
14	Dioxane	88.0522	$C_4H_8O_2$	+11.8	101.1	39.8	122.5	320.9	738.9	1532.2	2915.1	CRC	
	Ethyl Acetate	88.0522	$C_4H_8O_2$	-82.4	77.1	95.4	287.6	717.7	1550.5	2993.1	5282.6	Antoine	
15	Toluene	92.0624	C_7H_8	-95.0	110.6	28.4	92.1	244.3	556.3	1124.1	2065.1	Antoine	
16	Aniline	93.0577	C_6H_7N	-6.2	184.4	0.6	3.5	14.1	45.4	122.2	285.2	Antoine	
17	Phenol	94.0417	C_6H_6O	+40.6	181.9	0.4	2.4	11.6	41.3	119.1	291.8	Antoine	
18	Furfural	96.0210	$C_5H_4O_2$	-36.5	161.8	1.6	7.4	27.2	83.8	224.4	534.9	CRC	
19	Furfuryl Alcohol	98.0366	$C_5H_6O_2$	-	170.0	0.6	3.3	14.0	48.8	145.1	379.6	CRC	
20	Mesityl Oxide	98.0729	$C_6H_{10}O$	-59	130.0	9.8	35.9	109.1	285.8	663.5	1394.4	CRC	
	Cyclohexanone	98.0729	$C_6H_{10}O$	-45.0	155.6	4.9	17.8	53.4	138.3	318.1	663.1	CRC	
21	Methyl Cyclohexane	98.1092	C_7H_{14}	-126.4	100.9	46.3	138.3	343.4	740.2	1428.2	2522.4	Antoine	
22	Cyclohexanol	100.0085	$C_6H_{12}O$	+23.9	161.0	1.6	7.3	27.9	83.7	225.2	538.8	CRC	
	2-Hexanone	100.0085	$C_6H_{12}O$	-56.9	127.5	4.1	20.0	77.6	250.8	699.3	1727.4	CRC	
23	Ethyl Acrylate	100.0522	$C_5H_8O_2$	-71.2	99.5	38.9	123.4	331.9	782.0	1654.3	3203.2	CRC	Polymerizes easily
	Methyl Methacrylate	100.0522	$C_5H_8O_2$	-	101.0	38.0	118.2	312.7	725.9	(1516.0)	2902.3	CRC	Polymerizes easily

(continued)

APPENDIX II (continued)

	Possible compound	Molecular weight	Formula	Melting Point, °C	Boiling point, °C at 760 mm	Vapor pressure (mmHg) at various temperatures 25°C	50°C	75°C	100°C	125°C	150°C	Ref	Comments
24	Heptane	100.1248	C_7H_{16}	-90.6	98.4	45.7	141.6	361.5	795.7	1560.9	2793.2	Antoine	
25	Styrene	104.0624	C_8H_8	-30.6	145.2	6.0	23.8	74.3	192.1p	430.6p	861.6p	Antoine	p = Polymerizes
26	Ethyl Benzene	106.0780	C_8H_{10}	-94.9	136.2	9.5	35.2	103.6	256.9	557.2	1086.0	Antoine	
	2-Xylene	106.0780	C_8H_{10}	-25.2	144.4	7.1	25.3	75.2	193.3	441.5	914.7	CRC	
	3-Xylene	106.0780	C_8H_{10}	-47.9	139.1	8.7	30.6	89.8	228.3	516.4	1060.5	CRC	
	4-Xylene	106.0780	C_8H_{10}	+13.3	138.3	9.2	31.9	93.1	235.3	529.1	1081.2	CRC	
27	Monomethylaniline	107.0733	C_7H_9N	-57	195.5	0.4	2.3	9.7	31.9	87.3	207.1	Antoine	
	o-Toluidine	107.0733	C_7H_9N	-16.3	199.7	0.3	1.7	7.5	26.0	73.7	179.3	Antoine	
28	p-Quinone	108.0210	$C_6H_4O_2$	+115.7	124 (decomp.)	0.1	0.7	3.8	16.2	(57.8)	-	SUB	SUB = Sublimation pressure Decomposes at 124°C
29	2-Cresol	108.0573	C_7H_8O	+30.8	190.8	0.3	1.8	8.7	31.6	92.2	227.1	Antoine	
	3-Cresol	108.0573	C_7H_8O	+10.9	202.8	0.2	1.1	5.2	19.4	59.3	154.8	Antoine	
	4-Cresol	108.0573	C_7H_8O	+35.5	201.8	0.1	0.8	4.5	18.3	58.5	154.8	Antoine	
30	Hydroquinone	110.0366	$C_6H_6O_2$	+173-4	285-7	8.6×10^{-6}	2.6×10^{-4}	4.8×10^{-3}	6.1×10^{-2}	0.6	3.9	CRC	
31	2-Methylcyclohexanone (dl)	112.0885	$C_7H_{12}O$	-13.9	165	0.2	1.4	8.0	35.3	129.3	405.7	CRC	dl = racemic mixture Reported values based on only two P-T data points
32	Allylglycidylether	114.0678	$C_6H_{10}O$	-100	153.9	4.6	17.0	52.1	137.5	321.1	678.3	VER.	
33	Octane	114.1404	C_8H_{18}	-56.8	125.6	14.0	50.4	144.8	351.2	746.0	1427.1	Antoine	
34	Vinyl Toluene	118.0780	C_9H_{10}	-	171.1	2.1	8.8	29.5	82.2	198.1	425.1	Dreis.	
	α-Methyl Styrene	118.0780	C_9H_{10}	-23.2	165.4 (Polymerizes)	2.4	10.8	36.6	101.6	241.1	506.2	Antoine	Polymerizes
35	Cumene	120.0936	C_9H_{12}	-96.0	152.4	5.1	18.6	56.9	149.7	348.7	734.9	CRC	
36	Naphthalene	128.0624	$C_{10}H_8$	+80.2	217.9	0.2	1.2	5.2	17.9	50.2	120.7	Antoine	
37	Isophorone	138.1041	$C_9H_{14}O$	-	215.2	0.5	2.0	7.3	22.2	58.8	138.8	CRC	
38	Phthalic Anhydride	148.0159	$C_8H_4O_3$	+131.6	295.1	5.2×10^{-4}	8.2×10^{-3}	8.8×10^{-2}	1.3	5.2	17.4	SUB/CRC	
39	p-tert-Butyltoluene	148.1248	$C_{11}H_{16}$	-62.5	192.8	0.8	3.7	13.0	39.1	101.9	237.4	CRC	Values reported are those for 3-ethylcumene
40	Phenylglycidylether	150.0678	$C_9H_{10}O_2$	+3.5	245	1.5×10^{-2}	0.1	0.6	2.6	9.2	28.4	VER.	Reported values based on only two P-T data points
41	Camphor	152.1197	$C_{10}H_{16}O$	+178.5	209.2	0.4	1.7	6.7	21.7	60.6	149.9	SUB	
42	Diphenyl	154.0782	$C_{12}H_{10}$	+69.5	254.9	0.1	0.3	1.3	4.5	13.7	36.0	CRC	

(continued)

APPENDIX II (continued)

	Possible compound	Molecular weight	Formula	Melting Point, °C	Boiling point, °C at 760 mm	Vapor pressure (mmHg) at various temperatures 25°C	50°C	75°C	100°C	125°C	150°C	Ref	Comments
43	Phenylether	170.0729	$C_{12}H_{10}O$	+27	258.5	3.3×10^{-2}	0.2	1.0	3.9	12.3	33.2	Antoine	
44	Anthracene	178.0780	$C_{14}H_{10}$	+217.5	342.0	6.2×10^{-6}	1.5×10^{-4}	2.3×10^{-3}	2.4×10^{-2}	0.2	1.4	SUB/CRC	
	Phenanthrene	178.0780	$C_{14}H_{10}$	+99.5	340.2	1.7×10^{-4}	2.5×10^{-3}	2.6×10^{-2}	0.2	1.4	4.1	SUB/CRC	
45	Dinitro-o-cresol	198.0275	$C_7H_6N_2O_5$	+87.5	-	1.1×10^{-4}	2.7×10^{-3}	4.3×10^{-2}	0.5	3.8	23.9	SUB	
46	Pyrene	202.0780	$C_{16}H_{10}$	+156	404	7.0×10^{-6}	1.3×10^{-4}	1.5×10^{-3}	1.3×10^{-2}	8.3×10^{-2}	4.3×10^{-1}	Pupp	
	Benz[a]anthracene	228.28	$C_{18}H_{12}$	=160	Sublimes	1.1×10^{-7}	3.9×10^{-6}	8.1×10^{-5}	1.1×10^{-3}	1.1×10^{-2}	8.4×10^{-2}	Murray	Vapor pressure data was found only for benz[a]anthracene. However, the compounds in this group are structurally similar and should all have very similar vapor pressures.
47	Chrysene	228.0936	$C_{18}H_{12}$	+225	448	1.1×10^{-7}	3.9×10^{-6}	8.1×10^{-5}	1.1×10^{-3}	1.1×10^{-2}	8.4×10^{-2}		
	Benzo[c]phenanthrene			+68	-	1.1×10^{-7}	3.9×10^{-6}	8.1×10^{-5}	1.1×10^{-3}	1.1×10^{-2}	8.4×10^{-2}		
48	7,12-Dimethyl-benz[a]anthracene	256.1248	$C_{20}H_{16}$	+122-3	-	1.1×10^{-7}	3.9×10^{-6}	8.1×10^{-5}	1.1×10^{-3}	1.1×10^{-2}	8.4×10^{-2}		
	Benzo[k]fluoranthene			+217	480	9.7×10^{-10}	5.6×10^{-8}	1.8×10^{-6}	3.7×10^{-5}	5.1×10^{-4}	5.2×10^{-3}	Pupp	Vapor pressure data was found only for benzo[k]fluoranthene. However, the compounds in this group are structurally similar and should all have very similar vapor pressures. V.P. values of benzo[k]-fluoranthene based on measurements from samples with significant impurities (~10%).
49	Benzo[b]fluoranthene	252.0936	$C_{20}H_{12}$	+168	-	9.7×10^{-10}	5.6×10^{-8}	1.8×10^{-6}	3.7×10^{-5}	5.1×10^{-4}	5.2×10^{-3}		
49	Benzo[j]fluoranthene	252.0936	$C_{20}H_{12}$	+166	-	9.7×10^{-10}	5.6×10^{-8}	1.8×10^{-6}	3.7×10^{-5}	5.1×10^{-4}	5.2×10^{-3}		
50	Cholanthrene	254.1092	$C_{20}H_{14}$	+175 d	Sublimes	9.7×10^{-10}	5.6×10^{-8}	1.8×10^{-6}	3.7×10^{-5}	5.1×10^{-4}	5.2×10^{-3}		
49	Benzo[e]pyrene	252.0936	$C_{20}H_{12}$	=177	-	5.6×10^{-9}	2.3×10^{-7}	5.4×10^{-6}	8.3×10^{-5}	9.1×10^{-4}	7.5×10^{-3}	Murray	

(continued)

APPENDIX II (concluded)

Additional possible compounds	Molecular weight	Formula	Melting Point, °C	Boiling point, °C at 760 mm	Vapor pressure (mmHg) at various temperatures 25°C	50°C	75°C	100°C	125°C	150°C	Ref	Conc'n in diesel exhaust, ppm[†]	Comments
VAPOR PRESSURE VS. TEMPERATURE DATA ON ADDITIONAL ORGANIC COMPOUNDS[†]													
Formaldehyde	30.03	CH_2O	-92	-21	← GAS →						-	18.3 ppm	
Acetaldehyde	44.05	C_2H_4O	-121	+20.8	910.2	2096.0	4029.5	7606.6	12646.2	19664.3	Smith	3.2 ppm	
Acrolein	56.06	C_3H_4O	-87	53	272.0	700.7	-	-	-	-	CRC		
Acetone	58.08	C_3H_6O	-95	56.2	230.0	612.7	1385.2	2761.4	4986.8	8321.3	Antoine	2.9 ppm	
Proprionaldehyde	58.08	C_3H_6O	-81	48.8	318.7	816.5	1793.1	3495.2	6201.6	10204.1	Smith		Reported values based on only two P-T data points.
Isobutyraldehyde	72.10	C_4H_8O	-66	64	208.2	521.6	-	-	-	-	VER.		
n-Butyraldehyde	72.10	C_4H_8O	-99	76	112.3	319.4	765.8	1608.1	3041.8	5290.9	Smith	0.3 ppm	Reported values based on only two P-T data points.
n-Valeraldehyde	86.13	$C_5H_{10}O$	-92	103	50.0	138.0	329.2	699.0	-	-	VER.	0.4 ppm[‡]	
Hexaldehyde	100.16	$C_6H_{12}O$	-56	128	13.1	44.5	126.9	314.6	695.6	-	VER.	0.2 ppm	Reported values based on only two P-T data points.
Benzaldehyde	106.12	C_7H_6O	-26	178.1	1.0	4.8	18.1	57.5	157.7	384.2	CRC	0.2 ppm	

Key to References

CRC - Vapor pressure values were obtained from a linear least squares analysis of $\log_{10}P$ (mmHg) vs $1/T(^\circ K)$ from data given in the Handbook of Chemistry and Physics, 57th ed, Robert C. Weast, Ed. CRC Press, Cleveland, Ohio, 1976.

Antoine - Vapor pressure values were calculated from the Antoine Equation: $\log_{10}P(mm) = A - B/[C+t(^\circ C)]$. Values of A, B, and C were obtained from Lange's Handbook of Chemistry, 11th ed., J.A. Dean, Ed., McGraw Hill Book Company, New York, N.Y., 1967.

SUB - Vapor pressure values were calculated from the empirical equation: $\log_{10}P(mm) = A - B/T(^\circ K)$. Values of A and B were obtained from the Handbook of Chemistry and Physics, 57th ed, "Sublimation Data For Organic Compounds."

VER. - Vapor pressure values were obtained from a linear least squares anslysis of $\log_{10}P(mm)$ vs. $1/T(^\circ K)$ from data given in Karel Verschueren's "Handbook of Environmental Data on Organic Chemicals," Van Nostrand Reinhold Company, New York, N.Y., 1977, 659 pp.

Dreis. - Vapor pressure values were calculated from the Antoine equation. Values of A, B, and C were obtained from: Dreisbach, R.R. and R.A. Martin, Ind. Eng. Chem. 41, 2875 (1949).

Pupp - Vapor pressure values were calculated from the empirical equation $\log_{10}P(mm) = \frac{A}{T(^\circ K)} + B$. Values of A and B were obtained from: Pupp, C., R.C. Lao, J.J. Murray, and R.F. Pottie, Atmos. Envir., 8, 915 (1974).

Murray - Vapor pressure values were calculated from the empirical equation $\log_{10}P(mm) = \frac{A}{T(^\circ K)} + B$. Values of A and B were obtained from: Murray, J.J., R.F. Pottie, and C. Pupp, Can. J. Chem., 52, 557 (1974).

Smith - Vapor pressure values were calculated from the Antoine equation. Values of A, B, and C were obtained from: Smith, T.E. and R.F. Bonner, Ind. Eng. Chem., 43, 1169 (1951).

[†] Vogh, J.W. Nature of Odor Components in Diesel Exhaust. J. Air. Pollut. Control Assoc., 19, 773 (1969).

[‡] Combined concentration of crotonaldehyde and n-valeraldehyde

BIBLIOGRAPHY

GENERAL INFORMATION

Ramchandani, M. and N. D. Whitehouse. Heat Transfer in a Piston of a Four Stroke Diesel Engine. Applied Technology Associates, Inc. and Institute of Science and Technology, Univ. of Manchester, United Kingdom. SAE Paper No. 760007.

Das, P. K. Analysis of Piston Ring Lubrication. John Deere Product Engineering Center.

Davison, C. H. Plain Bearings for the High Speed Diesel Engine. Vandervell Products, Ltd., United Kingdom. SAE Paper No. 760009.

Grundy, J. R., L. R. Kiley, and E. A. Brevick. AVCR 1360-2 High Specific Output-Variable Compression Ratio Diesel Engine. TELEDYNE CONTINENTAL MOTORS, General Products Division. SAE Paper No. 760051.

Larkinson, D. E., R. J. Neal, and W. J. Schultz. The Perkins 6.247 - The High Speed, High Economy Diesel Engine for North American Light Duty Applications. Perkins Engines Co. SAE Paper No. 760052.

Parker, R. F. Future Fuel Injection System Requirements of Diesel Engines for Mobile Power. John Deere Product Engineering Center. SAE Paper No. 760125.

Zimmermann, K. D. New Robert Busch Developments for Diesel Fuel Injection. Robert Busch GmbH, Germany. SAE Paper No. 760127.

Chiu, W. S., S. M. Shabed, and W. T. Lyn. A Transient Spray Mixing Model for Diesel Combustion. Cummins Engine Co., Inc. SAE Paper No. 760128.

Hiroyasu, H. and T. Kadota. Models for Combustion and Formation of Nitric Oxide and Soot in Direct Injection. University of Hiroshima. SAE Paper No. 760129.

Bechtold, R. L. and S. S. Lestz. Combustion Characteristics of Diesel Fuel Blends. Pennsylvania State University. SAE Paper No. 760132.

Becker, K. The Influence of an Ignition Accelerator on the Ignition Quality and Anti-Knock Properties of Light Hydrocarbons in the Diesel Engine. Umweltbundesamt, West Germany. SAE Paper No. 760163.

Uyehara, O. A. Diesel Vehicles? - Crude Oil Scene. Dept. of Mechanical Engineering, University of Wisconsin, Madison. SAE Paper No. 760210.

Hayashi, Y. A Series of Light Duty Indirect Injection Engines. Nissan Diesel Motor Co., Japan. SAE Paper No. 760212.

Matsuoka, S., K. Yokota, T. Kamimoto, and M. Igoshi. A Study of Fuel Injection Systems in Diesel Engines. Matsuoka-Tokyo Institute of Technology, Yokota-Isuzu Motors Co., Kaminoto-Tokyo Institute of Technology and Igoshi-Japan Soc. for Promotion of Mach. Indus., Japan. SAE Paper No. 760551.

McFarland, R. A. and C. D. Wood. An Analog Heat Release Computer for Engine Combustion Evaluation. Dept. of Engine and Vehicle Research, Southwest Research Institute. SAE Paper No. 760553.

Fleming, R. D. Fuel Economy of Light-Duty Diesel Vehicles. Bartlesville Energy Research Center. SAE Paper No. 760592.

Roehrle, M. D. Pistons for High Output Diesel Engines. Mable GmbH, Germany. SAE Paper No. 770031.

Neu, E. A., J. A. Wade, and A. C. Chu. Simulating the Lubricating System of a Diesel Engine. Cummins Engine Co. SAE Paper No. 770032.

Bertodo, R. Design and Development Criteria for Automotive Diesels. Perkins Engines Group Ltd., United Kingdom. SAE Paper No. 770033.

Benson, R. S. and G. I. Alexander. The Application of Pulse Converters to Automotive Four Stroke Cycle Engines. Benson-University of Manchester Institute of Science and Technology and Alexander-Liverpool Polytechnic, United Kingdom. SAE Paper No. 770034.

Voss, J. R. and R. E. Vanderpoel. The Shuttle Distributor for a Diesel Fuel Injection Pump. American Bosch Div., AMBAC Industries, Inc. SAE Paper No. 770083.

Kimberley, J. A. and R. A. DiDomenico. UFIS - A New Diesel Injection System. American Bosch Div., AMBAC Industries, Inc. SAE Paper No. 770084.

Hofbauer, P. and K. Sator. Advanced Automotive Power Systems, Part 2: A Diesel for a Sub-compact Car. Volkswagenwerk AG. SAE Paper No. 770113.

Winterbone, D. E., R. S. Benson, A. G. Mortimer, P. Kenyon, and A. Stotter. Transient Response of Turbo-charged Diesel Engines. Winterbone, Benson, Mortimer, and Kenyon - The University of Manchester Institute of Science and Technology, United Kingdom and Stotter-Technion-Israel Institute of Technology, Israel. SAE Paper No. 770122.

Watson, N. and M. Marzouk. A Non-Linear Digital Simulation of Turbocharged Diesel Engines Under Transient Conditions. Watson-Imperial College of Science and Technology and Marzouk-Imperial College of Science and Technology. SAE Paper No. 770123.

Winterbone, D. E., C. Thiruarooran, and P. E. Wellstead. A Wholly Dynamic Model of a Turbocharged Diesel Engine for Transfer Function Evaluation. Univ. of Manchester Inst. of Science and Technology, United Kingdom. SAE Paper No. 770124.

Bolis, D. A., J. Johnson, and R. Callen. A Study of the Effect of Oil and Coolant Temperatures on Diesel Engine Brake Specific Fuel Consumption. Michigan Technological University. SAE Paper No. 770313.

Haefele, K. Considerations in Redesigning a Gasoline Engine into a Diesel Engine for Passenger Car Service. Adam Opel A.G. SAE Paper No. 770314.

Barry, E. G., A. Ramella, and R. B. Smith. Potential Passenger Car Demand for Diesel Fuel and Refining Implications. Mobil Research and Development Corp. SAE Paper No. 770315.

Tippelmann, G. A New Method of Investigation of Swirl Ports. Consulting Engineer, Germany. SAE Paper No. 770404.

Tindal, M. J. and T. J. Williams. An Investigation of Cylinder Gas Motion in the Direct Injection Diesel Engine. Dept. of Mechanical Engineering, Univ. of London King's College. SAE Paper No. 770405.

Jagadeesan, T. R. and B. S. Murthy. Study of Air Motion in a Compression Ignition Engine Cylinder. Jagadeesan-Guindy Engineering College, India and Murthy-Indian Institute of Technology, India. SAE Paper No. 770406.

Dent, J. C. and S. J. Sulaiman. Convective and Radiative Heat Transfer in a High Swirl Direct Injection Diesel Engine. Dent-Univ. of Technology, Loughborough and Sulaiman-Univ. of Mosul, Mosul, Iraq. SAE Paper No. 770407.

Strahle, W. C. and J. C. Handley. Stochastic Combustion and Diesel Engine Noise. School of Aerospace Engineering, Georgia Inst. of Technology. SAE Paper No. 770408.

Whitehouse, N. D., E. Clough, and P. S. Roberts. Investigating Diesel Engine Combustion by Means of a Timed Sampling Valve. Dept. of Mechnical Engineering, The University of Manchester, Institute of Science and Technology. SAE Paper No. 770409.

Whitehouse, N. D. and N. Baluswamy. Calculations of Gaseous Products During Combustion in a Diesel Engine Using a Four Zone Model. Department of Mechanical Engineering, The University of Manchester, Institute of Science and Technology. SAE Paper No. 770410.

Woods, W. A. and A. Allison. Effective Flow Area of Piston Controlled Exhaust and Inlet Ports. Woods-Department of Mechanical Engineering, University of Liverpool, United Kingdom and Allison-Imperial Chemical Industries Ltd., United Kingdom. SAE Paper No. 770411.

Way, R. J. B. Investigation of Interaction Between Swirl and Jets in Direct Injection Diesel Engines Using a Water Model. Dept. of Mechanical Engineering, University of Bath, United Kingdom. SAE Paper No. 770412.

Kamimoto, T. and S. Matsuoka. Prediction of Spray Evaporation in Reciprocating Engines. Dept. of Mechanical Engineering. Tokyo Institute of Technology. SAE Paper No. 770413.

Hill, S. H. and J. L. Dodd. A Low NOx Lightweight Car Diesel Engine. Teledyne Continental Motors, General Products Division. SAE Paper No. 770430.

Suzuki, T. and T. Shiozaki. A New Combustion System for the Diesel Engine and Its Analysis Via High Speed Photography. Hino Motors, Ltd., Japan. SAE Paper No. 770674.

Martin, B. and G. Wright. High Output Diesel Engine Design Philosophy. Advanced Engines Dept., John Deere Product Engineering Center. SAE Paper No. 770755.

Wallace, F. J. and G. Winkler. Very High Output Diesel Engines - A Critical Comparison of Two Stage Turbocharged, Hyperbar, and Differential Compound Engines. University of Bath, United Kingdom. SAE Paper No. 770756.

Barnes-Moss, H. W., A. R. Crouch, P. J. S. Ritchie, and K. C. Barnes-Moss. The Design and Development of a Heavy-Duty, Off-Highway Diesel Engine Family: Part 1 - Engine Concept and Design. Part 2 - Component Testing and Engine Development. Ricardo & Co. Engineers (1927) Ltd., England. SAE Paper No. 770775.

Kanesaka, H., K. Akiba, and H. Sakai. A New Method of Valve Cam Design. Kanesaka and Akiba-Isuzu Motors Ltd., Japan and Sakai-University of Tokyo. SAE Paper No. 770777.

Dent, J. C., J. H. Keightley, and C. D. DeBoer. The Application of Interferometry to Air Fuel Ratio Measurement in Quiescent Chamber Diesel Engines. Loughborough University of Technology, England. SAE Paper No. 770825.

Rounds, F. G. Carbon: Cause of Diesel Engine Wear? G. M. Research Laboratories. SAE Paper No. 770829.

Henein, N. A. and J. D. Rozanski. A Technique for the Diagnosis of Malfunctions in Diesel Injection Systems. Wayne State Univ. and U.S. Army TARADCOM. SAE Paper No. 780033.

Kamo, R. and W. Bryzik. Adiabatic Turbocompound Engine Performance Prediction. Cummins Engine Co. and U.S. Army TARADCOM. SAE Paper No. 780068.

Stang, J. H. Designing Adiabatic Engine Components. Cummins Engine Co., Inc., Columbus, IN. SAE Paper No. 780069.

Torti, M. L., J. W. Lucek, and G. Q. Weaver. Densified Silicon Carbide - An Interesting Material for Diesel Applications. Norton Co., Worcester, MA. SAE Paper No. 780071.

Scullen, R. S. and R. J. Hames. Computer Simulation of the GM Unit Injector. Detroit Diesel Allison Div., General Motors Corp. SAE Paper No. 780161.

Goyal, M. Modular Approach to Fuel Injection System Simulation. John Deere Product Engineering Center. SAE Paper No. 780162.

Mowbray, D. F. and M. Drori. The CAV DP15 Fuel Injection Pump. CAV Ltd., United Kingdom. SAE Paper No. 780163.

Meguerdichian, M. and N. Watson. Prediction of Mixture Formation and Heat Release in Diesel Engines. Imperial College of Science and Technology, London, England. SAE Paper No. 780225.

Voiculescu, I. A. and G. L. Borman. An Experimental Study of Diesel Engine Cylinder - Averaged NOx Histories. Voiculescu-National Institute for Thermal Engines, Brasov, Rumania and Burman-Mech. Eng. Dept., Univ. of Wisconsin-Madison, Madison, Wisconsin. SAE Paper No. 780228.

Talder, R. W., J. D. Fleming, D. C. Siegla, and C. A. Amann. Dynamometer-Based Evaluation of Low Oxides of Nitrogen, Advanced Concept Diesel Engine for a Passenger Car. General Motors Research Lab. SAE Paper No. 780343.

Arai, Y., Y. Yoshida, and M. Matsushita. Isuzu's New 5.8L Direct Injection Diesel Engine. Isuz Motors Ltd., Japan. SAE Paper No. 780349.

Jones, J. H., W. L. Kingsbury, H. H. Lyon, P. R. Mutty, and K. W. Thurston. Development of a 5.7 Litre V8 Automobile Diesel Engine. Oldsmobile Div. GMC. SAE Paper No. 780412.

Patton, D. W. Improving Serviceability. Cummins Engine Co., Inc. SAE Paper No. 780431.

Scott, W. M. Looking in on Diesel Combustion. SAE Publication No. SP-345.

Diesels from the Woodshed. SAE Publication No. SP-357.

Diesel Engine Noise. SAE Publication No. SP-397.

Boyce, T. R., G. A. Karim, and H. P. W. Moore. The Effects of Some Chemical Factors on Combustion Processes in Diesel Engines - Diesel Engine Combustion. Proceedings: Inst. of Mech. Engineers 184:Part 3J (1969-1970).

Gaal, S. L., J. P. Peer, G. L. Muntean, and H. L. Wilson. The PT-Econ-A New Injector Concept for the DI Diesel to Improve Smoke and Fuel Consumption at Low Emission Levels. Paper presented at the Eleventh International Congress on Combustion Engines, Barcelona, 1975.

Schmidt, P. R. Diesel Fuel Oils. Chapter 26, page 244 from Fuel Oil Manual. Industrial Press, New York, New York, 1969.

Standard Classification of Diesel Fuel Oils. D975, Annual Book of ASTM Standards, Part 17, p. 325, 1973. American Society for Testing and Materials, Philadelphia, PA.

Shamah, E. and T. O. Wagner. Fuel Quality or Engine Design: Which Controls Diesel Emissions, January 1973. SAE Paper No. 730168.

Mickel, B. L. and L. D. Fergesen. Dimensions of Diesel Fuel Performance - Design, Depressants and Response, June 1966. SAE Paper No. 660371.

Bayreis, K. A., V. P. Catto, and E. S. Swanson. Role of Flow Improvers in Solving Auto-Diesel Winter Fuel Problems, 1966. SAE Paper No. 660372.

Khan, I. M., C. H. T. Wang, and B. E. Langridge. Coagulation and Combustion of Soot Particles in Diesel Engines. Combustion and Flame 17:409 (1971).

Khan, I. M. Formation and Combustion of Carbon in a Diesel Engine, from Diesel Engine Combusiton. Proceedings - Inst. of Mech. Engineers 184:36, Part 3J (1969-1970).

Used Diesel Crankcase Oil - If You Can't Recycle It, Why Not Burn It in the Engine? Chevron Research Special Report, Chevron Research Co., 1975.

Weatherford, W. D., Jr., and B. R. Wright. Corrective Action Program for Bromochloromethane - Containing Fire-Safe Diesel Fuels. SwRI Final Report AFLRL No. 81, September 1976.

Gray, J. T. and A. A. Johnston. Engine Experiments with Fire Safe Fuels. SwRI Final Report AFLRL No. 31, January 1975.

Wimer, W. W., B. R. Wright, and W. D. Weatherford, Jr. Ignition and Flammability Properties of "Fail-Safe Fuels". SwRI Interim Report AFLRL No. 39.

Karlovsky, J., Jr. Engineering Criteria for Selecting Diesel- or Electric-Powered Equipment for Underground Mining Application. IC8666, U.S. Department of the Interior, Proceedings of the Symposium on the Use of Diesel-Powered Equipment in Underground Mining, Pittsburg, Pennsylvania, January 30-31, 1973.

Fischer, W. G. Case History of Diesel Use: FMC Corporation Green River Trona Mine, Wyoming. IC8666, U.S. Department of the Interior, Proceedings of the Symposium on the Use of Diesel-Powered Equipment in Underground Mining, Pittsburg, Pennsylvania, January 30-31, 1973.

Henderson, R. D. Diesel Technology. IC8666, U.S. Department of the Interior, Proceedings of the Symposium on the Use of Diesel-Powered Equipment in Underground Mining, Pittsburgh, Pennsylvania, January 30-31, 1973.

Higginson, N. Use of Diesel Engines Underground in British Coal Mines. IC8666, U.S. Department of the Interior, Proceedings of the Symposium on the Use of Diesel-Powered Equipment in Underground Mining, Pittsburgh, Pennsylvania, January 30-31, 1973.

Goldrath, B. Diesels in Underground Mining. Diesel and Gas Turbine Progress, 33-34, August 1977.

Countryman, D. L. Diesel Powered Underground Mining Equipment, Sept. 13-16, 1976. SAE Paper No. 760651.

Zorychta, H. Canadian Experience Using Diesels in Underground Coal Mines. Proceedings of the Symposium on the Use of Diesel-Powered Equipment in Underground Mines, Pittsburg, Pennsylvania, January 30-31, 1973.

Bosecker, R. E. and D. F. Webster. Precombustion Chamber Diesel Engine Emissions - A Progress Report. SAE Paper No. 710672.

General Motors Response to EPA Notice of Proposed Regulation for Light-Duty Diesel Vehicles. Submitted to the Environmental Protection Agency, April 19, 1979.

Russell, M. F. Recent CAV Research into Noise, Emissions, and Fuel Economy of Diesel Engines, 1977. SAE Paper No. 770257.

Summary Report on the Evaluation of Light-Duty Diesel Vehicles. Technology Assessment and Evaluation Branch, Emission Control Technology Division, Office of Mobile Source Air Pollution Control, Environmental Protection Agency, March 1975.

Bolis, D. A. The Effect of Oil and Coolant Temperatures on Diesel Engine Specific Fuel Consumption and Wear. M.S. Thesis, Michigan Technological University, 1976.

Bolis, D. A., J. H. Johnson, and D. A. Daavettila. The Effect of Oil and Coolant Temperature on Diesel Engine Wear, 1977. SAE Paper No. 770086.

Hofman, M. V. and J. H. Johnson. The Development of Ferrography as a Laboratory Wear Measurement Method for the Study of Engine Operating Conditions on Diesel Engine Wear. WEAR (Pub. in 1977) (also M.S. Thesis, Michigan Technological University, 1977, for M. V. Hofman.

Springer, K. J. An Investigation of Diesel-Powered Vehicle Odor and Smoke - Part I. Final Report to the Department of Health, Education, and Welfare under Contract No. PH86-66-93, March, 1967.

Springer, K. J. and R. C. Stahman. An Investigation of Diesel-Powered Vehicle Odor and Smoke. Paper FL-66-46 presented at the NPRA Fuels and Lubricants Meeting, Philadelphia, September 15-16, 1966.

Springer, K. J. An Investigation of Diesel-Powered Vehicle Odor and Smoke - Part II. Final Report to the Department of Health, Education, and Welfare under Contract No. PH 86-67-72, February 1968.

Springer, K. J. An Investigation of Diesel-Powered Vehicle Odor and Smoke - Part III. Final Report to the Department of Health, Education, and Welfare under Contract No. PH 22-68-23, October 1969.

Springer, K. J. and H. E. Dietzmann. An Investigation of Diesel-Powered Vehicle Odor and Smoke - Part IV. Final Report to the Department of Health, Education, and Welfare under Contract No. PH 22-68-23, April 1971.

Springer, K. J. Emissions from Diesel and Stratified Charge-Powered Cars. Final Report to the Environmental Protection Agency under Contract No. PH 22-68-23, Dec. 1974. EPA-460/3-75-001-a.

Springer, K. J. and R. C. Stahman. Emissions and Economy of Four Diesel Cars. Presented at SAE Automotive Engineering Congress and Exposition, Detroit, February 24-28, 1975. SAE Paper No. 750332.

Springer, K. J. and A. H. Ashby. The Low Emission Car for 1975 - Enter the Diesel. Paper 739133 presented at Eighth Annual IECEC Meeting, Philadelphia, August 13-16, 1973.

Oblander, K. and M. Fortnagel. Design and Results of the Five-Cylinder Mercedes-Benz Diesel Engine. Presented at SAE Automobile Engineering Meeting, Detroit, October 13-17, 1975. SAE Paper No. 750870.

Diesel Fuel Oils, 1973. Bureau of Mines Petroleum Products Survey, No. 82, November 1973.

Springer, K. J. and R. C. Stahman. Unregulated Emissions from Diesels Used in Trucks and Buses. Presented at the International Automotive Engineering Congress and Exposition, Cobo Hall, Detroit, February 28-March 4, 1977. SAE Paper No. 770258.

Stahman, R. C., J. P. Dekany. The Diesel Emission Program of the Environmental Protection Agency. Presented at the API Farm and Construction Equipment Fuels and Lubricants Forum, Mariott Motor Inn, Chicago, Illinois, February 1973.

Duggal, V. K. and T. Priede. A Study of Pollutant Formation within the Combustion Space of a Diesel Engine. Paper presented at the Congress and Exposition, Cobo Hall, Detroit, February 27-March 3, 1978. SAE Paper No. 780227.

Alcock, J. F. and W. M. Scott. Some More Light on Diesel Combustion. I. Mech. E. Auto. Div. Proc., 1962-1963.

Lyn, W. T. Study of Burning Rate and Nature of Combustion in Diesel Engines. Ninth Symposium (International) on Combustion, 1963.

Duggal, V. K. Studies in Pollutant Formation in Diesel Engines. Ph.D. Thesis, Faculty of Engineering - University of Southampton, 1977.

Jackson, P. P. Combustion in Diesel Engines. Ph.D. Thesis, Birmingham University, 1965.

Urlaub, A. and E. Müller. Experimental and Theoretical Investigations into the Question of the Exhaust Gas Quality of M-Diesel Engines. CIMAC, p. 463, 1973.

Shelton, E. M. Diesel Fuel Oils, 1976. Technical Information Center, Energy Research and Development Administration, BERC/PPS-76/5, November 1976.

Henein, N. A. A Diesel Engine Combustion and Emission. In: Engine Emissions, G. S. Springer and D. J. Patterson, Eds., Plenum Press, New York, N. Y., 1973.

Monaghan, M. L., C. C. J. French, and R. G. Freese. A Study of the Diesel as a Light-Duty Power Plant. Report to the Environmental Protection Agency, Research Triangle Park, North Carolina, 1974. EPA No. 460/3-74-011.

Doerfler, P. K. Comprex Supercharging of Vehicle Diesel Engines, 1975. SAE Paper No. 750335.

Eisele, E., H. Hiereth, and H. Polz. Experience with Comprex Pressure Wave Supercharger on the High Speed Passenger Car Diesel Engine, 1975. SAE Paper No. 750334.

How Dirty are Diesel Emissions? Consumer Reports, p. 354, June 1979.

Gretch, S. Ford Diesel Emissions Review. Presentation to DOE, March 1979.

Marshall, W. F. and R. W. Hurn. Factors Influencing Diesel Emissions. SAE Transactions, Vol. 77, 1968. SAE Paper No. 680528.

French, C. C. J. Taking the Heat Off the Highly Boosted Diesel. SAE Transactions, Vol. 78, 1969. SAE Paper No. 690463.

Walder, C. J. Some Problems Encountered in the Design and Development of High Speed Diesel Engines. Paper 978A presented at SAE International Automotive Engineering Congress, Detroit, January 1965.

Forrest, L., W. B. Lee, and W. M. Smalley. Impacts of Light-Duty Vehicle Dieselization on Urban Air Quality. Paper presented at the 72nd Annual Meeting of the Air Pollution Control Association, Cincinnati, Ohio, June 24-29, 1979.

Barnes-Moss and M. W. Scott. The Light-Duty Diesel Engine for Private Transportation, February 1975. SAE Paper No. 750331.

Monaghan, M. L. and J. J. McFadden. A Light-Duty Diesel for America?, February 1975. SAE Paper No. 750330.

Improving the Diesel Engine. Automotive Engineering Journal, 83(8):24, August 1975.

Schultz, W. J., C. E. Miesiak, A. E. Hamilton, and D. E. Larkinson. Credibility of Diesel over Gasoline Fuel Economy Claims by Association, Feb. 1976. SAE Paper No. 760047.

Cass, G. R. Cost and Performance of Automotive Emission Control Technologies. California Institute of Technology, December 1973.

Briggs, T., J. Throgmorton, and M. Karaffa. Air Quality Assessment of Particulate Emissions from Diesel-Powered Vehicles. PEDCo Environmental, Inc. for U.S. Environmental Protection Agency, Research Triangle Park, North Carolina, March 1978. EPA-450/3-78-038.

Eisele, E. and K. Binder. Increasing the Power Output of Direct Injection Diesel Engines by means of a Double Mixture-System. Int. Congress on Combustion Engines, 12th, Tokyo, Japan, May 22-31, 1977.

Barry, E. G., F. J. Hills, A. Pamella, and R. B. Smith. Diesel Engines for Passenger Cars - Emissions, Performance, Fuel Demand, and Refining Implications. Proc. Am. Pet. Inst. Refin. Dep., 42nd Midyear Meeting, Chicago, Illinois, May 9-12, 1977.

Can Diesel Specific Power Be Increased? Automotive Eng., 85(12): 66-69, Dec. 1977.

How Do Diesel and Gasoline Emissions Compare? Automotive Eng., 85(11):50-55, Nov. 1977.

AD-209: A Light-Duty Diesel with Heavy-Duty Heritage. Automotive Eng., 85(7):39-42, July 1977.

Simanitis, D. J. Oldsmobile Opts for Diesel Power. Automotive Eng., 85(11):24-27, Nov. 1977.

Pike, D. A. and M. J. Wright. Comparison Between Diesel and Gasoline Passenger Cars. Entropie, 13(74):45-56, Mar.-Apr. 1977.

Volkswagen Develops a Diesel. Automotive Eng., 85(6):62-68, June 1977.

Hare, C. T. and R. L. Bradow. Light-Duty Diesel Emission Correction Factors for Ambient Conditions. SAE Preprint No. 770717 for Meeting, Sept. 12-15, 1977.

Fairweather, R. G. Gas Emissions and Fuel Economy of the Light-Duty Diesel Truck. SAE Paper No. 770256 for Meeting Feb. 28-Mar. 4, 1977.

Combustion in Engines. Combustion in Engines Conference, Cransfield Inst. of Technol., Bedfordshire, England, July 7-9, 1975. Available from Mech. Eng. Publ., New York, N. Y.

Diesel Engine for Automobiles Automotive Eng., 83(12):24-28, December 1975.

Hartley, J. Light Diesel Engines. Automot. Des. Eng., 14:16-17, July-Aug.-Sept. 1975.

Pachernegg, S. J. Efficient and Clean Diesel Combustion. SAE Preprint No. 750787 for Meeting, Sept. 8-11, 1975.

Whitehouse, N. D., E. Clough, and J. B. Way. Effect of Changes in Design and Operating Conditions on Heat Release in Direct-Injection Diesel Engines. SAE Preprint No. 740085 for Meeting Feb. 25-March 1, 1974.

Brisson, B., A. Ecomard, and P. Eyzat. New Diesel Combustion Chamber - The Variable-Throat Chamber. SAE Preprint No. 730167 for Meeting January 8-12, 1973.

Lindgren, Olle. Scania's New DS14 Diesel Engine. SAE Preprint No. 720782 for Meeting Sept. 11-14, 1972.

Potter, J. H. and M. S. Nutkis. Study of Smoke in Diesel Engine Exhaust Products. ASME Paper No. 71-WA/PID-4 for Meeting Nov. 28-Dec. 2, 1971.

Hill, S. H. Automotive Diesel Technology Program. Final Report, June 1975-April 1977. Teledyne Continental Motors, Muskegan, Mich., General Products Div., Dept. of Energy. Contract No. FY-76-C-03-1099. NTIS No. SAN-1099-1.

Lehmann, E. J. Diesel Exhaust Emissions, March 1977. NTIS No. PS-77/0104/8ST.

Marshall, W. F. and K. R. Stamper. Engine Performance Test of the 1975 Chrysler-Nissan Model CN633 Diesel Engine. Energy Research and Development Administration, Bartlesville, Oklahoma, Bartlesville Energy Research Center. NTIS No. DOT-TSC-OST-75-44.

NATURE OF DIESEL EMISSIONS

Motoyoshi, E., T. Yamada, and M. Mori. The Combustion and Exhaust Emission Characteristics and Starting Ability of Y.P.C. Combustion System. Yanmar Diesel Engine Co., Ltd., Japan. SAE Paper No. 760215.

Russell, M. F. Recent CAV Research into Noise, Emissions, and Fuel Economy of Diesel Engines. CAV Ltd., United Kingdom. SAE Paper No. 770257.

Springer, K. J. and T. Baines. Emissions from Diesel Versions of Production Passenger Cars. Presented at the Passenger Car Meeting, Detroit Plaza, Detroit, Sept. 26-30, 1977. SAE Paper No. 770818.

Lipkea, W. H., J. H. Johnson, and C. T. Vuk. The Physical and Chemical Character of Diesel Particulate Emissions - Measurement Techniques and Fundamental Considerations. Paper presented at the Congress and Exposition, Cobo Hall, Detroit, Michigan, February 27-March 3, 1978. SAE Paper No. 780108.

Jones, M. A. The Effect of Engine Load and Speed on the Physical Characteristics of Diesel Particulate Emissions. M.S. Thesis, Michigan Technological University, 1975.

Khan, I. M. Factors Affecting Emissions of Smoke and Gaseous Pollutants from Direct Injection Diesel Engines. Lucas Engineering Review, 6:36, November 1973.

Broome, D. The Mechanisms of Soot Release from Combustion of Hydrocarbon Fuels with Particular Reference to the Diesel Engine. Lucas Engineering Review, 6:36, November 1973.

Harmes, R. J., D. F. Merrion, and H. S. Ford. Some Effects of Fuel Injection System Parameters on Diesel Exhaust Emissions, August 1971. SAE Paper No. 710671.

Size Distribution and Mass Output of Particulate from Diesel Engines. U.S. Dept. of Interior, Bureau of Mines, RI 8141, 1976.

Frey, J. W. and M. Corn. Physical and Chemical Characteristics of Particulates in Diesel Exhaust. J. Am. Industrial Hygiene Assoc., pp. 468-478, Sept.-Oct. 1967.

Greeves, G. Origins of Hydrocarbon Emissions from Diesel Engines, March 1977. SAE Paper No. 770259.

Bechtold, R. L. and S. S. Lestz. Combustion Characteristics of Diesel Fuel Blends Containing Used Lubricating Oil, February 1976. SAE Paper No. 760132.

Owens, E. C. and B. R. Wright. Engine Performance and Fire-Safety Characteristics of Water-Containing Diesel Fuels. SwRI Interim Report, AFLRL No. 83, December 1976.

Johnson, J. H. Diesel Engine Design, Performance, and Emission Characteristics. IC8666, U.S. Department of the Interior, Proceedings of the Symposium on the Use of Diesel-Powered Equipment in Underground Mining, Pittsburg, Pennsylvania, January 30-31, 1973.

Lawson, A. and H. Vergeer. Analysis of Diesel Exhaust Emitted from Water Scrubber and Catalytic Purifiers. CANMET Energy, Mines and Resources Canada. Final Report ORF77-01.

Rehnberg, O. What are Constituents of Exhaust from Underground Diesel Trucks? World Mining V29:42-46, Feb. 1976.

Wilson, R. P., Jr., E. B. Muir, and F. A. Pellicciotti. Emissions Study of A Single-Cylinder Diesel Engine. SAE Paper No. 740123.

Shahed, S. M., W. S. Chiu, and V. S. Yumlu. A Preliminary Model for the Formation of Nitric Oxide in Direct Injection Diesel Engines and Its Application in Parametric Studies. SAE Paper No. 730083.

Melton, C. W., R. I. Mitchell, W. M. Henry, P. R. Webb, and W. E. Chase. The Physical-Chemical Characteristics of Particles Associated with Polynuclear Aromatic Hydrocarbons Present in Automobile Exhaust. Final Report to Coordinating Research Council by Battelle Memorial Institute, January 1970.

Wilson, R. P., Jr., C. H. Waldman, and L. J. Muzio. Foundation for Modeling NOx and Smoke Formation in Diesel Flames. Final Report for Phase 1, prepared for Coordinating Research Council, Inc., New York, 1973.

Tyler, J. C., J. T. Gray, and W. D. Weatherford. An Investigation of Diesel Fuel Composition - Exhaust Emission Relationships. Report prepared by Southwest Research Institute for the Army Mobility Equipment Research and Development Centre, October 1974. NTIS No. AD-A-005-077.

Perez, J. Cooperative Evaluation of Techniques for Measuring NO and CO in Diesel Exhaust. Coordinating Research Council, January 1975. NTIS No. PB 241710.

Dietzmann, H. E. Protocol to Characterize Gaseous Emissions as a Function of Fuel and Additive Composition. Southwest Research Institute, September 1975. NTIS No. PB 253363.

Gentel, J. E., O. J. Manary, and J. C. Valenta. Characterization of Particulates and Other Non-Regulated Emissions from Mobile Sources and the Effects of Exhaust Emission Control Devices on These Emissions. Dow Chemical, March 1973. NTIS No. PB 224243.

Hare, C. T. Methodology for Determining Fuel Effects on Diesel Particulate Emissions. Prepared by Southwest Research Institute for the Environmental Protection Agency, Research Triangle Park, North Carolina, March 1975. NTIS No. PB 245163. EPA-650/2-75-056.

Gentel, J. E., O. J. Manary, and J. C. Valenta. Development of a Methodology for the Assessment of the Effects of Fuels and Additives on Control Devices. Dow Chemical, July 1974. NTIS No. PB 253911.

Frisch, L. E., J. H. Johnson, and D. G. Leddy. Effect of Fuels and Dilution Ratio on Diesel Particulate Emissions. Paper presented at the Congress and Exposition, Cobo Hall, Detroit, Feb. 26-March 2, 1979. SAE Paper No. 790417.

Frisch, L. E. The Effect of Exhaust Dilution and Fuel Properties on the Character of Diesel Particulate Emissions. M.S. Thesis, Michigan Technological University, 1978.

Scofield, G. L. Diesel Engines and Their Particle Signatures. Paper presented to the Automobile Division of the Institution of Mechanical Engineers at St. Mary's Hall, Coventry, England, June 15, 1977. SAE Paper No. 780426.

Braddock, J. N. and R. L. Bradow. Emission Patterns of Diesel-Powered Passenger Cars. Paper presented at Fuels and Lubricants Meeting, Houston, Texas, June 1975. SAE Paper No. 750682.

Braddock, J. N. and P. A. Gabele. Emission Patterns of Diesel-Powered Passenger Cars - Part II. Paper presented at SAE Congress, Detroit, Michigan, February 1977. SAE Paper No. 770168.

Black, F. M. and L. E. High. Diesel Hydrocarbon Emissions, Particulate and Gas Phase. EPA Symposium on Diesel Particulate Emissions Measurement and Characterization, Ann Arbor, Michigan, May 1978.

Coordinating Research Council. A Study of the Atmospheric Behavior of Diesel Particles. CRC-APRAC Project No. CAPA-13-76, 30 Rockefeller Plaza, New York, New York.

Nightingale, D. R. A Fundamental Investigation into the Problem of NO Formation in Diesel Engines. Presented at the SAE FCIM Meeting, Milwaukee, September 1975. SAE Paper No. 750848.

Dietzmann, H. E., K. J. Springer, and R. C. Stahman. Diesel Emissions as Predictors of Observed Diesel Odor. Presented at the SAE National Combined Farm, Construction, and Industrial Machinery and Powerplant Meetings, Milwaukee, September 11-14, 1972. SAE Paper No. 720757.

Springer, K. J. Emissions from a Gasoline- and Diesel-Powered Mercedes 220 Passenger Car. Report to the Environmental Protection Agency under Contract No. CPA70-44, June 1971.

Stewart, D. B., P. Mogan, and E. D. Dainty. Some Characteristics of Particulate Emissions in Diesel Exhaust. CIM Bull. (Canadian Mining Met. Bull.), 68(756):62-69, April 1975.

Mogan, P., D. B. Stewart, A. D'Aoust, and E. D. Dainty. A Comparison of Probe vs Total Particulate Collection from the Exhaust of a V-6 Diesel Engine. Divisional Report (FRC 74/10 - CEAL No. 306 - limited distribution) of the Department of Energy, Mines and Resources, Mines Branch, Fuels Research Centre, Ottawa.

Mogan, P., D. B. Stewart, A. D'Aoust, and E. D. Dainty. A Gaseous and Particulate Emissions Investigation of an Air-Cooled, Indirect-Injection Six-Cylinder Diesel Engine Derated to 117 13HP, Divisional Report (FRC 74/8 - CEAL No. 304 - limited distribution) of the Department of Energy, Mines and Resources, Mines Branch, Fuels Research Centre, Ottawa.

Stewart, D. B., A. D'Aoust, P. Mogan, and E. D. Dainty. A Detailed Electron Microscope Examination of the Particulate Emissions from a V-6, Air-Cooled Indirect-Injection Diesel Engine, Divisional Report (FRC 74/6 - CEAL No. 302 - limited distribution) of the Department of Energy, Mines and Resources, Mines Branch, Fuels Research Centre, Ottawa.

Baluswamy, N. Spatial and Temporal Distribution of Gaseous Pollutants in a Diesel Engine Combustion Chamber. Ph.D. Thesis, University of Manchester, Institute of Science and Technology, 1976.

Holtz, J. C., et al. Diesel Engines Underground. I. Composition of Exhaust Gas from Engines in Proper Mechanical Condition. U.S. Bur. Mines Rept. Invest. 3508, 1940.

Elliot, M. A., G. J. Nebel, and F. G. Rounds. The Composition of Exhaust Gases from Diesel, Gasoline, and Propane Powered Motor Coaches. J. Air Pollution Control Assoc., 5:103, August 1955.

McKee, H. C., W. A. McMahon, and L. R. Roberts. A Study of Particulates in Automobile Exhaust. Proceedings of the Semi-annual Technical Conference, Air Pollution Control Association, pp. 208-227, November 1957.

Linnell, R. H. and W. E. Scott. Diesel Exhaust Composition and Odor Studies. J. Air Pollution Control Assoc., 12:510, November 1962.

Gross-Gronomski, L. Diesel Smoke, Flame Cooling as the Main Cause. Automobile Eng., p. 531, December 1964.

Linnell, R. H. and W. E. Scott. Diesel Exhaust Analysis, Preliminary Results. Arch. Environ. Health, 5:616, December 1962.

Reckner, L. R., W. E. Scott, and W. F. Biller. The Composition and Odor of Diesel Exhaust. Proc. Amer. Petrol. Inst., Sect. III 45:133, 1965.

Hills, F. J. and C. G. Schleyerbach. Diesel Fuel Properties and Engine Performance. Paper presented at the International Automotive Engineering Congress and Exposition, Cobo Hall, Detroit, February 28-March 4, 1977. SAE Paper No. 770316.

Funkenbusch, E. F., D. G. Leddy, and J. H. Johnson. The Characterization of the Soluble Organic Fraction of Diesel Particulate Matter. Paper presented at the Congress and Exposition, Cobo Hall, Detroit, February 26-March 2, 1979. SAE Paper No. 790418.

Menster, M. and A. J. Sharkey, Jr. Chemical Characterization of Diesel Exhaust Particulates. Final Report on RIMS No. 07032, prepared for the United States Department of the Interior, Bureau of Mines, 1976.

Schreck, R. M., J. J. McGrath, S. J. Swarin, W. E. Hering, P. J. Groblicki, and J. S. MacDonald. Characterization of Diesel Exhaust Particulate Under Different Engine Load Conditions. Paper presented at the 71st Annual Meeting of the Air Pollution Control Association, Houston, June 25-30, 1978.

Khatri, N. J., J. H. Johnson, and D. G. Leddy. The Characterization of the Hydrocarbon and Sulfate Fractions of Diesel Particulate Matter. Paper presented at the Congress and Exposition, Cobo Hall, Detroit, February 27-March 3, 1978. SAE Paper No. 780111.

Springer, K. J. and R. C. Stahman. Diesel Car Emissions - Emphasis on Particulate and Sulfate, 1977. SAE Paper No. 770254.

Breslin, J. A., A. J. Strazisar, and R. L. Stein. Size Distribution and Mass Output of Particulate from Diesel Engine Exhausts. Report of Investigations 8141r, U.S. Dept. of the Interior, Bureau of Mines, 1976.

Groblicki, P. J. and C. R. Begeman. Particle Size Variation in Diesel Exhaust, 1979. SAE Paper No. 790421.

Exhaust Emissions from a Diesel-Powered Volkswagen Rabbit. Technology Assessment and Evaluation Branch, Environmental Protection Agency, Research Triangle Park, October 1975.

Duggal, V. K. and J. S. Howarth. A Preliminary Study of the Structure of Diesel Smoke. Journal of the Institute of Fuel, 48(394):38-44, March 1975.

Rockner, L. R., W. E. Scott, and W. F. Biller. The Composition and Odor of Diesel Exhaust. Proceedings, American Petroleum Institute, Section III, 45:133, 1965.

Khan, I. M., G. Greeves, and D. M. Probert. Prediction of Soot and Nitric Oxide Concentrations in Diesel Exhaust. Symposium on Air Pollution Control in Transport Engines. I. Mech. E., 1971.

Marshall, W. F. NO_2 Levels in Diesel Exhaust. Dept. of Energy, Bartlesville Energy Research Center, Bartlesville, Oklahoma, for the U.S. Dept. of Energy, Technical Information Center, January 1978. BERC/TPR-78/1.

Murayama, T., N. Miyamoto, S. Sasaki, and N. Kojima. Relation Between Nitric Oxide Formation and Combustion Process in Diesel Engines. Twelfth Int. Congr. on Combust. Engines, Tokyo, Japan, May 22-31, 1977.

Hoelzer, J. C. Emission Formation Characteristics of the Diesel Combustion Process and Estimated Future Development Trends. SAE Special Publ. SP-396, Aug. 1975, Paper No. 751002.

Cakir, H. Nitric Oxide Formation in Diesel Engines. Inst. Mech. Eng. (Lond.) Proc., 188(46):477-483, 1974.

Karim, G. A. and S. Khanna. Effect of Very Low Air Intake Temperature on the Performance and Exhaust Emission Characteristics of a Diesel Engine. SAE Preprint No. 740718 for Meeting Sept. 9-12, 1974.

Cioffi, G., A. Polletta, and A. Scognamiglio. Characteristics of Diesel Engines Exhaust Gas (In Italian). Termotecnica (Milan), 25(12):645-659, December 1971.

CONTROL OF DIESEL EMISSIONS

Grigg, H. C. The Role of Fuel Injection Equipment in Reducing 4-Stroke Diesel Engine Emissions. CAV Ltd. SAE Paper No. 760126.

Hare, C. T., K. J. Springer, and R. L. Bradow. Fuel and Additive Effects on Diesel Particulate - Development and Demonstration of Methodology. Hare and Springer - Southwest Research Institute, Bradow - Environmental Protection Agency. SAE Paper No. 760130.

Suzuki, T. and K. Usaml. A Modification of Combustion Systems for Low Exhaust Emission and Its Effect on Durability of Prechamber Diesel Engine. Hino Motors Ltd., Japan. SAE Paper No. 760213.

Nakagawa, H., M. Tateishi, and M. Sekino. Application of Fuel Spray Theory to Exhaust Emission Control in a D.I. Diesel Engine. Nakagawa and Tateishi-Mitsubishi Heavy Industries Ltd., Japan and Sekino-Mitsubishi Motors Corp., Japan. SAE Paper No. 760214.

Apostolescu, N. D., R. D. Matthew, and R. F. Sawyer. Effects of a Barium-Based Fuel Additive on Particulate Emissions from Diesel Engines. University of California-Berkeley, September 1977. SAE Paper No. 770828.

Murayama, T., Morishama, Y., Tsukahara, M., and Miyamoto, N. Experimental Reduction of NOx, Smoke, and BSFC in a Diesel Engine Using Uniquely Produced Water (0 - 80%) to Fuel Emulsion, February 1978. Murayama - Visiting Professor, Univ. of Wisconsin-Madison, Hokkaido Univ., Japan, Morishima-Toray Co., Ltd., Japan, Tsukahara-Muroran Inst. of Tech., Japan, and Miyamoto-Hokkaido Univ. SAE Paper No. 780224.

Brandes, J. G. Diesel Fuel Specification and Smoke Suppressant Additive Evaluation, May 1970. SAE Paper No. 700522.

Saito, T. and M. Nabetani. Surveying Tests of Diesel Smoke Suppression with Fuel Additive, January 1973. SAE Paper No. 730170.

Norman, G. R. New Approach to Diesel Smoke Suppression, 1966. SAE Paper No. 660339.

Golothan, D. W. Diesel Engine Exhaust Smoke: The Influence of Fuel Properties and the Effects of Using a Barium-Containing Fuel Additive. SAE Trans., 76:616, 1967. SAE Paper No. 670092.

Turley, D. C., D. L. Brenchley, and R. R. Landolt. Barium Additives as Diesel Smoke Suppressants. J. of Air Pollution Control Assoc., 23:783, 1973.

Bryzik, W. and C. O. Smith. Relationships Between Exhaust Smoke Emissions and Operating Variable in Diesel Engines, September 1977. SAE Paper No. 770718.

Soebar, R. F. and F. B. Parks. Emission Control with Lean Operation Using Hydrogen Supplemented Fuel. SAE Paper No. 740187.

Cook, D. H. and C. K. Law. A Preliminary Study on the Utilization of Water-in-Oil Emulsions in Diesel Engines. Combustion Science and Technology, 1978.

Barnes, K. O., D. B. Kittelson, T. E. Murphy. Effect of Alcohols as Supplemental Fuels for Turbocharged Diesel Engines, February 1975. SAE Paper No. 750469.

Johnston, A. A., C. D. Wood, and K. Springer. A Proposal for Control of Diesel Exhaust Emissions in Underground Mines, by Southwest Research Institute, May 1978.

Knight, B. E. and C. H. T. Wang. Some Experiments on the Mode of Action of a Diesel Smoke Suppressant Additive. Symposium on Motor Vehicle Air Pollution Control, London, England, November 1968.

Reducing Exhaust Emissions from Diesels. Society of Automotive Engineers, September 1971.

Hurn, R. W. Diesel Emissions Measurement and Control. IC8666, U.S. Department of the Interior, Proceedings of the Symposium on the Use of Diesel-Powered Equipment in Underground Mining, Pittsburgh, Pennsylvania, January 30-31, 1973.

Schaub, F. S. and K. V. Beightol. Effect of Operating Conditions on Exhaust Gas Emissions of Diesel, Gas Diesel, and Spark Ignited Stationary Engines. Engineering Research Laboratory, Cooper-Bessemer Company, Mount Vernon, Ohio, June 1973.

Bascom, R. C., L. C. Broering, and D. E. Wulfhorst. Design Factors that Affect Diesel Emissions, June 1971. SAE Paper No. 710484.

Mooney, J. J., C. E. Thompson, and J. C. Dettling. Three-Way Conversion Catalysts: Part of the New Emission Control System. SAE Paper No. 770365.

Kulnig, H. Exhaust Gas Catalysers for Underground Use. Mining Magazine V129(4) 351-353, October 1973.

Kulnig, H. Bench Testing of the Kiruna Diesel Exhaust Fumes Catalytic Afterburner. Erzmetall, V27(6) 292-298, June 1974.

Wilson, R. P., Jr., D. W. Lee, and P. G. Gott. Potential Emission-Control Concepts for Large-Bore Stationary Engines. Preliminary Draft Phase I Report, March 1978. EPA Contract 68-02-2664.

Masuda, G., Contractor. 1. Particulate Control System for Diesel-Engine Exhaust Gas and Its Associated Informations. 2. A Simple Collecting Device "Aut-Ainer Collector", November 17, 1978. EPA Contract No. 68-02-2697.

Masuda, S. Design of Test Models of Aut-Ainer Collector, Feb. 24, 1979. EPA Contract No. 68-02-2697.

El Nesr, M. S., S. Satcunanathan, and B. J. Kaczek. Diesel Engine Exhaust Emissions and Effect of Additives. Conference on Air Pollution Control in Transport Engines, Institute of Mechanical Engineers, November 1971.

Springer, K. J. Investigation of Diesel-Powered Vehicle Emissions: VIII. Removal of Exhaust Particulate from Mercedes 300D Diesel Car. Prepared for U.S. Environmental Protection Agency, June 1977. EPA-460/3-77-007.

Stahman, R. C., G. D. Kittredge, and K. J. Springer. Smoke and Odor Control for Diesel-Powered Trucks and Buses. Presented at the SAE Mid-Year Meeting, Detroit, May 20-24, 1968. SAE Paper No. 680443.

Springer, K. J. and C. T. Hare. Four Years of Diesel Odor and Smoke Control Technology Evaluations - A Summary. ASME Paper 69-WA/APC-3 presented at the ASME Winter Annual Meeting, Los Angeles, November 16-20, 1969.

Springer, K. J. An Investigation of Diesel-Powered Vehicle Emissions-Part V. Final Report to the Environmental Protection Agency under Contract No. PH 22-68-23, April 1974.

Springer, K. J. and R. C. Stahman. Control of Diesel Exhaust Odors. Paper 26 presented at New York Academy of Sciences Conference on Odors: Evaluation, Utilization and Control, New York, October 1-3, 1973.

Springer, K. J. Field Demonstration of General Motors Environmental Improvement Proposal (EIP) - A Retrofit Kit for GMC City Buses. Final Report to the Environmental Protection Agency under Contract No. PH 22-68-23, December 1972.

Springer, K. J. and R. C. Stahman. Diesel Emission Control Through Retrofits. Presented at SAE Automotive Engineering Congress and Exposition, Detroit, February 24-28, 1975. SAE Paper No. 750205.

Hare, C. T., K. J. Springer, and R. L. Bradow. Fuel and Additive Effects on Diesel Particulate Emissions - Development and Demonstration of Methodology. Presented at SAE Automotive Engineering Congress and Exposition, Detroit, February 23-27, 1976. SAE Paper No. 760130.

Springer, K. J. Investigation of Diesel-Powered Vehicle Emissions-Part VII. Final Report to the Environmental Protection Agency under Contract No. 68-03-2116, August 1976.

Mogan, P., D. B. Stewart, A. D'Aoust, and E. D. Dainty. A Particulate Emissions Evaluation of an Annular Radial Flow Platinum Catalytic Purifier Applied to a V-6, Air-Cooled, Indirect-Injection Diesel Engine. Divisional Report (FRC 74/12 - CEAL No. 308 - limited distribution) of the Department of Energy, Mines and Resources, Mines Branch, Fuels Research Centre, Ottawa.

Mogan, P., D. B. Stewart, A. D'Aoust, and E. D. Dainty. An Evaluation of Particulate Emissions from a Catalytic Diesel Exhaust Purifier During Extended Steady-State Operation. (FRC 74/58 - CEAL No. 327 - limited distribution) of the Department of Energy, Mines and Resources, Mines Branch, Fuels Research Centre, Ottawa.

Test Results on a Mercedes-Benz 220D Diesel Sedan Equipped with a Comprex Pressure Wave Supercharger. Technology Assessment and Evaluation Branch, Emission Control Technology Division, Office of Mobile Source Air Pollution Control, Environmental Protection Agency, August 1975.

Texhirogi, N. and K. Kontani. Control of Exhaust Emissions from Diesel Engines. Kuki Seijo, 12(6):32-45, February 1975 (Japanese).

Sudar, S. and L. Grantham. Diesel Exhaust Emission Control Program. Final Report prepared by Atomics International, Canoga Park, California for the Department of Transportation, Washington, D.C., January 1974. PB 234 752.

Amano, M., H. Sami, S. Nakagawa, and H. Yoshizaki. Approaches to Low Emission Levels for Light-Duty Diesel Vehicles. Paper presented to the Automotive Engineering Congress and Exposition, Detroit, Michigan, February 23-27, 1976. SAE Paper No. 760211.

Hames, H. J., D. F. Merrion, and H. S. Ford. Some Effects of Fuel Injection System Parameters on Diesel Exhaust Emissions. Presented at SAE National West Coast Meeting, Vancouver, August 1971. SAE Paper No. 710671.

Walder, C. J. Reduction of Emissions from Diesel Engines. Presented at SAE International Automotive Engineering Congress, Detroit, January 1973. SAE Paper No. 730214.

Marshall, W. F., D. E. Seizinger, and R. W. Freedman. Effects of Catalytic Reactors on Diesel Exhaust Composition. Health and Safety Research - Coal Mines Program, Technical Progress Report 105, April 1978.

Markworth, V. O. and C. D. Wood, III. Large Diesel Engine Testing for Oil Shale Mining. Prepared for U.S. Dept. of the Interior, Bureau of Mines by Southwest Research Institute, Contract No. J0265023, July 1978.

Broering, L. C. and L. W. Holtmann. Effect of Diesel Fuel Properties on Emissions and Performance, September 1974. SAE Paper No. 740692.

Marshall, W. F. and R. D. Fleming. Diesel Emissions as Related to Engine Variables and Fuel Characteristics, October 1971. SAE Paper No. 710836.

Burt, R. and K. A. Troth. Influence of Fuel Properties on Diesel Exhaust Emissions. Symposium on Motor Vehicle Air Pollution Control, London, England, November 1968.

Torpy, P. M., M. J. Whitehead, and J. Wright. Experiments in the Control of Diesel Emissions. I. Mech. E. (London) Conference in Air Pollution Control in Transport Engines, 1971.

Ford, H. S., D. F. Merrion, and R. J. Hames. Reducing Hydrocarbons and Odor in Diesel Exhaust by Fuel Injector Design. SAE Paper No. 700734.

Stumpp, G. and W. Banzhaf. An Exhaust Gas Recirculation System for Diesel Engines. Paper presented at the Congress and Exposition, Cobo Hall, Detroit, February 27-March 3, 1978. SAE Paper No. 780222.

Stumpp, G. Reduction of Exhaust Emissions of Diesel Engines by Means of the Injection Equipment. CIMAC, pp. 441-456, 1973.

Tholen, P., K. Streicher. New Experiences in the Development of Air-Cooled Diesel Engines with Particular Regard to the Human Development. CIMAC, p. 521, 1973.

Hill and E. A. Dodd. An Advanced Low Emission Diesel Engine Concept. ERDA NATO/CCMS Fourth International Symposium, Automotive Propulsion Systems, Washington, D.C., April 18-22, 1977.

Broome, D. and Wright. The Regulation and Reduction of Gaseous Exhaust Emissions from Direct Injection Automotive Diesel Engines. Seventh National Conference on Internal Combustion Engine Theory and Practice, Warsaw, Poland, November 4-5, 1975.

Wood, C. D. and J. W. Colburn, Jr. Control Technology for Diesel Equipment in the Underground Mining Environment - A Review of Selected Topics. Final Report prepared by Southwest Research Institute for U.S. Dept. of the Interior, Bureau of Mines, January 1979.

Sullivan, H. F., L. P. Tessier, C. E. Hermance, and G. M. Bragg. Reduction of Diesel Exhaust Emissions. Prepared for Dept. of Energy, Mines and Resources, Ottawa, May 1977.

Murphy, J. J., L. J. Hillenbrand, and D. A. Trayser. Oxidation of Diesel Particulate. Prepared by Battelle for U.S. Environmental Protection Agency, Research Triangle Park, North Carolina, June 21, 1979.

Duleep, K. G. and R. G. Dulla. Survey and Analysis of Collection Methods for Automotive Particulate Emissions. Presented at the 72nd Annual Meeting of the Air Pollution Control Association, Cincinnati, Ohio, June 24-29, 1979.

Fortnagel, M. Influencing Exhaust Gas Composition by Means of Exhaust Gas Recirculation in a Pressure Charged Swirl Chamber Diesel Engine. Paper presented at Symposium on Technical and Legal Problems of the Protection of the Environment, University of Trier-Kaiserslantern, Sept. 1971.

Valdmanis, E. and E. E. Wulfhorst. The Effects of Emulsified Fuels and Water Induction on Diesel Combustion. SAE Transactions, Vol. 79, 1970. SAE Paper No. 700736.

Springer, K. J. and R. C. Stahman. Removal of Exhaust Particulate from a Mercedes 300D Diesel Car. SAE Paper No. 770716.

Greeves, G., I. M. Khan, and G. Onion. Effects of Water Introduction on Diesel Engine Combustion and Emissions. Paper No. 25, 16th Symposium (International) on Combustion, The Combustion Institute, 1976.

Kabele, D. F. and G. A. Anderkay. Techniques for Quieting the Diesel, September 1975. SAE Paper No. 750839.

The Point of the Planning and the Necessary Conditions for Equipping "Aut-Ainer" with Automobiles (diesel engine). Eikosha Co., Ltd., Tokyo, Japan, June 10, 1979.

Azuma, T. and N. Nakato. Noise and Exhaust Gas Pollution Caused by Engines in Small- and Medium-Sized Construction Equipment in Japan. SAE Preprint No. 780490 for Meeting April 10-12, 1978.

EGR Lowers Diesel NOx Emissions. Automotive Eng., 86(7):46-51, July 1978.

Geometry Controls Diesel Emissions. Automotive Eng., 86(5):42-47, May 1978.

Insulated Pistons Raise Diesel Efficiency. Automotive Eng., 86 (6):72-76, June 1978.

Mercedes Turbocharges Five-Cylinder Diesel. Automotive Eng., 86(6):40-45, June 1978.

Murayama, T. and M. Tsukahara. Study on the Reduction of NOx of Diesel Engine by the Use of Lighter Fuel. Bull JSME, 20(150):1615-1622, December 1977.

Murayama, T., Y. Morishima, N. Miyamoto, and M. Tsukahara. Experimental Reduction of NOx, Smoke, and BSFC in a Diesel Engine Using Uniquely Reduced Water (0-80%) to Fuel Emulsion. SAE Paper No. 780224.

Malyavinskii, L. V. and V. M. Rossinskii. Effectiveness of Smoke Suppression Additives for Diesel Fuels. Chem. Technol. Fuels Oils, 12(11-12):875-877, Nov.-Dec. 1976.

Tholen, P. and I. Killmann. Investigations on Highly Turbocharged Air-Cooled Diesel Engines. ASME Paper No. 77-DGP-11 for Meeting Sept. 18-22, 1977.

Pearce, J. F., R. J. Hames, and D. F. Merrion. Two-Stroke Cycle Diesel Engine Fuel Economy Improvement and Emission Reduction. SAE Paper No. 770255 for Meeting Feb. 28-Mar. 4, 1977.

Starkman, E. S. and F. W. Bowditch. Vehicular Emission Control. Adv. Environ. Sci. Technol., Vol. 7, published by John Wiley and Sons, New York, N. Y., 1977.

Tucker, L. E. Diesel Smoke: Legislation and Control. Int. Conf. on Air Pollution, Univ. of Pretoria, South Africa, April 26-29, 1976.

Anderton, D. and V. K. Duggal. Effect of Turbocharging on Diesel Engine Noise, Emissions, and Performance. SAE Spec. Publ. No. 397, Aug. 1975, Diesel Engine Noise Conf., Paper No. 750797.

Anderton, D. and V. K. Duggal. Diesel Engine Emissions and Noise. J. Inst. Fuel, 49(398):20-25, March 1976.

Ikegami, M., E. Kawai, and Y. Kihara. Reducing Oxides of Nitrogen in a Diesel Engine by Means of Exhaust Gas Recirculation. Bull., JSAE (6):65-74, April 1974.

Fukazawa, S., T. Murayama, and Y. Fujiwara. Experimental Study on Exhaust Smoke in Diesel Engine. Bull. JSAE, (6):22-32, April 1974.

Radwan, M. S. and N. D. C. Tee. Highly Turbocharged Small Automotive Diesel Engines. J. Automot. Eng., 6(2):17-22, April 1975.

Mathur, H. B. Exhaust Odor and Smoke Emission from Diesel Engines and Their Control. J. Inst. Eng. (India) Mech. Eng. Div., 55:169-173, March 1975.

Springer, K. J. Investigation of Diesel-Powered Vehicle Emissions: VIII. Removal of Exhaust Particulate from Mercedes 300D Diesel Car. Prepared for U.S. Environmental Protection Agency, Ann Arbor, Michigan, June 1977. EPA-460/3-77-007.

Storment, J. O., K. J. Springer, and K. M. Hergenrother. NOx Studies with EMD 2-567 Diesel Engine. ASME Paper No. 74-DGP-14 for Meeting April 28-May 2, 1974.

Bly, R. L. Clean Exhaust - Good Diesel Performance. Pit Quarry, 66(4):75-79, October 1973.

Dai, J., S. Ozaki, Y. Uchiyama, and K. Motohaski. Reduction of Nitrogen Oxides by Exhaust Gas Recirculation and Water Injection on Diesel Engine. J. Fuel Soc. Jap., 52(550):113-120, February 1973.

Scott, W. M. Recent Developments in Diesel Engine Research at the Ricardo Laboratories. Entropie, 8(48):69-79, Nov.-Dec. 1972.

Bernhardt, W. E., R. W. Hura, B. H. Eccleston, I. M. Khan, C. H. T. Wang, T. Muroki, and C. E. Moser, et al. Air Pollution Control in Transport Engines, Symposium. Air Pollution Control in Transp. Engines, Symposium, Shirley, Solihull, England, Nov. 9-11, 1971.

Krause, S. P., D. F. Merrion, and G. L. Green. Effect of Inlet Air Humidity and Temperature on Diesel Exhaust Emissions. SAE Preprint No. 730213 for Meeting Jan. 8-12, 1973.

Pischinger, R. Emission Control Investigations on Diesel Engines (German). Automobiltech Z, 74(3):111-116, March 1972.

McCreath, C. G. Effect of Fuel Additives on the Exhaust Emissions from Diesel Engines. Combust. Flame, 17(3):359-366, December 1971.

Losikov, B. V., K. N. Golovanov, and S. M. Livshits. Use of Fuel Additives to Reduce Diesel Exhaust Smoke. Chem. Technol. Fuels Oils, (7-8):634-638, July-August, 1970.

Walter, R. A. The Emissions and Fuel Economy of a Detroit Diesel 6-71 Engine Burning a 10-Percent Water-in-Fuel Emulsion. Transportation Systems Center, Cambridge, Mass. Rept. No. TSC-USCG-78-1.

Cavagnaro, D. M. Diesel Exhaust Emission Control for Motor Vehicles, Feb. 1978. NTIS No. PS-78/0110/3ST.

Cavagnaro, D. M. Diesel Exhaust Emissions, Feb. 1978. NTIS No. PS-78/0109/5ST.

Lehmann, E. J. Diesel Exhaust Emission Control for Motor Vehicles, March 1977. NTIS No. PS-77/0105/5ST.

Springer, K. J. and A. C. Ludwig. Documentation of the Guide to Good Practice for Minimum Odor and Smoke from Diesel-Powered Vehicles. Final Report to the Department of Health, Eucation, and Welfare under Contract No. CPA 22-69-71, November 1967.

Lenane, D. L. Status Report-Trapping Systems for Automotive Exhaust Particulates, October 1973.

Lenane, D. L. Particulate Lead Traps. Report to the French Association of Petroleum Technicians, Application Technology Section, Paris, France, January 23, 1975.

Cernansky, N. P., C. W. Savery, I. H. Suffet, and R. S. Cohen. Diesel Odor Sampling and Analysis Using the Diesel Odor Analysis System (DOAS). Dept. of Mechanical Engineering and Mechanics and Environmental Studies Institute, Drexel Univ., Philadelphia, PA. SAE Paper No. 780223.

Rhee, K. T., P. S. Myers, and O. A. Uyehara. Time- and Space-Resolved Species Determination in Diesel Combustion Using Continuous Flow Gas Sampling. Mechanical Eng. Rhee- Dept., Univ. of Miami, Coral Gables, FL, and Myers and Uyehara- Mech. Eng. Dept., U. of Wisconsin, Madison, WI. SAE Paper No. 780226.

Vuk, C. T. The Development and Application of Techniques for the Measurement and Analysis of Diesel Particulate Emissions. M.S. Thesis, Michigan Technological University, 1975.

Khatri, N. J. The Measurement of Diesel Particulate Matter Size Distributions Using the Electrical Aerosol Analyzer and the Analysis of the Sulfate Fraction Using the Barium Chloranilate Method. M.S. Thesis, Michigan Technological University, 1977.

Diesel Smoke Measurement Procedure. SAE J35 (SAE Recommended Practice). SAE Handbook, 1977.

Measurement Procedure for Evaluation of Full-Flow, Light-Extinction Smoke-meter Performance. SAE J1157 (SAE Recommended Practice), SAE Handbook, 1978.

Control of Air Pollution from New Motor Vehicles and New Motor Vehicle Engines Certification and Test Procedures. Federal Register (40 CFR Part 86), 44(23):6650-6671, February 1, 1979.

Bascom, R. C., W. S. Chiu, and R. J. Padd. Measurement and Evaluation of Diesel Smoke, 1973. SAE Paper No. 730212.

Durant, J. B. CRC Investigation of Diesel Smoke Measurement, Vehicle Emissions, 3:352. Society of Automotive Engineers.

Hurn, R. W. and W. F. Marshall. Techniques for Diesel Emissions Measurement. SAE Vehicle Emissions, 3:120.

Williams, G., F. W. Hartman, and G. R. Mackey. Diesel Smoke Analysis on a Chassis Dynamometer, June 1973. SAE Paper No. 730660.

Greeves, G. and J. O. Meehan. Measurement of Instantaneous Soot Concentration in a Diesel Combustion Chamber, from Combustion in Engines. Inst. of Mech. Engineers - Automobile Division, 1976.

Leddy, D. G. Measurement of Sulphate in Diesel Exhaust Particulate Matter. Paper presented at CRC-APRAC Diesel Exhaust Measurement Symposium, Chicago, 1977.

Carpenter, K. The Design and Development of a Dilution Tunnel for the Physical and Chemical Characterization of Diesel Particulate Matter. M.S. Thesis, Michigan Technological University, 1978.

Recommended Practice for Measurement of Exhaust Sulfate Emissions from Light-Duty Vehicles and Trucks, September 1977. U.S. Environmental Protection Agency.

Dolan, D. F., D. B. Kittelson, and K. T. Whitby. Measurement of Diesel Exhaust Particle Size Distributions. Paper presented at the Winter Annual Meeting of The American Society of Mechanical Engineers, Houston, Texas, November 30-December 4, 1975.

Pinolini, F. and J. Spiers. Diesel Smoke - A Comparison of Test Methods and Smokemeters on Engine Test Bed and Vehicle, 1969. SAE Paper No. 690491.

Carey, A. W., Jr. Steady State Correlation of Diesel Smoke Meters-An SAE Task Force, 1969. SAE Paper No. 690493.

Vuk, C. T. and J. H. Johnson. Measurement and Analysis of Particles Emitted from a Diesel Combustion Process. Paper presented at the Combustion Institute Central States-Western States 1975 Spring Technical Meeting, April 1975.

Kittelson, D. B. and D. F. Dolan. Dynamics of Sampling and Measurement of Diesel Engine Exhaust Aerosols. Paper presented at the Conference on Carbonaceous Particles in the Atmosphere, March 20-22, 1978.

Laresgoiti, A., A. C. Loos, and G. S. Springer. Particulate and Smoke Emission from a Light-Duty Diesel Engine. Environmental Science and Technology, 11(10):973-978, October 1977.

Dolan, D. F. and D. B. Kittelson. Diesel Exhaust Aerosol Particle Size Distributions - Comparison of Theory and Experiment. Paper presented at the Congress and bxposition, Cobo Hall, Detroit, February 27-March 3, 1978. SAE Paper No. 780110.

Kittelson, D. B., D. F. Dolan, and J. A. Verrant. Investigation of a Diesel Exhaust Aerosol. Paper presented at the Congress and Exposition, Cobo Hall, Detroit, February 27-March 3, 1978. SAE Paper No. 780109.

Verrant, J. A. and D. B. Kittelson. Sampling and Physical Characterization of Diesel Exhaust Aerosols. Paper presented at the Off-Highway Vehicle Meeting and Exhibition, MECCA, Milwaukee, September 12-15, 1977. SAE Paper No. 770720.

Vuk, C. T., M. A. Jones, and J. H. Johnson. The Measurement and Analysis of the Physical Character of Diesel Particulate Emissions. Paper presented at the Automotive Engineering Congress and Exposition, Detroit, Michigan, February 23-27, 1976. SAE Paper No. 760131.

Black, F. and L. High. Methodology for Determining Particulate and Gaseous Diesel Hydrocarbon Emissions. Paper presented at the Congress and Exposition, Cobo Hall, Detroit, February 26-March 2, 1979. SAE Paper No. 790422.

Stinton, H. C. Development of a Methodology for the Determination of Diesel Total Hydrocarbon Emission Rates for Cyclic Driving Condition. EPA Contract No. 68-02-2751, Progress Report, September 1978.

Zweidinger, R. B., S. B. Tejada, D. Dropkin, J. Huisingh, and L. Claxton. Characterization of Extractable Organics in Diesel Exhaust Particles. EPA Symposium on Diesel Particulate Emissions Measurement and Characterization, Ann Arbor, Michigan, May 1978.

Huisingh, J. et al. Application of Bioassay to Characterization of Diesel Particle Emissions. EPA Symposium on Application of Short-Term Bioassays in the Fractionation and Analysis of Complex Environmental Mixtures, Williamsburg, Virginia, February 1978.

Bennethum, J. E., J. N. Mattavi, and R. R. Toepel. Diesel Combustion Chamber Sampling - Hardware, Procedures, and Data Interpretation. Paper presented at the 1975 SAE Off-Highway Vehicle Meeting, Milwaukee, Wisconsin, September 8-11, 1975. SAE Paper No. 750849.

Springer, K. J. and H. E. Dietzmann. Diesel Exhaust Hydrocarbon Measurement - A Flame Ionization Method. Presented at SAE Meeting, Detroit, January 12-16, 1970. SAE Paper No. 700106.

Williams, R. L. and S. J. Swarin. Benzo(a)pyrene Emissions from Gasoline and Diesel Automobiles. Paper presented at the Congress and Exposition, Cobo Hall, Detroit, February 26-March 2, 1979. SAE Paper No. 790419.

Lyons, M. J. Comparison of Aromatic Polycyclic Hydrocarbons from Gasoline-engine and Diesel-engine Exhaust, General Atmospheric Dust and Cigarette Smoke Condensate. NCI Monograph No. 9, pp. 193-199, Washington, D.C., 1962.

Recommend Practice for Measurement of Gaseous and Particulate Emissions from Light-Duty Diesel Vehicles. Draft Report, U.S. Environmental Protection Agency, March 1978.

Greeves, G. and J. O. Meehan. Measurement of Instantaneous Soot Concentration in a Diesel Combustion Chamber. I. Mech. E. (London) Conference Paper C8.

Knuth, E. L. Direct Sampling Studies of Combustion Processes. Engine Emissions - Pollutant Formation and Measurement. Editors: G. S. Springer and D. J. Patterson, Plenum Press, 1973.

McKee, H. C., J. M. Clark, and R. J. Wheeler. Measurement of Diesel Engine Emissions. J. Air Pollution Control Assoc., 12:516, November 1962.

Bricklemeyer, B. A. and R. S. Spindt. Measurement of Polynuclear Aromatic Hydrocarbons in Diesel Exhaust Gases. Presented at the SAE Congress and Exposition, February 27-March 3, 1978. SAE Paper No. 780115.

Sawicki, E., R. C. Corey, A. E. Dooley, et al. Tentative Method of Microanalysis for Benzo(a)pyrene in Airborne Particulates and Source Effluents. Health Lab. Sci. 7(Suppl. 1),:56-59, January 1970.

Sawicki, E., R. C. Corey, A. E. Dooley, et al. Tentative Method of Analysis of Polynuclear Aromatic Hydrocarbon Content of Atmospheric Particulate Matter. Health Lab. Sci. 7 (Suppl. 1),:31-44, January 1970.

Sawicki, E., R. C. Corey, A. E. Dooley, et al. Tentative Method of Routine Analysis for Polynuclear Aromatic Hydrocarbon content Atmospheric Particulate Matter. Health Lab. Sci. 7 (Suppl. 1),:45-55, January 1970.

Golden, C. and E. Sawicki. Ultrasonic Extraction of Total Particulate Aromatic Hydrocarbons (TpAH) from Airborna Particles at Room Temperature. Int. J. Environ. Anal. Chem. in press, 1975.

Bailey, C., A. Javes, and J. Lock. Investigation into the Composition of Diesel Engine Exhausts. Fifth World Petroleum Congress, Section VI, Paper 13, p. 209, New York, N. Y., 1959.

Oldham, R. G. Quantitative Analysis of Polynuclear Aromatic Hydrocarbons in Liquid Fuels. U.S. Environmental Protection Agency, Contract No. 68-02-2446, initiated September 1976.

Kau, C. J., M. P. Heap, T. J. Tyson, and R. P. Wilson. Prediction of Nitric Oxide Formation in a Direct Injection Diesel Engine. Sixteenth Symposium (Int) on Combustion, MIT, Cambridge, Mass., Aug. 15-20, 1976.

McGuire, D. W. Diesel Smoke Meters for Army Use, November 1976. NTIS No. AD-A035210/4ST.

Springer, K. J. and H. E. Dietzmann. Diesel Exhaust Hydrocarbon Measurement - A Flame Ionization Method. Paper presented at SAE Meeting, Detroit, January 12-16, 1970. SAE Paper No. 700106.

HEALTH EFFECTS

Johnston, A. A., K. Springer, D. Johnson, D. Boenig, and F. Newman. Toxicity of Engine Exhaust Gases Diesel - Bromochloromethane Fuel Blend. SwRI Final Report AFLRL No. 51, February 1975.

Bradburn, R. A. Diesel Haulage Experience in the Martin County Coal Corporation with Emphasis on Health and Safety Aspects. IC8666, U.S. Department of the Interior, Proceedings of the Symposium on the Use of Diesel-Powered Equipment in Underground Mining, Pittsburg, Pennsylvania, Jan. 30-31, 1973.

Alcock, K. Safe Use of Diesels in Underground Coal Mines. Diesel and Gas Turbine Progress, 80-82, March 1977.

Dimick, D. L. Particulate Control Development Status. Workshop on Unregulated Diesel Emissions and Their Potential Health Effects, DOT-NHTSA, DOE and EPA, April 27-28, 1978.

Barth, D. S. and S. M. Blacker. The EPA Program to Assess the Public Health Significance of Diesel Emissions. Journal of the Air Pollution Control Association, 28(8):769-771, August 1978.

Wang, Y. Y., et al. Direct-Acting Mutagens in Automobile Exhaust. Cancer Letters, 5:39-47, 1978.

Pitts, J. N., et al. Proceedings of the Workshop on Unregulated Diesel Emissions and Their Potential Health Effects. DOT-NHTSA, DOE and EPA, Washington, D.C., April 27-28, 1978.

Turner, D. W. Workshop on Unregulated Diesel Emissions and Their Potential Heal Effects, April 27-28, 1978. DOT-NHTSA, DOE and EPA, Washington, D.C.

Mogan, P., D. B. Stewart, A. D'Aoust, and E. D. Dainty. The Respirability of Exhaust Particulates Generated by a V-6, Air-Cooled, Indirect-Injection Diesel Engine. Divisional Report (FRC 74/9 - CEAL No. 305 - limited distribution) of the Department of Energy, Mines and Resources, Mines Branch, Fuels Research Centre, Ottawa.

Kotin, P., H. L. Falk, and M. Thomas. Aromatic Hydrocarbons: III. Precence in the Particulate Phase of Diesel Engine Exhausts and the Carcinogenicity of Exhaust Extracts. AMA Arch. Indust. Health, 11:113, 1955.

Battigelli, M. C., T. F. Hatch, R. J. Mannella, and F. Hengstenberg. Dose Response Relations from Inhalation of Diesel Exhaust. Terminal Report, U.S. Public Health Service, Grant No. OH-00191-02, University of Pittsburg, 1967.

Unregulated Diesel Emissions and Their Potential Health Effects. Edited Transcript of Proceedings, Department of Transportation, Department of Energy, Environmental Protection Agency, April 27-28, 1978.

Health Effects of Diesel Exhaust Emissions. A Report Prepared for the American Mining Congress by Environmental Health Associates, Inc., January 1978.

Begeman, C. R. Carcinogenic Aromatic Hydrocarbons in Automobile Effluents. Society of Automotive Engineers, Inc., Warrendale, Pennsylvania, 1962. SAE Paper No. 440C.

Workshop On: Unregulated Diesel Emissions and Their Potential Health Effects. Edited Transcript of Proceedings, April 27-28, 1978. Sponsored by the Department of Transportation, National Highway Traffic Safety Admin., The Department of Energy, and the Environmental Protection Agency.

Lassiter, D. V. and T. H. Milby. Health Effects of Diesel Exhaust Emissions: A Comprehensive Literature Review, Evaluation and Research Gaps Analysis. Environmental Health Associates, Inc., Berkeley, California, American Mining Congress, Washington, D.C., Jan. 25, 1978. NTIS No. PB-282795/4ST.

TECHNICAL REPORT DATA
(Please read Instructions on the reverse before completing)

1. REPORT NO.	2.	3. RECIPIENT'S ACCESSION NO.
EPA-600/7-79-232a		

4. TITLE AND SUBTITLE	5. REPORT DATE
Assessment of Diesel Particulate Control: Filters, Scrubbers, and Precipitators	October 1979
	6. PERFORMING ORGANIZATION CODE
7. AUTHOR(S)	8. PERFORMING ORGANIZATION REPORT NO.
M.G. Faulkner, E.B. Dismukes, J.R. McDonald, D.H. Pontius, and A.H. Dean	SORI-EAS-79-564 Project 3858-14-FR
9. PERFORMING ORGANIZATION NAME AND ADDRESS	10. PROGRAM ELEMENT NO.
Southern Research Institute 2000 Ninth Avenue South Birmingham, Alabama 35205	EHE624A
	11. CONTRACT/GRANT NO.
	68-02-2610, Task 14
12. SPONSORING AGENCY NAME AND ADDRESS	13. TYPE OF REPORT AND PERIOD COVERED
EPA, Office of Research and Development **Industrial Environmental Research Laboratory** **Research Triangle Park, NC 27711**	Final; 3/79 - 7/79
	14. SPONSORING AGENCY CODE
	EPA/600/13

15. SUPPLEMENTARY NOTES IERL-RTP project officer is Dennis C. Drehmel, Mail Drop 61, 919/541-2925.

16. ABSTRACT The report discusses an investigation of three types of devices that might be used for the aftertreatment of diesel exhaust to lower particulate emissions from light-duty vehicles. The devices are filters, electrostatic precipitators (ESPs), and wet scrubbers. The conclusions reached are that filters and ESPs merit further consideration, but wet scrubbers do not. Wet scrubbers were eliminated from further consideration on the basis of excessive size, low efficiency, and excessive fluid loss by evaporation (assuming that water is the fluid of choice). Filters and ESPs, although appearing to offer significant potential, have possible disadvantages that can only be assessed experimentally. Prototype filters and electrostatic devices that appear worthy of experimental study are described.

17. KEY WORDS AND DOCUMENT ANALYSIS

a. DESCRIPTORS	b. IDENTIFIERS/OPEN ENDED TERMS	c. COSATI Field/Group
Pollution	Pollution Control	13B
Diesel Fuels	Stationary Sources	21D
Diesel Engines	Particulate	21G 13F
Dust		11G
Aerosols		07D
Dust Filters		13J
Scrubbers		07A, 13I
Electrostatic Precipitators		
Ground Vehicles		

18. DISTRIBUTION STATEMENT	19. SECURITY CLASS *(This Report)*	21. NO. OF PAGES
Release to Public	**Unclassified**	174
	20. SECURITY CLASS *(This page)*	22. PRICE
	Unclassified	

EPA Form 2220-1 (9-73)